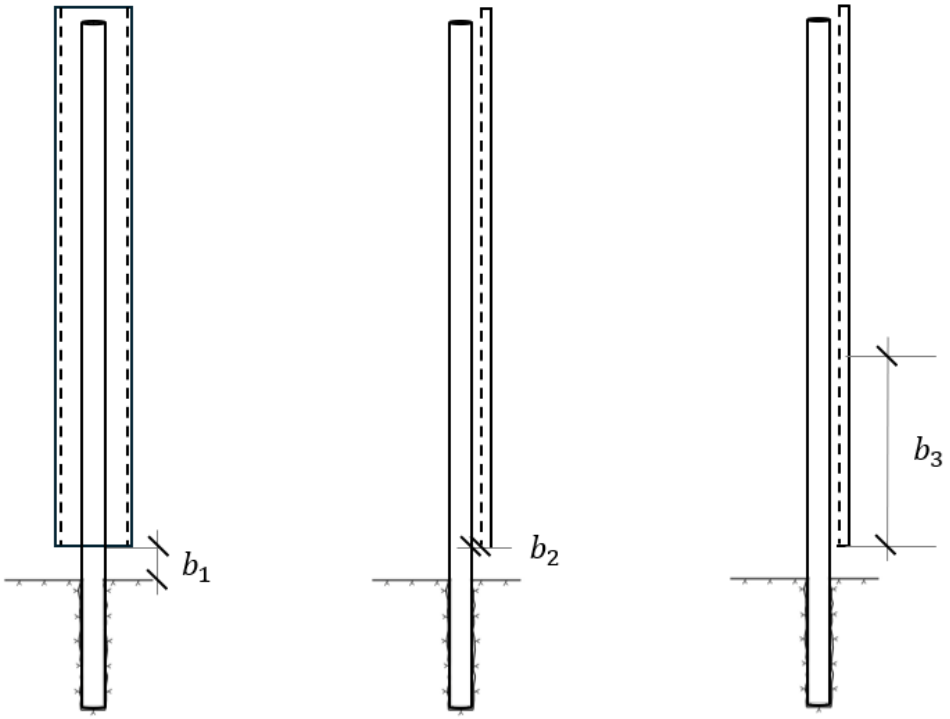

Drilled Piles used as Rock Supports for Sheet Piles

An investigation into the structural behavior and gap effects of drilled piles, with a comparative analysis of rock dowel design approaches

Master's thesis in the Master's Programme Infrastructure and Environmental Engineering

RIHAM EBRAHIM
SOFIA SANDVIK

DEPARTMENT OF ARCHITECTURE AND CIVIL ENGINEERING
CHALMERS UNIVERSITY OF TECHNOLOGY
Master's thesis ACEX30
Gothenburg, Sweden 2025

MASTER'S THESIS 2025

Drilled Piles used as Rock Supports for Sheet Piles

An investigation into the structural behavior and gap effects of drilled piles, with a comparative analysis of rock dowel design approaches

Master's Thesis in the Master's Programme
Infrastructure and Environmental Engineering

RIHAM EBRAHIM
SOFIA SANDVIK

CHALMERS
UNIVERSITY OF TECHNOLOGY

Department of Architecture and Civil Engineering
Division of Geology and Geotechnics
CHALMERS UNIVERSITY OF TECHNOLOGY
Gothenburg, Sweden 2025

Drilled Piles used as Rock Supports for Sheet Piles
An investigation into the structural behavior and gap effects of drilled piles, with a comparative analysis of rock dowel design approaches
Master's Thesis in the Master's Programme Infrastructure and Environmental Engineering
RIHAM EBRAHIM
SOFIA SANDVIK

Supervisor: Andreas Flyckt, WSP
Supervisor: Mats Karlsson, Department of Architecture and Civil Engineering
Examiner: Mats Karlsson, Department of Architecture and Civil Engineering

Master's Thesis 2025
Department of Architecture and Civil Engineering
Division of Geology and Geotechnics
Chalmers University of Technology
SE-412 96 Göteborg
Telephone +46 31 772 1000

Cover:
Conceptual model of the three gaps/distances analyzed in the thesis.

Typeset in LaTeX
Department of Architecture and Civil Engineering
Gothenburg, Sweden, 2025

Drilled piles Used As Rock Supports For Sheet Piles
An investigation into the structural behavior and gap effects of drilled piles, with a comparative analysis of rock dowel design approaches

Master's thesis in the Master's Programme Infrastructure and Environmental Engineering

RIHAM EBRAHIM

SOFIA SANDVIK

Department of Architecture and Civil Engineering
Division of Geology and Geotechnics
Chalmers University of Technology

ABSTRACT

Drilled piles are used as rock supports for deep excavations where passive resistance is insufficient due to proximity to bedrock. Conventional methods primarily include the use of rock dowels; however, there is growing industry interest in adapting drilled piles as a primary alternative rather than just a backup. Available design methods in standards and guidelines do not adequately address the forces that occur in the bedrock, especially when gaps exist between the sheet pile wall and the bedrock due to uneven levels or obstacles that hinder the sheet pile. This thesis aims to investigates how varying horizontal and vertical gaps between the sheet pile and bedrock affect the structural behavior of drilled piles acting as supports. Numerical simulations in PLAXIS 2D were performed using data from the Sahlgrenska Life project, and interviews were conducted to provide further insight into the installation processes.

The results show that the horizontal distance, b_2, between the sheet pile and drilled pile contributes to minimal changes in forces within the two structures. For the vertical gap, b_1, between the toe of the sheet pile and the bedrock, the drilled pile exhibits an increase in shear force as the gap increases, while the bending moment remains relatively unaffected. However, this applies only to cases where redistributed net earth pressure remains low. For cases with higher redistributed earth pressure, the bending moment increases with a gradient of approximately $3{\cdot}b_1$, whereas the shear force remains relatively unchanged. This indicates that the conventional design method for rock dowels does not show the same correlation between design shear force Q_{ed} and design bending moment M_{ed}. Variations in toe modeling were also examined, concluding that modeling the drilled pile as close to realistic conditions as possible resulted in unrealistic shear forces within the drilled pile. This is assumed to be caused by numerical point loading effects due to the significant stiffness contrast between the soil layer and the bedrock.

Key words: Geotechnics, Retaining structures, Drilled piles, Sheet pile wall, Anchor methods, Rock anchors, PLAXIS 2D, Finite element method, Geotechnical construction

Användning av borrade stålrör som bergförankring för spont
En undersökning av borrade pålars beteende och glappens inverkan, med en jämförande analys av dimensioneringsmetoder för bergdubb

Examensarbete inom masterprogrammet Infrastruktur och miljöteknik

RIHAM EBRAHIM

SOFIA SANDVIK

Institutionen för arkitektur och samhällsbyggnadsteknik
Avdelningen för Geologi och Geoteknik
Chalmers tekniska högskola

SAMMANFATTNING

Borrade pålar används som bergförankring vid djupa schakter där det passiva jordtrycket inte är tillräckligt på grund av närhet till berg. Dimensioneringen bygger traditionellt på användning av bergdubb, men intresset i branschen för att använda borrade pålar som ett primärt alternativ har ökat. Befintliga standarder och riktlinjer behandlar därmed inte fullt ut de krafter som uppstår i den borrade pålen, särskilt inte i de fall med glapp mellan sponten och bergytan på grund av ojämna nivåskillnader eller hinder som förhindrar neddrivning av sponten. Syftet med detta examensarbete är att undersöka hur variationer i horisontella och vertikala glapp mellan spont och berg påverkar den borrade pålens berförmåga och beteende. Numeriska simuleringar i PLAXIS 2D har genomförts baserat på data från Sahlgrenska Life-projektet, och intervjuer har genomförts för att ge ytterligare inblick i installationsprocessen.

Resultaten visar att det horisontella avståndet, b_2,mellan spont och borrad påle har liten inverkan på kraftfördelningen i konstruktionen. För det vertikala glappet, b_1, mellan underkant spont och bergytan ses en tydlig ökning av tvärkraften i den borrade pålen i takt med att avståndet ökar medan böjmomentet i dessa fall förblir relativt konstant. Detta gäller dock främst för fall där det omfördelade resulterande jordtrycket är lågt. Vid högre omfördelat jordtryck ökar istället böjmomentet linjärt med en koefficient på cirka $3 \cdot b_1$, medan tvärkraften påverkas minimalt. Detta indikerar att nuvarande dimensioneringsmetod för bergdubb, där böjmomentet beräknas linjärt från tvärkraften, inte fullt ut representerar kraftfördelningen i borrade pålar. Vidare har olika sätt att modellera förankring med berget analyserats, vilket visar att en realistisk representation kan ge upphov till orimliga tvärkrafter i modellen. Detta antas bero på numeriska punktbelastningar till följd av stor styvhetsskillnad mellan jordlager och berg.

Nyckelord: Geoteknik, Stödkonstruktioner, Borrade pålar, Spont, Förankringsmetoder, Bergförankringar, PLAXIS 2D, Finita element metoden, Geokonstruktion

Contents

Acknowledgments

This thesis has been conducted through continuous work and iterative testing of various model setups in PLAXIS 2D, in combination with data processing and analysis using Excel. The project was carried out at both Chalmers University of Technology and WSP Sweden, whom provided the project framework, support, and necessary resources. The construction project forming the basis of this thesis was executed by Aarsleff, who also offered valuable insights into the production process through an interview with Mathias Matsman. We also extend our sincere thanks to Johan Eriksson at Hercules for taking the time to share his insight in the industry that would have been difficult to obtain otherwise. Our supervisor and examiner at Chalmers, Mats Karlsson, has been of great help with his guidance and technical expertise throughout the process and helped navigate various challenges along the way. Finally, we would like to express our deepest thanks to our supervisor at WSP, Andreas Flyckt, for continuous support and in-depth knowledge in the subject. His engagement and enthusiasm for the thesis has been a key source of motivation for us during this spring.

Gothenburg, June 2025
Riham Ebrahim & Sofia Sandvik

Notations

Roman upper case letters

E	Young's modulus
G	Shear modulus
M	Bending moment
Q	Shear force
N	Normal force
H	Excavtion depth
K	Earth pressure coefficient (e.g. K_a, K_p, and K_0)

Roman lower case letters

b_1	Vertical distance between sheet pile toe and bedrock
b_2	Horizontal distance between sheet pile and drilled pile
b_3	Vertical distance of support
c	Distance between rock dowels
d	Lever arm
$l_{spacing}$	The actual distance between the drilled piles
u	Pore water pressure
m_b, s, a	Hoek-Brown parameters

Greek letters

ν	Poisson's ratio
σ	Total stress
σ'	Effective stress
τ	Shear stress
γ	Unit weight
ϕ'	Effective friction angle
σ_v, σ_h	Vertical and horizontal stress
σ_{ci}	Uniaxial compressive strength of intact rock

Abbreviations

PLAXIS	Finite element software for geotechnical analysis
SLS	Serviceability Limit State
ULS	Ultimate Limit State
SP	Sheet pile
DP	Drilled pile
MC	Mohr-Coulomb
HB	Hoek-Brown

1

Introduction

The ongoing urbanization contributes to the development and reconstruction of cities. As population density increases, the available space for construction becomes more confined and projects that require deep excavations must therefore protect the adjacent structures (Jin et al., 2021). This is done by installing retaining structures that ensure a minimal impact on ground movement and groundwater variations. Depending on the forces generated by surrounding earth pressure, different types of support structures are required (Knappett & Craig, 2012). These systems can include diaphragm walls, sheet piles, or piles. Factors influencing the choice of method are, among others, excavation depth, soil stratigraphy, whether the structure is temporary or permanent, the type of loads involved, and the availability of space on-site. One of the most common methods for retaining soil masses is the use of sheet piles, typically made of steel, however, can also be constructed from concrete or wood. The steel sheet piles are composed of alternating angles, where two common designs of a sheet pile wall are the U-shaped and Z-shaped profiles.

In projects with shallow depths to bedrock, it is quite common that the sheet piles need extra support due to lack of passive resistance, lack of stability and lack of strength (Knappett & Craig, 2012). This is particularly relevant in Sweden, where layers of soft clay often is found overlaying bedrock, causing complex geotechnical conditions in need of careful design considerations (ArcelorMittal Sheet Piling, 2018). For extra support, the sheet piles are typically anchored by plate anchors, ground anchors or rock anchors, or varying types of shoring systems (Knappett & Craig, 2012). These anchoring systems are placed at different heights along the sheet pile wall to resist the forces that could lead to structural failure.

For failures that occur due to lack of lateral support at the toe, rock dowels have been used as a bedrock anchoring method, which results in a fixed end. An observed problem within the industry regarding rock dowels is that specific conditions are required for each unit to be successfully installed. A drawback of the method is the uncertainty of the conditions during installation, which are not always according to design. If conditions on site are different from the expected it is common to add additional rock anchoring support to the structure by adding a drilled pile next to the defected rock dowel. Because of the uncertainties related to rock dowels, an alternative method of using drilled piles instead have been introduced to the geotechnical industry (Matsman, 2025). These drilled piles are today dimensioned using the same calculation method as for rock dowels.

1.1 Project description: Sahlgrenska Life

The area of Gothenburg contains a varying soil depth, with thicknesses surpassing 50 m in areas close to the rivers Göta älv, Mölndalsån and Säveån, as seen in Figure 1.1. The remaining area is primarily covered by bedrock with soil layers ranging between 0-20 m, thereby contributing to the usage of retaining structures that need to be adapted to a variation of bedrock and soil properties.

Figure 1.1: Overviewing map of depths of soil Gothenburg from SGU.

Swedens largest hospital, Sahlgrenska universitetssjukhus, located in Gothenburg is undergoing large reconstructions of some of the old facilities that have been around since year 1899 (Sahlgrenska Universitetssjukhus VGR, 2023). This to allow for the conditions necessary for continued modernization of equipment and technology within the different categories of medicine, as well as to adapt to an increase and aging population. Another contributing factor is that the current buildings require a higher energy usage, which will be reduced with the development of new amenities.

As a result of this, the project Sahlgrenska Life has been developed and primarily aims to increase patient capacity through innovation (Västra Götalandsregionen, 2025). Three new buildings are planned for, which requires the demolition of the three existing buildings; the otorhinolaryngology building (commonly known as the ear-nose-throat division), an ambulance hall and the Per Dubbs building shown in Figure 2.3. To enable this, preparatory works need to be done which includes the installation of retaining structures necessary for excavations in order to conduct work with minimal effect on the surrounding buildings.

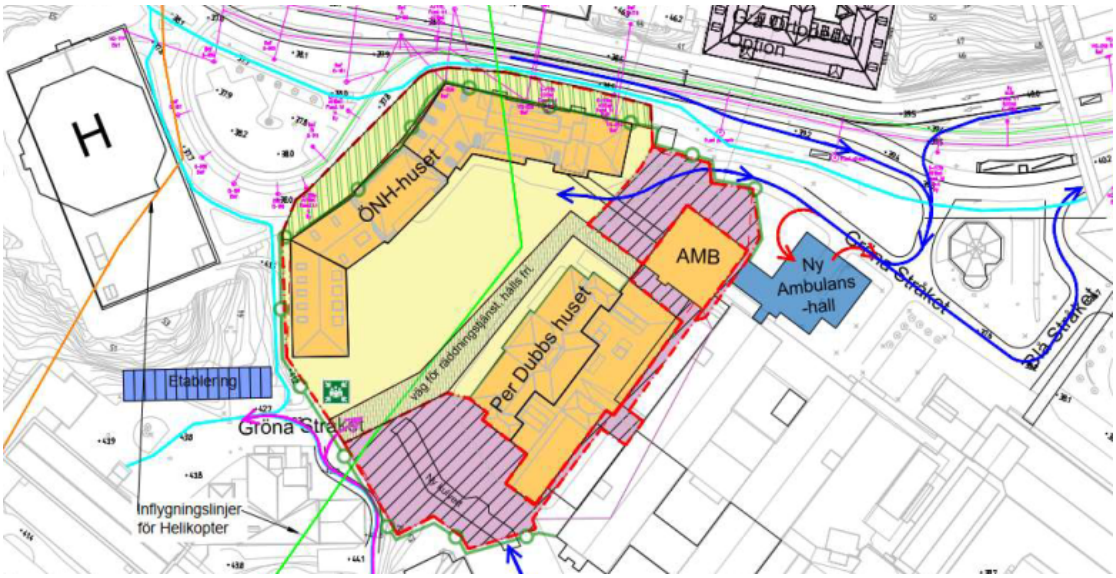

Figure 1.2: Overview of the project area showing the locations of future buildings and their relative positions within the site.

DACO Contractor AB have taken on the project and together with consulting firm WSP are responsible for the designs of the temporary substructures in the area. A solution involving sheet piles, anchors and steel pipes have been designed with the methodology that is used for the dimensioning of rock dowels, in accordance to Eurocode SS_EN_1993_5:2007 and SS_EN_1997_1:2005. Inclinometers will be installed on some of the sheet piles and data from the project will be used both to monitor the structure during it's design life and to better understand the behavior of the retaining structure in comparison to expected movements from calculations.

1.2 Aim and objectives

This thesis aims to investigate the use of steel piles drilled in front of the sheet piles and their interaction.

Research questions:

- What is the interaction distance (b_3) between a sheet pile and drilled piles when used as a bedrock anchor?
- How do vertical and horizontal distances (b_1 and b_2) affect the forces in the drilled pile and sheet pile?
- What are the benefits of using the method of drilled piles in comparison with rock dowels?

1.3 Limitations

- Only sheet piles used as temporary constructions are considered, long term effects are not analyzed.
- The method aims to include projects with a proximity to bedrock at 8-16m.
- Three dimensional effects are disregarded.

1.4 Method

To begin, this thesis will review relevant reports and sources in a literature analysis which will contribute to the theory that the results will be based on. As the project Sahlgrenska Life applies the method of using drilled piles as rock anchors, which is the basis of the research questions for this thesis, the theory will cover information regarding the conditions that prevail at the site. To enable an objective perspective, the search engines that will be used are the following:

- Sciencedirect
- Google scholar
- Chalmers Library Portal

The thesis utilization of the Sahlgrenska project requires a thorough understanding of the conditions, thus site visits will be made continuously throughout the time frame but primarily for the phases of installation of sheet piles and drilled piles. Both analytical calculations and numerical geotechnical finite element software analyses will be carried out and compared to each other with the intention of calibrating and validating the models that the analyses are based on.

An interview with the contractor of the project will be carried out with the aim of deepening the understanding of experiences from general projects and as a base of the advantages and disadvantages of the installation process. For further understanding, an additional interview will be conducted to broaden the view of the opinions within the industry. The methods of calculations will be covered in chapter 3. Lastly, AI-tools such as ChatGPT and Microsoft Copilot will be used consistently throughout the report to support different stages of the writing and analysis process.

2

Theory

In the following sections, theories and relevant knowledge for the aim and objectives of this report will be covered briefly, to enable comprehensiveness for the reader.

2.1 Theoretical framework for soil behavior

The load from total stress, to effective and lastly to horizontal stress is defined in different theories and the determination of which theory that is applicable can have consequences on the precision of the problem. The earth pressure theories that will be covered in this chapter are the following:

- Terzaghis principle of effective stresses
- Linear elasticity and soil plasticity
- Mohr Coulombs failure criteria
- Rankine´s theory

These terms are deemed most relevant for this thesis in terms of understanding the properties of soil and the behavior under shear stresses. By establishing the correlations between different parameters, the conditions that the principles are based on and the required geotechnical data for gathering is clarified. The definitions of all theories are based on *Craig's Soil Mechanics* (Knappett & Craig, 2012).

2.1.1 Terzaghi's principle

One of the primary concepts and theories regarding the transferal of forces within soil are based on Terzaghis principle of effective stress. The relationship is based on conditions that it is a fully saturated soil and establishes the relationship of vertical total stress σ, pore water pressure u and vertical effective stress σ'. The sum of the weight given by the mass from the soil, results in the total vertical stress at depth z, per unit area. The equations for all are as seen in Equations 2.3, 2.2 and 2.3

$$\sigma_v = \gamma_{sat} * z \tag{2.1}$$

$$u = \gamma_w * z \tag{2.2}$$

$$\sigma'_v = \sigma_v - u = (\gamma_{sat} - \gamma_w) * z \tag{2.3}$$

It is the effective stress that determines the soil's mechanical behavior. This means that any deformation, strength, and consolidation are are all based on the

proportion of the total stress that is transferred through the particles, which is independent of the pore water. The principal is also based on the assumption that both the soil grains and water are assumed to be incompressible, meaning that the solid volume is considered constant during mechanical loading.

2.1.2 Linear elasticity and soil plasticity

There are multiple stages of identifying soil behavior, the first one being the simple linear elastic behavior and is modeled with shear strain linear to the applied shear stress. This gradient is known as the the shear modulus G. By applying Hooke's law of relationships between strain caused by normal stress for elastic cases, using Young's Modulus E calculated as shown in Equation 2.4 and Poisson's ratio of soil behavior, the correlation between the parameters is determined as seen in Equation 2.5.

The characterization of soil behavior typically begins with the assumption of linear elasticity, which is often used in early-stage analysis and for small-strain approximations. In this model, shear strain is proportional to the applied shear stress, and the gradient of this relationship is defined as the shear modulus G. Normal strains resulting from applied normal stresses are similarly assumed to follow a linear relationship, determined by Young's modulus E and Poisson's ratio ν.

$$E = \sigma/\epsilon \tag{2.4}$$

$$G = \frac{E}{2(1+\nu)} \tag{2.5}$$

Linear elasticity assumes that the material response is fully reversible and independent of loading history. However, this is a significant simplification, as real geotechnical materials typically exhibit highly non-linear, irreversible behavior even at relatively low stress levels. For this reason, plasticity models are introduced to capture the yield and post-yield behavior of soils.

In plasticity theory, soil deformations are divided into recoverable (elastic) and permanent (plastic) components. Plastic deformation is typically defined by a yield surface in which the material no longer follows Hooke's law. Various constitutive models exist to describe this behavior, including the Mohr–Coulomb and Soft Soil models, which are widely used in numerical geotechnical analysis.

2.1.3 Mohr-Coulomb's circle theory

Mohr–Coulomb's circle theory illustrates the relationship between shear stress and effective (or normal) stress at failure and is one of the most widely used failure criteria in geotechnical engineering due to its simplicity and empirical relevance. The model assumes that failure occurs along a plane when the shear stress reaches a critical value, defined by the material's internal friction and cohesion.

Based on empirical observations, the relationship between principal effective stresses σ_1' and σ_3' can be established at different depths or for varying slope conditions. The key mechanisms that contribute to shear strength are grain interlocking, internal friction, and cohesion. These are captured in the Mohr–Coulomb failure

criterion:

$$\tau_f = c' + \sigma' \tan \phi' \tag{2.6}$$

where τ_f is the shear stress at failure, c' is the effective cohesion, σ' is the effective normal stress on the failure plane, and ϕ' is the effective angle of internal friction.

The Mohr–Coulomb model simplifies the three-dimensional stress state into a two-dimensional plane strain representation, in which shear strength is plotted against effective normal stress. The failure condition is represented as a linear envelope tangent to the Mohr circle, as shown in Figure 2.1. The point of contact between the circle and the envelope marks the start of failure.

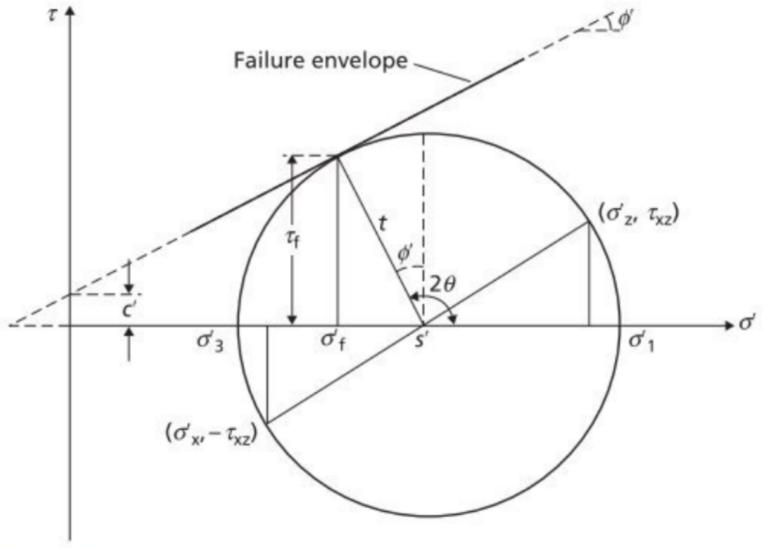

Figure 2.1: Plastic equilibrium state based on Mohr Coulomb's failure criteria (Knappett & Craig, 2012).

2.1.4 Rankine´s theory

Rankine's theory is a method used for analyzing how stresses in soil transfer to lateral earth pressure, in order to calculate what loads acting on retaining structures. The theory is based on the following assumptions:

- Homogeneous and isotropic properties of the soil
- Failure according to Mohr Coulomb
- Infinite soil mass in the horizontal direction
- No friction between the wall-soil interface
- Small displacements of the soil

In this theory, earth pressures are divided into three categories: active, passive, and at-rest earth pressure. The active earth pressure p_a develops when the wall moves away from the soil, causing expansion and mobilization of shear strength. This is due to the cohesion factor which shows how much of the vertical stresses

contribute to lateral movement of the retaining structure caused by expansion. K_a and p_a is calculated with Equation 2.7 resp. 2.8.

The active earth pressure coefficient K_a is calculated from the effective friction angle ϕ' using:

$$K_a = \frac{1 - sin\phi'}{1 + sin\phi'} \tag{2.7}$$

$$p_a(z) = \sigma_h(z) = K_a\sigma'_v(z) - 2c'\sqrt{K_a} + u(z) \tag{2.8}$$

The same principal applies for the calculation of the passive earth pressure, however for the soil that is compressed or moves toward the retaining structure. The cohesion factor for passive earth pressure K_p is determined with Equation 2.9, which enables the calculation of the passive earth pressure using Equation 2.10.

$$K_p = \frac{1 + sin\phi'}{1 - sin\phi'} \tag{2.9}$$

$$p_p(z) = \sigma_h(z) = K_p\sigma'_v(z) + 2c'\sqrt{K_p} + u(z) \tag{2.10}$$

The net pressure acting on the sheet pile is therefore seen as the difference between the active and the passive forces, demonstrated with the Equation 2.11.

$$p_{net}(z) = p_a - p_p \tag{2.11}$$

Before any active or passive pressures are mobilized, the soil mobilizes a lateral pressure on the retaining structure which is referred to as the earth pressure at rest, p_0 and is calculated using Equation 2.12 , where K_0 is the earth pressure at-rest coefficient calculated by Equation 2.13.

$$p_0 = K_0 * \sigma_v \rightarrow p'_0 = K_0 * \sigma'_v \tag{2.12}$$

$$K_{0,\mathrm{NC}} = 1 - sin\phi' \tag{2.13}$$

Rankine's theory does not account for wall roughness, wall flexibility, or non-linear stress–strain behavior, but remains a widely used method due to its simplicity and reasonable accuracy for preliminary design.

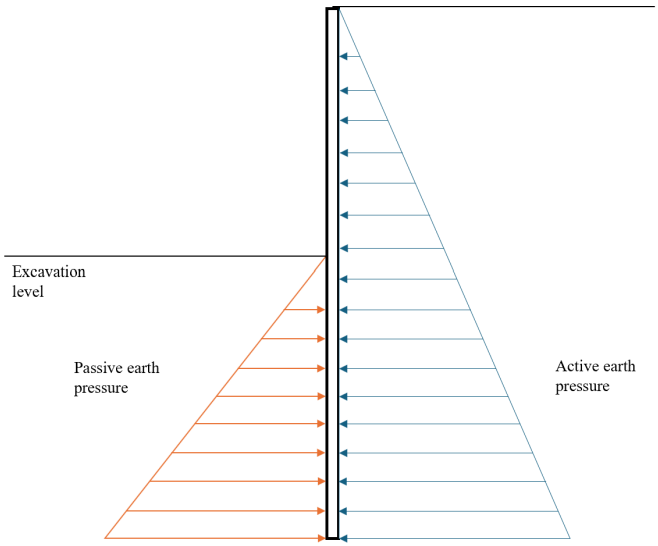

Figure 2.2: Illustration of active and passive earth pressure.

2.1.5 Redistribution of earth pressure between support levels

In order to estimate the distribution of loads acting on different support levels in a retaining system, the net earth pressure is often assumed to act evenly over a limited portion of the wall. According to practical guidance, such as that found in Fredriksson et al., 2024, the redistributed pressure can be considered uniform from a level approximately $0.2 * H$ below the excavation surface (where H is the excavation depth) down to the toe of the sheet pile. This simplification is valid for structures with top and bottom anchorage, and allows for a more workable calculation of support reactions and is commonly used in analytical design of embedded retaining structures.

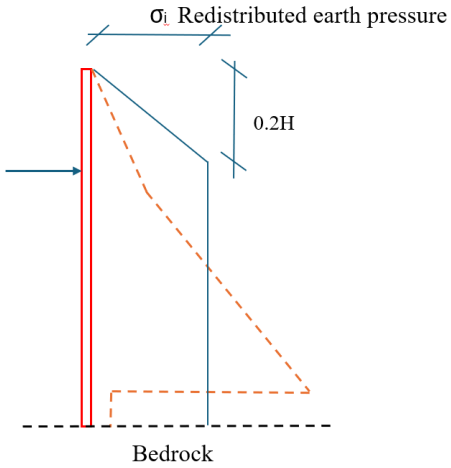

Figure 2.3: Simplified sketch of the redistributed earth pressure, for a sheet pile with top and bottom anchor. Inspired by Fredriksson et al. (2024)

2.2 Sheet piles

Sheet piling is a supportive structure used to retain earth masses and water during deep excavations in projects such as tunnel constructions, harbors, and excavations in densely populated areas (Fredriksson et al., 2024). Sheet piles use the passive earth pressure at the toe (bottom) of the pile to retain the earth masses on the active side of the wall. For the earth pressure at the toe to be sufficient, the depth of which the retaining wall must be driven to must be dimensioned. Sheet piles are either driven or vibrated into the ground as support for the sides of deep excavations or waterfront structures. By connecting joints to adjacent walls, the construction provides structural resistance and a relatively watertight configuration. The retaining structure can be used as both temporary and permanent structures, which is an advantage since they can be reused once the final construction is completed. Sheet piles are normally 12 meters long, but their length can be easily adjusted into both longer and shorter lengths (SSAB AB, 2025). The material used to make sheet piles is most commonly steel, but sometimes concrete or wood is used (Knappett & Craig, 2012). Steel sheet piles are preferred partly because of their high strength and potential for reuse and also because of the smoothness in installations especially in areas where space is limited or in challenging soil conditions (Das & Sobhan, 2018).

The structural design of sheet pile walls is dimensioned through calculating the internal forces, deciding which cross-sectional profile to use, and depending on what embedment depth is of interest (Knappett & Craig, 2012). Some key parameters regarding structural design are the wall's capacity to withstand bending moments caused by lateral soil and water pressures, shear forces, deflections, soil conditions, and installation methods. There are different profiles of sheet piles, and the two most commonly used are the Z-profile and the U-profile displayed in Figure 2.4. The Z-profiles can withstand a high bending moment because the interlock is symmetric and are used mainly during permanent structures such as harbor walls and dams. In comparison the U-profiles can withstand a lower bending moment due to the fact that their interlock is on the neutral axis (Piling, 2022). U-profiles are easier to drive into the ground and reuse, therefore, these are mostly used in temporary structures.

Figure 2.4: U-profile (left) and Z-profile (right) for sheet pile walls. Red circles highlight the interlocks (Piling, 2022).

The sheet pile's ability to retain soil masses is determined by the lateral earth pressures of the surrounding soils. To analyze the surrounding pressures, classical theories such as Rankine's Theory and Mohr-Coulomb's theory are used (Knappett

& Craig, 2012). Both active or passive earth pressure can be dominant depending on the wall movement. Depending on the groundwater level, hydrostatic pressure can also affect the sheet pile and in those cases the interlocks must be tight to prevent water from entering the excavation. Sheet pile walls can either be floating in the soil or driven to the surface of underlying bedrock. To counteract the risk of sliding against the bedrock, sheet piles can be anchored into the bedrock to transfer lateral force.

To determine the proper driving method for sheet piles, analysis of soil type, environmental constraints, and accessibility needs to be performed (Piling, 2022) For the safety of operatives and minimal environmental disturbance, the choice of driving system is of great importance. The three basic driving methods are impact driving, vibro-driving, and press-in piling. Roughly described, impact driving can be loud and take longer time than other methods, therefore, it is not preferred in sensitive areas. Vibro-driving, on the other hand, is not as noisy, and press-in piling is considered silent and is the most effective method in sensitive areas.

It is of great importance to consider the correct standards and guidelines when designing and executing sheet pile systems and other geotechnical designs. The structural design of steel piles is regulated by Eurocode 3 (EN 1993-5) and geotechnical design principles are regulated by Eurocode 7 (EN 1997-1).

2.2.1 Failure mechanisms for sheet piles

To determine the dimensions of sheet piles, the acting earth pressures need to be established in order to understand the vertical, lateral and rotational vulnerabilities. The failure mechanism occurring for sheet piles are mainly overturning, overstresses, general stability and bottom heave (SS-EN 1997-1:2005). To counteract the failure envelopes, different stabilizing methods can be used. Anchors and struts are used in different combinations, depending on what conditions that prevail on the site and where the stability needs to be reinforced. One large disadvantage of the usage of struts is the occupation of space within the excavation, and is not a suitable option for projects in which the construction is located in areas with limited space.

In projects with shallow depths to bedrock, lack of passive earth pressure resistance can contribute to the need to anchor the lower part of the sheet pile, in order to prevent general stability failure (SS-EN 1997-1:2005). Common measures include ground anchors to ensure that the structure can sustain given loads.

2.3 Bedrock anchoring methods

In projects with shallow depths to bedrock, it is common that sheet piles require additional support to stabilize the structure due to the lack of sufficient passive resistance (Knappett & Craig, 2012). For extra lateral support, sheet piles are typically anchored to the bedrock.

2.3.1 Rock dowels

Rock dowels is a commonly used method to support sheet piles with insufficient passive resistance, by anchoring the dowels into the underlaying bedrock as illustrated in Figure 2.5 (Knappett & Craig, 2012). This method involves installing steel bars (dowels) either through casings that are welded onto the excavation side of the sheet piles or through pre-drilled installation tubes, as illustrated in Figure 2.5. The welded casings ensure a more precise connection between the sheet pile and the casing though it is more time demanding than the pre-drilled tubes. Rock dowels ensure a connection between the toe of the sheet pile and the bedrock by bridging the gap referred to as b in Figure 2.6. The primary purpose of these rock dowels is to transfer lateral forces from the sheet pile wall to the bedrock, thus increasing stability and preventing movement at the toe.

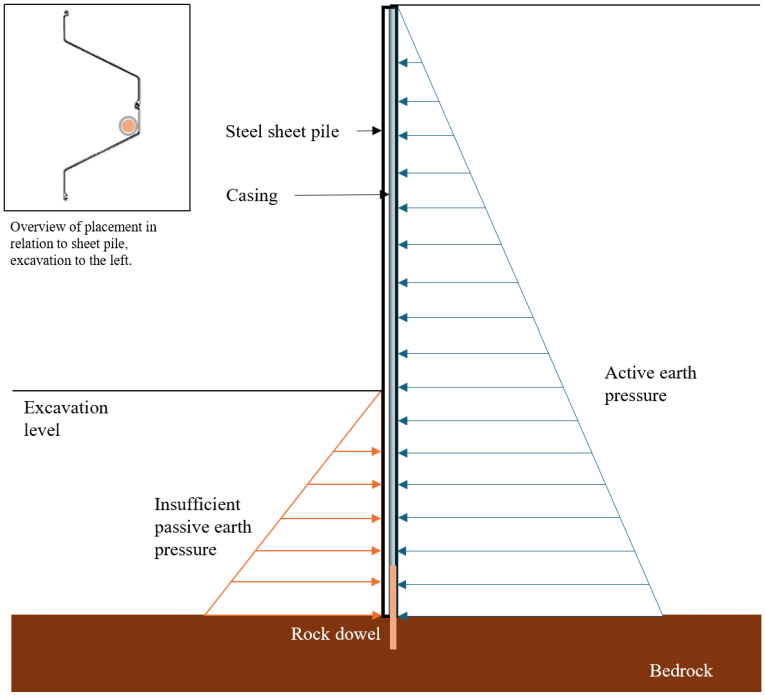

Figure 2.5: Illustration of a conceptual design for a sheet pile wall with a rock dowel used in an excavation support system.

2.3.1.1 Design and capacity

Shear force and bending moment are two important parameters when dimensioning a retaining structure using rock dowels as bedrock anchoring support(Knappett & Craig, 2012). The shear force for each dowel is calculated using the lateral load at the toe of the wall and the spacing between the dowels. The dowel must be dimensioned for the bending moment caused if there is a existing gap b shown in Figure 2.6. And the calculation is also affected by the dowel being grouted or not into the bedrock(Fredriksson et al., 2024). The capacity of the dowel is then calculated following the steps below.

According to (Fredriksson et al., 2024) each dowel must satisfy the following condition to ensure sufficient bending resistance : $M_{\mathrm{Ed}} \leq M_{\mathrm{Rd}}$

Where M_{Ed} is the bending moment capacity and M_{Rd} is the design moment capacity.

The normal load of each dowel N_{Ed} is calculated using:

$$N_{\mathrm{Ed}} = q_{h,\mathrm{dubb}} \cdot c \tag{2.14}$$

Where $q_{h,\mathrm{dubb}}$ is the governing lateral load of each dowel and c is the distance between the dowels.

To calculate the bending moment capacity under the circumstances where the dowel is grouted into bedrock:

$$M_{\mathrm{Ed}} = N_{\mathrm{Ed}} \cdot d \tag{2.15}$$

Where $d = b(from\ 2.6) + 0.06m$, and if the casing is pre-welded and the dowels are grouted $d = (b(sheetpile - bedrock) + 0.06m)/2$

$$M_{\mathrm{Rd}} = \frac{W_{\mathrm{pl}} \cdot f_y}{\gamma_{\mathrm{M0}}} \tag{2.16}$$

Where W_{pl} is the dowels' plastic section modulus of the dowel and f_y is the dowel material's yield strength.

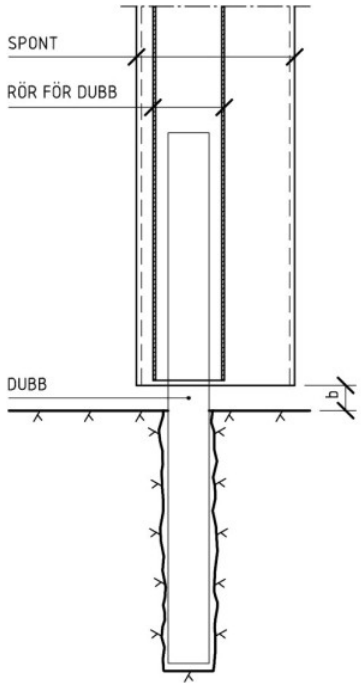

Figure 2.6: Conceptual model of rock dowel inspired by Figure 7-23 in (Fredriksson et al., 2024)

Rock dowels are dimensioned to resist bending moments if there is space between the sheet pile and the bedrock, see distance b in Figure 2.6, ensuring that lateral loads are effectively transferred (Knappett & Craig, 2012). However, a common issue encountered in construction projects is that the gap between the sheet pile and the bedrock often exceeds the designed maximum distance, reducing the effectiveness of the dowels (Eriksson, 2025). This phenomenon is most common if the bedrock surface is steeply sloping. In some projects where the distance b exceeds the designed maximum,one method to strengthen the construction further is to drill a pile close to the installation tube.

2.3.2 Drilled piles

Drilled steel pipe piles, commonly referred to as *drilled piles* or in some cases *RD piles* (shown in Figure 2.7), are widely used structural elements in geotechnical engineering due to their high strength, durability, and versatility (Piling, 2022). The use of drilled piles began to evolve in the 1970s, particularly in Finland, and the demand in Sweden has increased in recent decades (Bredenberg et al., 2010). Until recently, there were no specific Swedish regulations governing their use, indicating that large-scale adoption is still relatively new in Sweden and did not begin until the early 2000s.

The piles are typically manufactured from high-strength steel and standard dimensions for drilled steel pipe piles range from 100 mm to 800 mm in outer diameter, with wall thicknesses between 5 mm and 16 mm (Bredenberg et al., 2010) and according to one manufacturer (SSAB AB, 2025) larger piles can reach diameters up to 1200 mm. Unlike traditional steel core piles, drilled piles function as the primary load-bearing element (Bredenberg et al., 2010). They can support struc-

tures on their own, but in cases where increased capacity is needed, the pipe may be filled with concrete and, in some cases, reinforced with rebar .

The installation method of drilled piles is, as given by their name, by drilling a steel pipe down to load-bearing bedrock (Bredenberg et al., 2010). The installation method differs from driven piles in that drilling causes significantly less vibration, noise and soil disturbance, making it a less invasive alternative. Because of this, these piles are known for their minimal environmental impact during installation and are particularly effective in demanding ground conditions. This characteristic makes them suitable for modern construction projects in densely built areas requiring high-performance foundation solutions.

The drilled piles are effective elements supporting both vertical and horizontal loads in soil, making them suitable in several geotechnical applications like building foundations and retaining walls (SSAB Europe Oy, 2024). Further, in areas with soft soil or with shallow depth to bedrock, drilled piles are considered ideal.

Figure 2.7: Picture taken on-site of drilled piles used at the Sahlgrenska life project. Own image.

In projects with insufficient anchoring support due to the exceeded maximum distance b, drilled piles have shown to be an efficient way to strengthen the connection between the sheet piles and bedrock. Because of the drilled piles' capability to anchor the sheet piles to bedrock, it is today not unfamiliar to use the piles as a first choice rather than a complementary option. In Figure 2.8 a conceptual model is illustrated, showing the placement of the drilled pile in relation to the sheet pile.

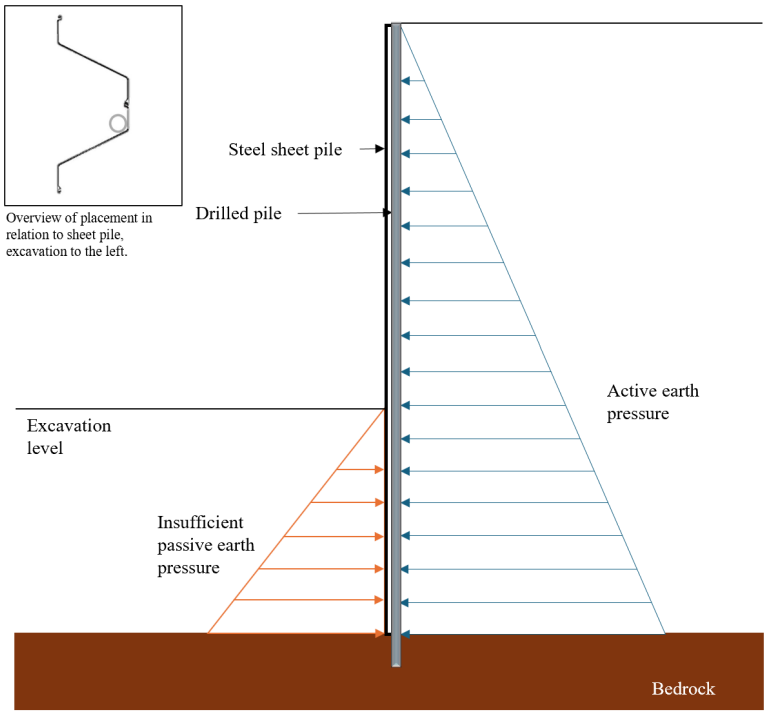

Figure 2.8: Conceptual model of drilled pile used as rock anchoring support for a sheet pile wall.

The relevant mechanical properties of drilled piles making them suitable as replacements for tension-resisting elements like rock dowels are, among others, the high axial load capacity in both tension and compression, as well as meaningful bending stiffness. Frictional resistance determines the load transfer mechanism between the drilled pile and surrounding soil or rock (Knappett & Craig, 2012).

Mathias Matsman mentioned in our interview that the drilled piles are more expensive but also more time-efficient than rock dowels (Matsman, 2025). Further, he highlights the advantage of drilled piles and their improved control over depth, and that in the worst of cases, the piles can be filled with a rock dowel to strengthen the construction.

2.4 Project details

The project area Sahlgrenska Life is located in Gothenburgs district Änggården, involving both demolition and new construction phases. An overview of the site layout, including all building names and the location of relevant cross-sections, is presented in Figure 2.9, where sections S7, S8 and S10 are also highlighted. The

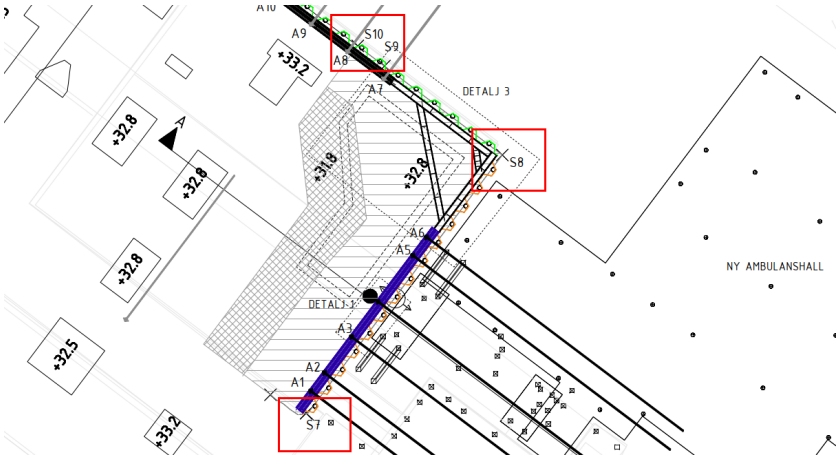

Figure 2.9: Plan view of the placements of the sheet pile, drilled piles and relevant sections. Taken from designs created by J. Pomery at WSP (2024).

demolition phase of the Sahlgrenska Life project required a thorough analysis of potential impacts on the surrounding structures. In order to construct new buildings with appropriate foundations and basement levels in level with the existing structures, the excavation must reach several meters below the current ground surface. Figure 2.10 shows the implemented retaining structure on site.

Figure 2.10: Picture taken on site of the area of interest at project Sahlgrenska life. Own image.

The existing ground elevation within the area ranges from approximately +37.5 m to +38.5 m along the sheet pile alignment, which is designed to protect the new ambulance hall and nearby infrastructure from ground movements. The excavation level varies between approximately +34 m and +32 m, depending on the location, while the depth to bedrock ranges significantly—from as shallow as 3 m to as deep as 13.8 m, this is seen in Figure 2.11.

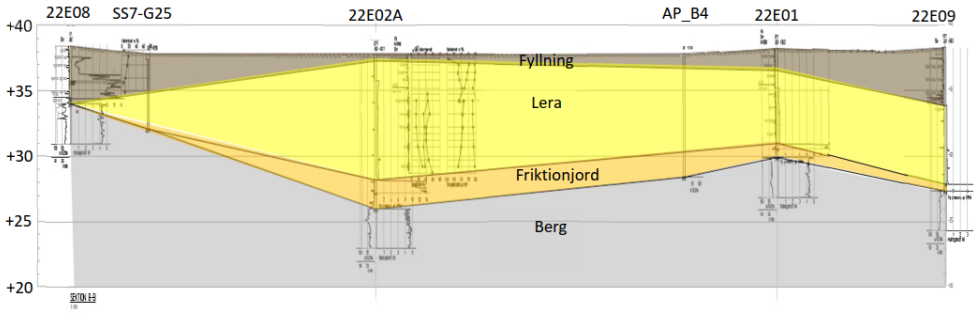

Figure 2.11: Elevation of soil profile determined from CPT evaluation (Pomery & Flyckt, 2024)

Due to these large variations in soil depth and soil stratigraphy, critical sections were selected along the sheet pile wall to represent the different earth pressures acting on the retaining structures. In these sections, the drilled pile method was chosen for bedrock anchoring, as the short distance to rock contributes to an insufficient passive earth pressure, hence requiring a support for failure at the toe of the sheet pile. The traffic and construction load are 10, 20, and 30 kN/m/m for section 7, 8 and 10 respectively.

A geotechnical investigation report was executed by ELU konsult AB which was used for analysis and establishment of the soil profile and its properties. The soil profiles general composition consists of a top layer of fill that ranges between 0.2-4.5 m depth, followed by a thin layer dry-crust-clay (torrskorpelera) of 0.5-1.7 m. Beneath the dry crust, a clay layer of approximately 1 m is found which transitions to a layered silty clay layer with a depth of up to 11 m.

The soil profiles for the three sections analyzed both analytically and numerically are as seen in Figure 2.12. The layers are composed of backfill-material with properties like frictional soils.

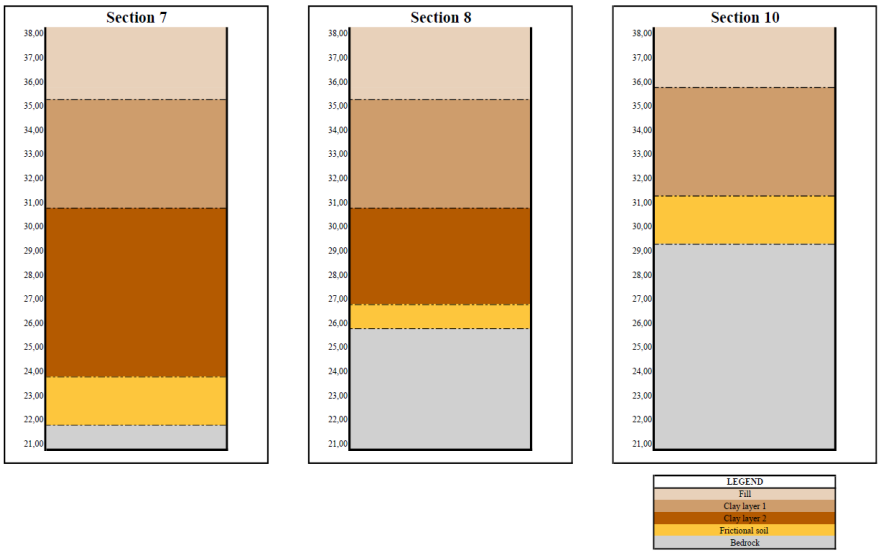

Figure 2.12: Soil profile for critical sections S7, S8 and S10. Chosen for numerical and analytical analysis.

3

Calculation methods

3.1 Numerical calculations

In order to model and simulate deformations of both drilled pile and sheet piles, PLAXIS 2D was used. The program, which is developed by Bentley Systems, is based on the finite element method, which defines the area of analysis in a mesh, allowing different reactions and behaviors to be calculated for each separate element. The aim of the software is to allow numerical analyses for geotechnical engineers, which does not require a deep understanding of numerical computation.

Numerical calculations were performed for the variations in vertical gaps between the bottom of the sheet pile wall and the bedrock level b_1, as well as for lateral gaps between the bottom of the sheet pile wall and the drilled pile b_2 as visualized in Figure 3.1. Distance named b_3 is the unknown interaction distance between the drilled pile and the sheet pile.

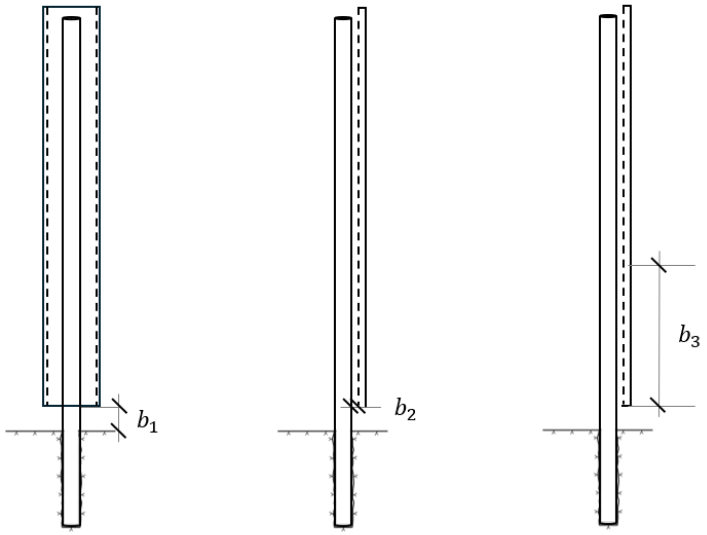

Figure 3.1: Conceptual model of the type of gaps/distances analyzed. For better visualization the model to the left is presented in front view and the model in the middle and to the right is presented in side view.

3.1.1 Soil layers

The primary step of establishing the model was to set up the geometry of the soil layers to be representative of the data gathered for the different critical sections. As described in section 2.4, the soil layers are composed of a layer of fill, two different types of clay, a frictional soil layer and lastly bedrock. The input data for clay soils can be seen in Table 3.1, with full input data found in Appendix A. The program allows for different soil behavior models, however, according to

Swedish standards, the Mohr-Coulomb failure criterion was applied for all soil layers, undrained conditions for the clay layers whereas the frictional soil layers were modeled as drained layers.

Table 3.1: Summary of input data relevant for soil layers, full input data for PLAXIS is found in Appendix A

Soil layer	Material parameter	Characteristic value
Fill	Unit weight γ_{unsat}	21 kN/m3
	Sat. unit weight γ_{sat}	11 kN/m3
	Friction angle ϕ'	35°
	Young's modulus E	20 MPa
Clay layer 1	Unit weight γ_{unsat}	17,7 kN/m3
	Sat. unit weight γ_{sat}	7,7 kN/m3
	Undrianed shear strength c_u	16,5 kPa
	Friction angle ϕ'	30°
	Young's modulus E	4,15 MPa
Clay layer 2	Unit weight γ_{unsat}	18,5 kN/m3
	Sat. unit weight γ_{sat}	8,5 kN/m3
	Undrained shear strength c_u	16,5 + 1*z1** kPa
	Friction angle ϕ'	30°
	Young's modulus E	250 x Cu MPa
Frictional soil	Unit weight γ_{unsat}	19 kN/m3*
	Sat. unit weight γ_{sat}	11 kN/m3*
	Friction angleϕ'	35°
	Young's modulus E	15 MPa*
Bedrock	Unit weight γ_{unsat}	22 kN/m3
	Sat. unit weight γ_{sat}	22 §kN/m3
	Young's modulus E	$2{\cdot}10^4$ MPa

* Empirical value from TRVINFRA-00230
**z_1 is the depth from elevation +31.0 m
** According to TRVINFRA-00230, the modulus of elasticity can be assumed to be $250 \cdot c_u$ for highly plastic clays

The bedrock parameters differ from the frictional soils as well as the clay soils as it is modeled as a Hoek-Brown, parameters as shown in Table found in Appendix A. This is to replicate the behavior between the structures and the bedrock as close to reality as possible. The stiffness of the bedrock is relatively high at 2,4*10^7 k/Nm^2, this is due to the assumption that the failure occurs in the soil first rather than in the bedrock. This can be be confirmed by adjusting the drilled depth of the drilled pile to reach a level where this assumption applies.

3.1.2 Structural elements

The following step was to model the structural components which consisted of a strip load, anchors, sheet pile walls and the drilled piles. The load was placed 1 m from the sheet pile wall, and measures 10, 20 and 30 kN/m/m for the sections 7, 8, and 10 respectively, representing the surface loads from traffic and equipment needed for installation of the retaining structures and executions of the excavations. The retaining wall was modeled as a plate structure, with a varying material assigned to the plate between the sections, depending on what sheet pile that was designed by WSP for the sections.

Common modeling assumptions were the following:

- Strength reduction activated.
- Fixed displacement in x-direction and free displacements for y-directions.
- Positive and negative interfaces to realistically simulate the interaction between the soil and the sheet pile.

All three sections are modeled with a waling beam, including a top anchor for section 7 and 8. The design parameters for these are taken from the calculations made by WSP, that follow standard, conventional design methods based on Eurocodes and Swedish guidelines (Pomery & Flyckt, 2024).

The sheet pile was assumed to have no gap initially between the toe of the sheet pile and the bedrock vertically. The placement of the drilled pile in relation to the sheet pile had a starting point of 0.05 m from the sheet pile horizontally, this was due to installation process disabling a non-existent gap.

3.1.2.1 Modeling of drilled pile

Due to one of the limitations which is that the analysis is only done in 2D, the modeling of the drilled pile was adjusted to represent the behavior of the bedrock anchors as close to reality as possible. This was achieved by treating the drilled piles as a cooperating group and modeling them as a continuous plate element. By assuming that each pile contributes linearly over the determined spacing, an equivalent plate could be calculated to represent the structural effect of the drilled piles on the sheet pile wall.

To define the plate in PLAXIS, the required material parameters included the unit weight w, axial stiffness EA, bending stiffness EI, and Poisson's ratio ν. These values were then converted into equivalent plate properties using Equations 3.1 ,3.2, and 3.3, taking into account the distance between each pile ($l_{spacing}$) .

$$w = \frac{m * g}{l_{spacing}} \tag{3.1}$$

$$EA' = \frac{EA_{pile}}{l_{spacing}} \tag{3.2}$$

$$EI' = \frac{EI_{pile}}{l_{spacing}} \tag{3.3}$$

The Poisson's ratio for steel was taken as 0.3. A summary of all input parameters used for the equivalent plate modeling of the drilled pile is presented in Table 3.2.

Table 3.2: Equivalent plate properties for drilled pile (S460, ∅273 mm, $t = 10$ mm)

Property	**Value**	**Unit**
Material type	Elastic	–
Colour	RGB (199, 82, 143)	–
Unit weight w	0.4548	kN/m/m
Diameter D	0.27	m
Thickness t	0.01	m
EA′	$1.24 \cdot 10^6$	kN/m
EI′	$1.07 \cdot 10^4$	kNm^2/m
Young's modulus E	$2.10 \cdot 10^8$	kN/m^2
Poisson's ratio ν	0.3	–

3.1.3 Mesh and flow conditions

In order to achieve accurate and stable numerical results, a very fine mesh was used in the analysis. The mesh quality was ensured by maintaining a minimum mesh quality requirement greater than 0.35, which allowed for improved resolution of stress and strain concentrations near and in between the structural elements, as well as more accurate groundwater flow simulations.

For flow and pore pressure conditions, the *Global water level* setting was applied during the stages before final excavation level, ensuring consistent hydraulic boundary conditions throughout the early phases of the simulation. From the first final excavation level, the *Interpolate pore pressures* option was applied in the first layer of the excavation side in order to provide a more realistic transition in pore pressure conditions between stages.

3.1.4 Staged construction

The staged construction was modeled using PLAXIS phase function and were determined to simulate realistic sequence of excavation and support installation. The following phases were defined in the model:

- **Initial Phase**: Earth pressure at rest K0 and initial pore pressure distribution.
- **Phase 1**: Installation of the sheet pile wall and drilled pile.
- **Phase 2**: Excavation down to the first support level
- **Phase 3**: Installation of first level support (tie rod/wailing beam).
- **Phase 4**: Further excavation down to final excavation level.
- **Phase 5**: Strength reduction analysis for phase 4 (phi-c reduction).
- **Phase 6**: Excavation to final depth with no surface load applied.
- **Phase 7**: Strength reduction analysis for phase 6 (phi-c reduction).

This sequence was designed to reflect the actual construction process and to eval-

uate both supported and unsupported stability conditions through the use of *phi-c reduction* analyses. However, for the evaluation and analysis of data between the varying measurements of b_1 and b_2, the values for phase 4 were determined most critical and therefore the basis of comparison. Figure 3.2 shows the model of section 7.

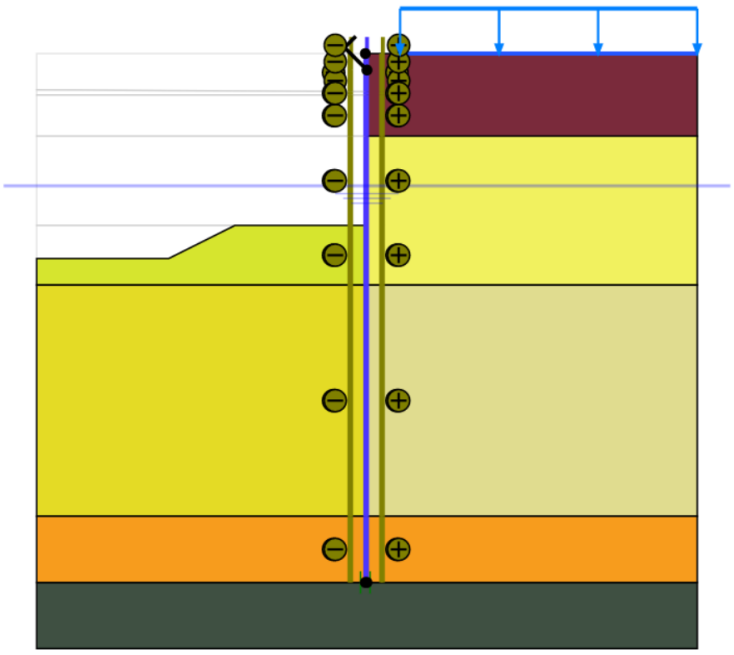

Figure 3.2: PLAXIS model for section 7.

3.1.5 PLAXIS output

After the generation of the models, data was extracted from PLAXIS output. The relevant data that were extracted from each section were the total and phase displacements, shear forces and bending moments for both the drilled pile and the sheet pile, as well as earth pressures from the initial phase.

To enable further analysis, data were also extracted for iterations where different displacements conditions were modeled. The variations of toe modeling where the following:

- x_{fixed}, y_{free}
- x_{fixed}, y_{fixed}
- x_{free}, y_{free}
- SP_{fixed}

The model with the x_{free}, y_{free} displacement condition was restricted by the bedrock, as the drilled pile was modeled to end 0.5 m beneath the top of the bedrock level. SP_{fixed} is the model which simulated the sheet pile behaving as fixed, as is described in the conventional guidelines (Fredriksson et al., 2024). The forces from the output were extracted and calculated for the drilled pile using the method for rock dowels, as seen in the equations described in Chapter 2.3.

3.2 Analytical calculations

Analytical calculations were carried out to estimate the active and passive earth pressures acting on the sheet pile wall for serviceability limit state conditions (SLS). In the SLS case, no partial safety factors are applied, meaning that the calculations are based solely on characteristic values of the obtained soil parameters and loads.

3.2.1 Input parameters and soil profile

The input data used in the calculations are based on the site conditions and geotechnical parameters described in previous chapters. The soil layers for each section have been modeled to reflect the variation in unit weight (γ), effective friction angle (ϕ'), and cohesion properties. These parameters are critical in determining the distribution of earth pressure along the wall.

The analyzed sections include:

- **Section S7**: 16 meters to bedrock, excavation depth at +34m
- **Section S8**: 11.8 meters to bedrock, excavation depth at +32m
- **Section S10**: 8 meters to bedrock, excavation depth at +32m

These sections were selected due to their varying depth to bedrock and representative soil layering, which influence the magnitude and distribution of earth pressure.

3.2.2 Earth pressure coefficients and net pressure

The earth pressure calculations are based on classic earth pressure theory. The active and passive earth pressure coefficients (K_a and K_p) were calculated from the effective friction angle ϕ' according to Rankine's theory:

$$K_a = \frac{1 - sin\phi'}{1 + sin\phi'} \tag{3.4}$$

$$K_p = \frac{1 + sin\phi'}{1 - sin\phi'} \tag{3.5}$$

Using these coefficients, the net lateral earth pressure (p_{net}) is calculated as the difference between the active (p_a) and passive (p_p) earth pressures:

$$p_{\text{net}} = p_a - p_p \tag{3.6}$$

For clay layers, simplifications of Equations in chapter 2.1.4 results in the following Equations 3.7 and 3.8.

$$p_a = \sigma - 2c_u \tag{3.7}$$

$$p_p = \sigma + 2c_u \tag{3.8}$$

Similar a simplifications were made for the layers with frictional soils, resulting in Equation 3.9 and 3.10

$$p_a = K_a * \sigma' + u \tag{3.9}$$

$$p_p = K_p * \sigma' + u \tag{3.10}$$

This net pressure is used as the basis for evaluating the forces acting on the retaining structure.

3.2.3 Distribution of net earth pressure

The net earth pressure was calculated along the full embedded depth of the sheet pile and was assumed to be evenly distributed. This assumption simplified the results and enabled a general analysis of the effects of the distances b_1, b_2 and b_3. By simplifying to a constant net pressure distribution, a simplified correlation was developed to compare the stresses from the earth pressure σ_i to the forces analyzed numerically. This relationship is later used to confirm and conclude how the development of forces relates to the magnitude of the earth pressures.

4

Results and Analysis

4.1 Numerical results

The numerical simulations made by the FEM program PLAXIS 2D were simulated for the variations in geometrical parameters b_1 (vertical distance from sheet pile to bedrock) and b_2 (lateral distance from the toe of the drilled pile to the sheet pile). The results were later extracted as tables from PLAXIS output and illustrated in Microsoft Excel.

4.1.1 Variations in b_1: S7

The most relevant parameters to visualize and compile were determined to be total displacements, shear forces and bending moments for both the sheet pile wall and the drilled pile. The distances analyzed for b_1 are most relevant for 0,1-0,8 m, however, more extreme scenarios were simulated, in order to draw comprehensive conclusions regarding the behavior of the drilled pile. The extreme scenarios were b_1 distances of 1,2 m and 1,6 m.

4.1.1.1 Total displacements

For section S7, the level at which the parameter b_3 was identified at approximately +32 m as shown in Figure 4.1. This level was consistent across both the phase and total displacement results in PLAXIS, and did not vary with changes in the parameter b_1. To better understand the behavior below this elevation, the distribution of forces beneath +32 m was analyzed. This analysis aims to evaluate how the net earth pressure is distributed over the lower part of the sheet pile wall and how it contributes to overall system stability through the support from the drilled-pile.

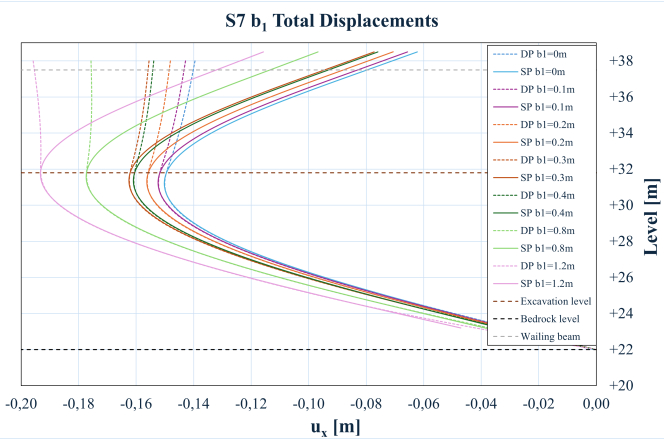

Figure 4.1: Section 7 Total displacement for variations in b_1 for the sheet pile (SP) and drilled pile (DP)

4.1.1.2 Shear force

Figure 4.2 shows that the shear force in the sheet pile was zero at +32 m, indicating a turning point in bending moment. The magnitude of the shear forces in the sheet pile is consistent with a peak at the top and bottom of the sheet pile, with peaks that also increase slightly in magnitude as the distance b_1 increases. A negative peak in shear force was observed in the drilled pile at approximately +32 m which is displayed in Figure 4.3. This indicates that load from the earth pressure acting on the sheet pile is being transferred in correlation to the excavation depth.

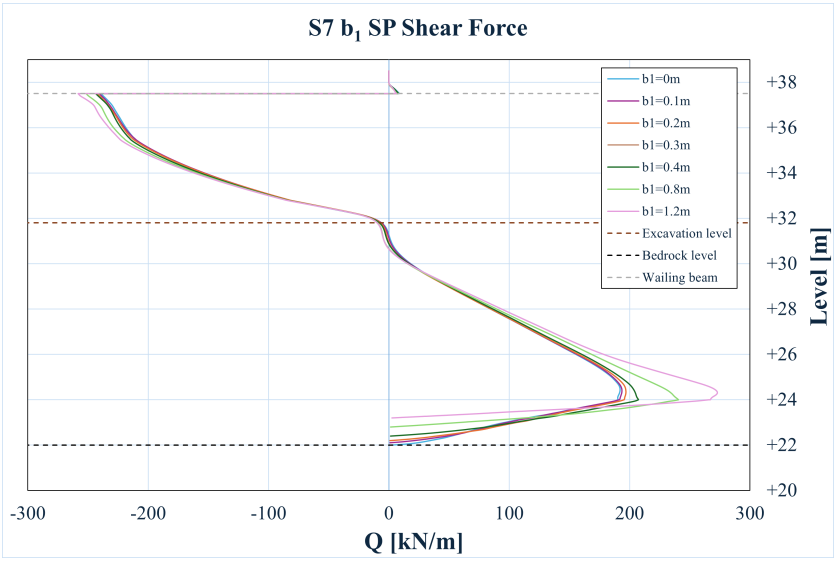

Figure 4.2: Section 7 Shear force in the sheet pile for variations in b_1

The shear force diagram seen in Figure 4.3 shows a positive maximum in shear force for the drilled pile closer to the toe of the sheet pile, however is much harder to interpret as the magnitude of the forces are relatively small.

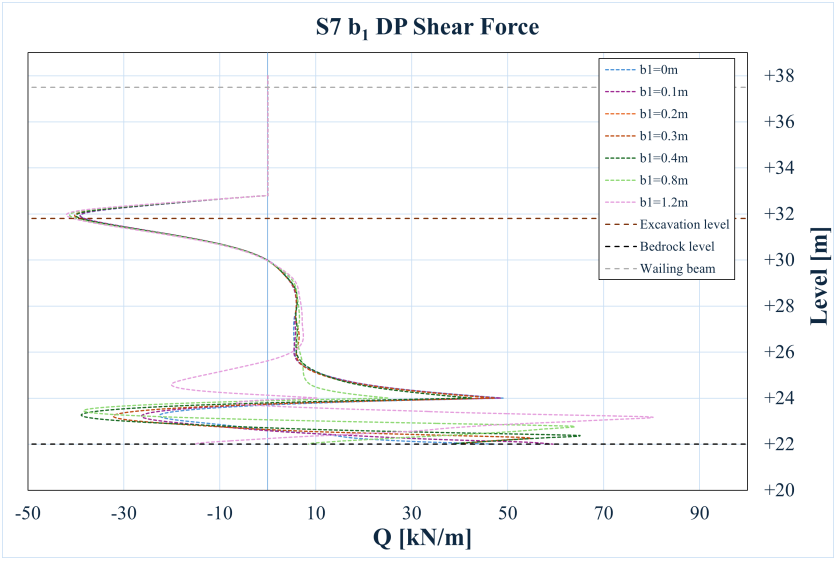

Figure 4.3: Section 7 Shear force in the drilled pile for variations in b_1

4.1.1.3 Bending moment

The sheet pile shows a typical bending moment profile, with the peak moment occurring between +32 and +30,m. This peak marks the largest distance from support levels, therefore generating a maximum structural demand, where the bending resistance is most critical, see Figure 4.4. The bending moment in the drilled pile decreases towards zero around +32 m, as seen in Figure 4.5, corresponding with the transition in shear described above.

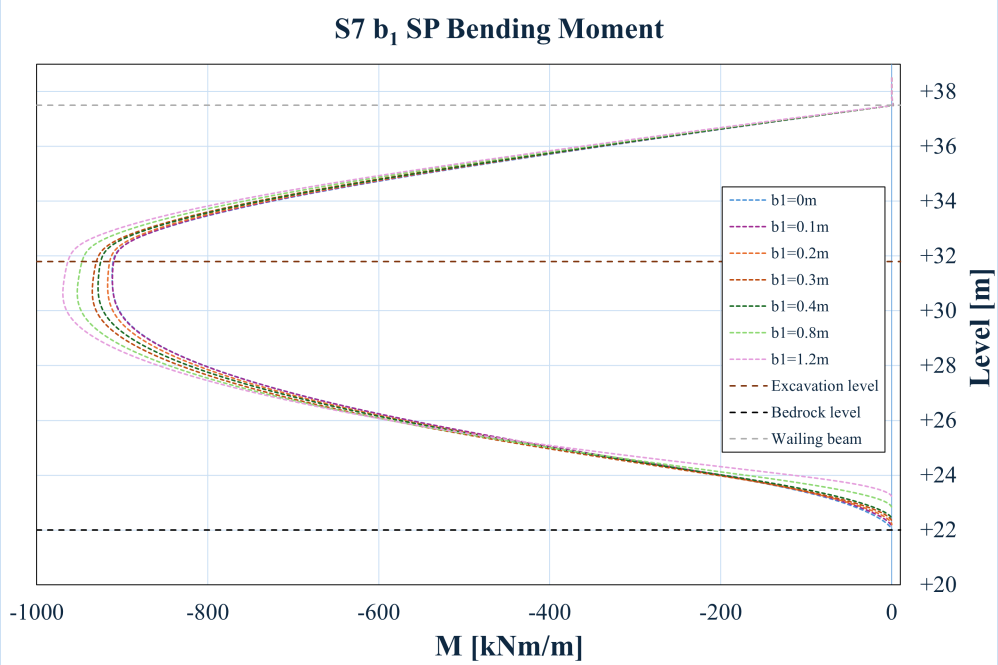

Figure 4.4: Section 7 Bending moment in the sheet pile for variations in b_1

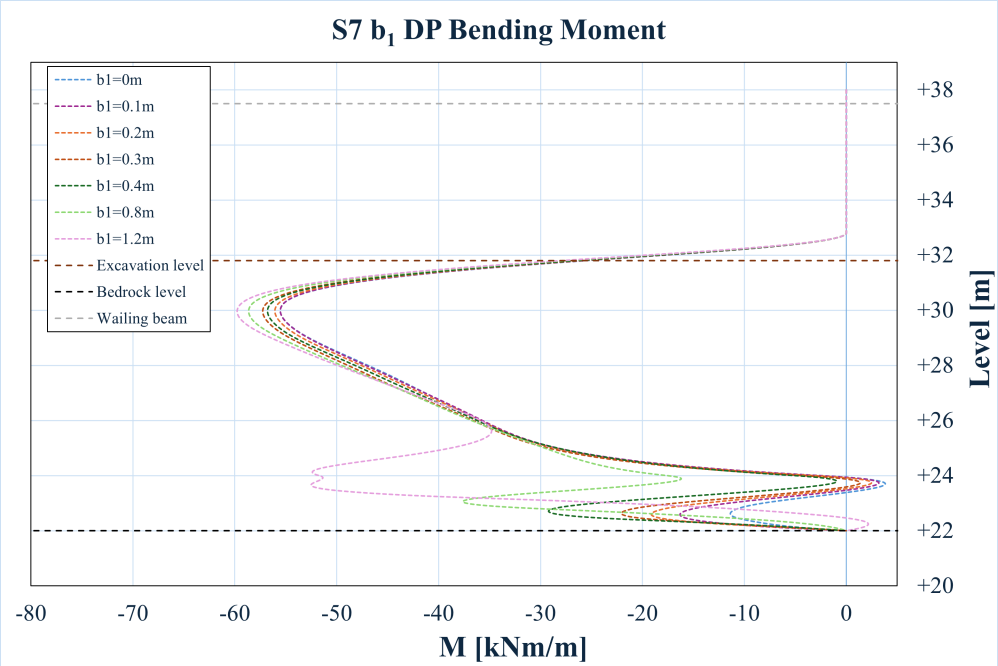

Figure 4.5: Section 7 Bending moment in the drilled pile for variations in b_1

4.1.2 Variations in b_1: S8

4.1.2.1 Total displacements

Following the behavior observed in S7, the interaction between the sheet pile and the drilled pile continues to be approximately +32 m as seen in Figure 4.6, even in this case where the distance to bedrock is significantly shorter. Due to the assumed initial lateral position of $b_2 = 0.05$ m between the drilled pile and the sheet pile, the drilled pile showcases a displacement trend which is directed toward the sheet pile after the interaction stops, showing that the distance decreases for $b_2 > 0.05$ m.

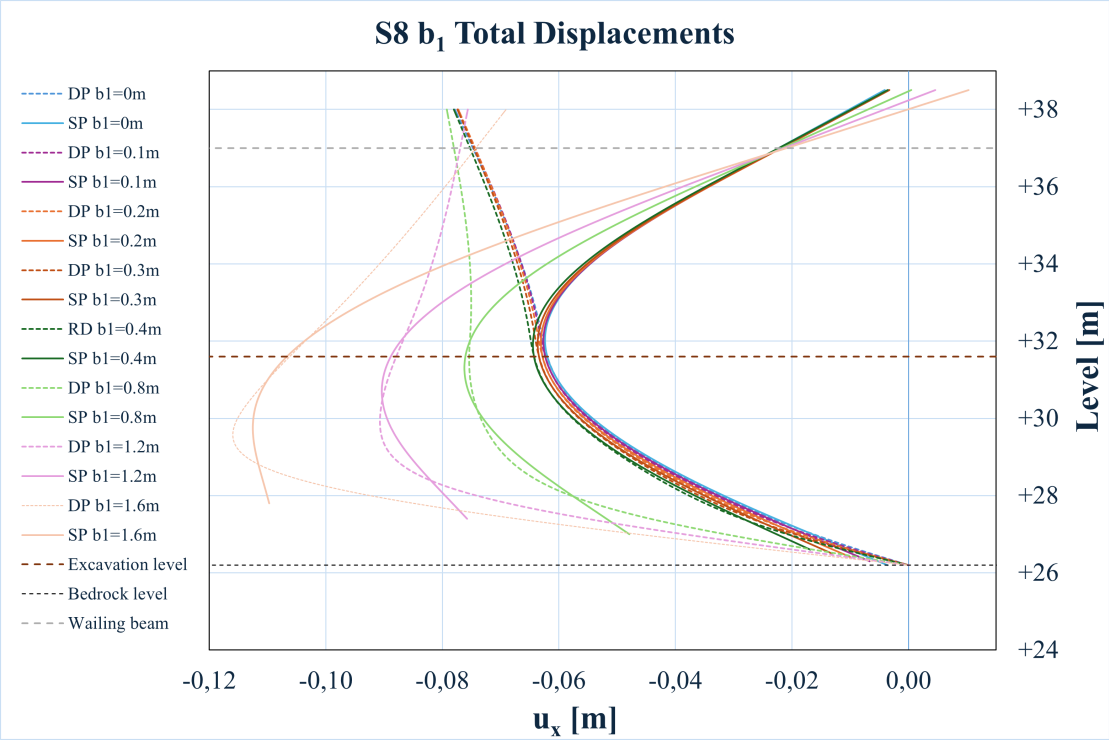

Figure 4.6: Section 8 Total displacement for variations in b_1

4.1.2.2 Shear force

In section S8, the shear force in the sheet pile increases as b_1 increases, as shown in Figure 4.7, which can suggest that the earth pressure acting needs to be distributed across a shorter distance, resulting in an increase in peak shear force. It increases especially toward the toe as the gap b_1 increases, the results are shown in Appendix B.1. An exception is seen for $b_1 = 0.8$ m, where the trend appears to deviate slightly, probably due to local redistribution effects or numerical sensitivity for that iteration. The shear force in the drilled pile reaches its maximum when b_1= 0.1 m, and decreases in magnitude with increasing distance b_1. This is due to a more intense force distribution along the drilled pile from +32 m down to the bedrock in both positive and negative directions.

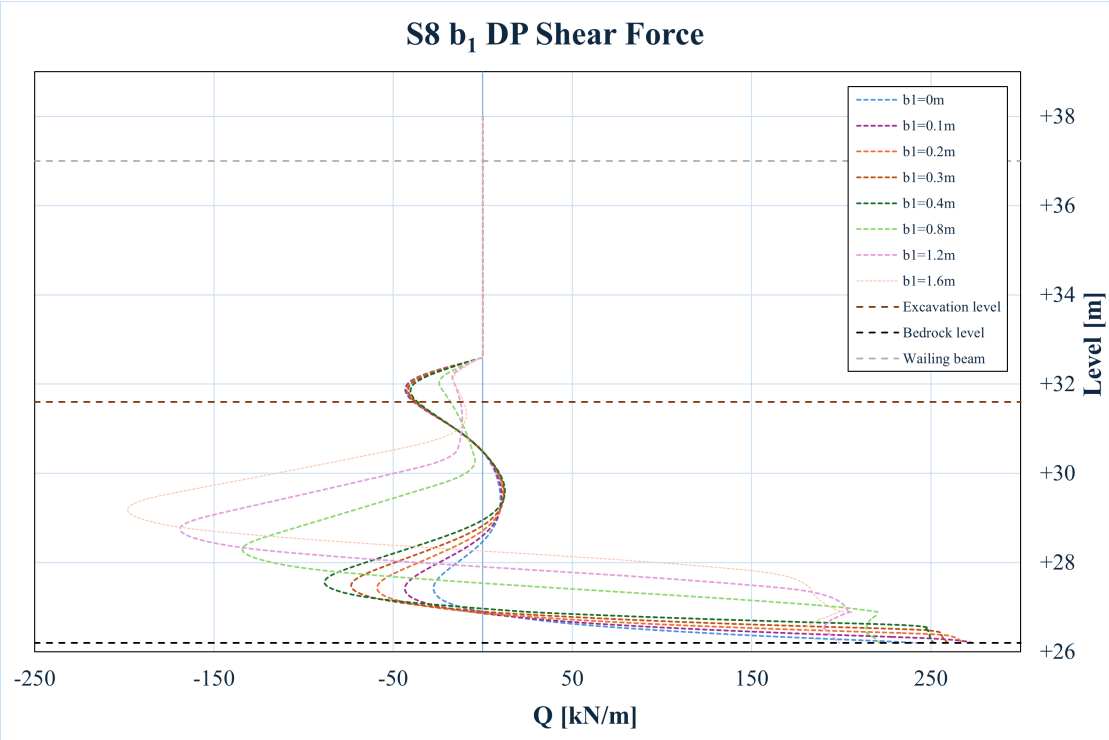

Figure 4.7: Section 8 Shear force in the drilled pile for variations in b_1

4.1.2.3 Bending moment

The results for the bending moment for the sheet pile are found in Appendix B.1, showing a general decreases as b_1 increases, with the exception of the case $b_1 = 0.8$ m, corresponding to the same deviation as seen in the shear force. However, the relative decrease in magnitude is not significantly large in terms of percentage. An intercept point of maximum moment in the drilled-pile for section 8 is a simplification made in order to be able to analyze the reaction of the drilled pile, as a structure which supports the sheet pile at two points. This is done in order for further analysis of the assumed behavior in chapter 4.3, a Figure for the intercept is seen in Appendix B.1.

Overall, peak bending moments in the drilled pile appear to increase in magnitude by increases in b_1, as seen in Figure 4.8. The interpretation of b_3 also increases for $b_1 > 0.4m$, which may not be relevant as the expected b_1 distances are those for $b_1 \leq 0.4m$.

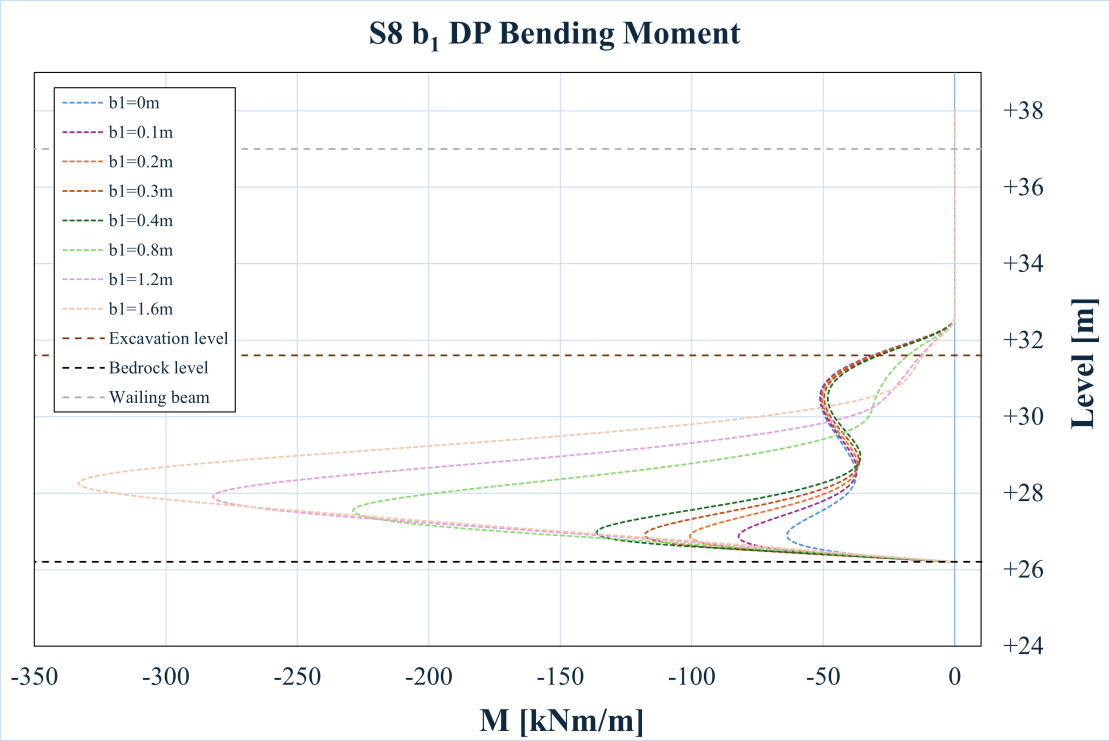

Figure 4.8: Section 8 Bending moment in the drilled pile for variations in b_1

4.1.3 Variations in b_1: S10

The results from section 10 indicate similar response and trends as section 7 and 8 in bending moment and shear force, therefore only the most relevant graphs will be displayed.

4.1.3.1 Shear force

Figure 4.9 show an initial increase in shear force and decrease in $Q_{\max}$ after $b_1 = 0.1\ m$. The negative shear force increases, distributing the force acting on the drilled pile along the length of the pile.

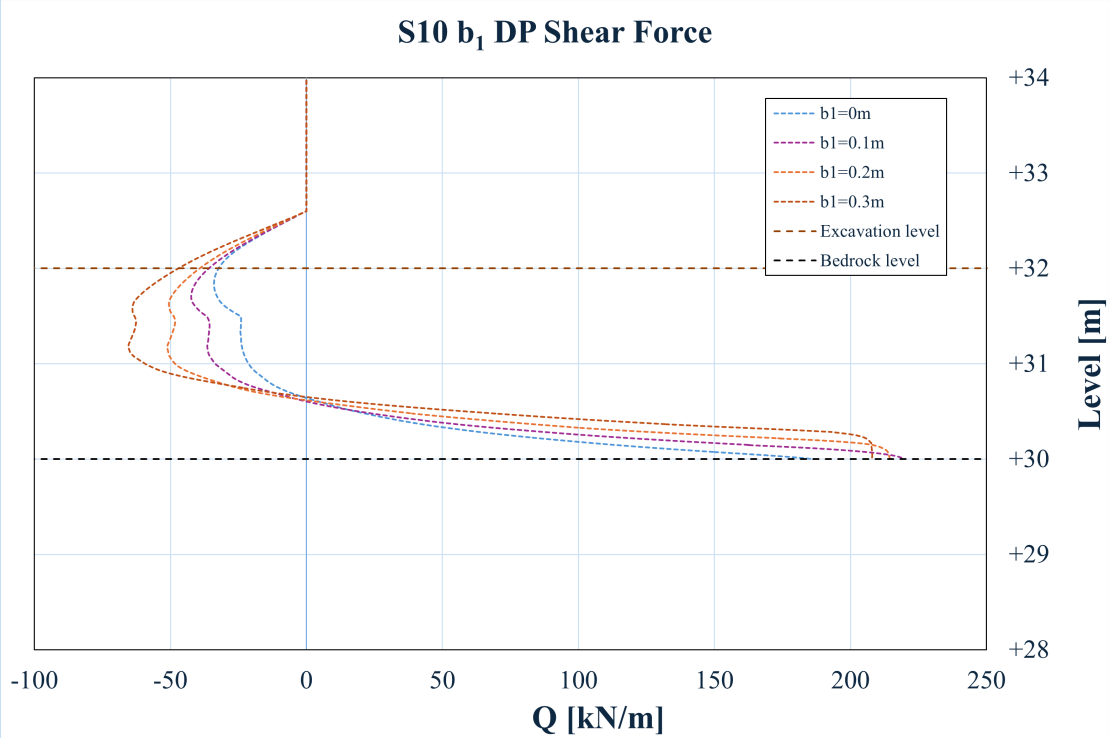

Figure 4.9: Section 10 Shear force in the drilled pile for variations in b_1

4.1.3.2 Bending moment

The bending moment within the drilled pile for section 10 is displayed in Figure 4.10, illustrating an even increase in $M_{\max}$ as the vertical distance b_1 increases.

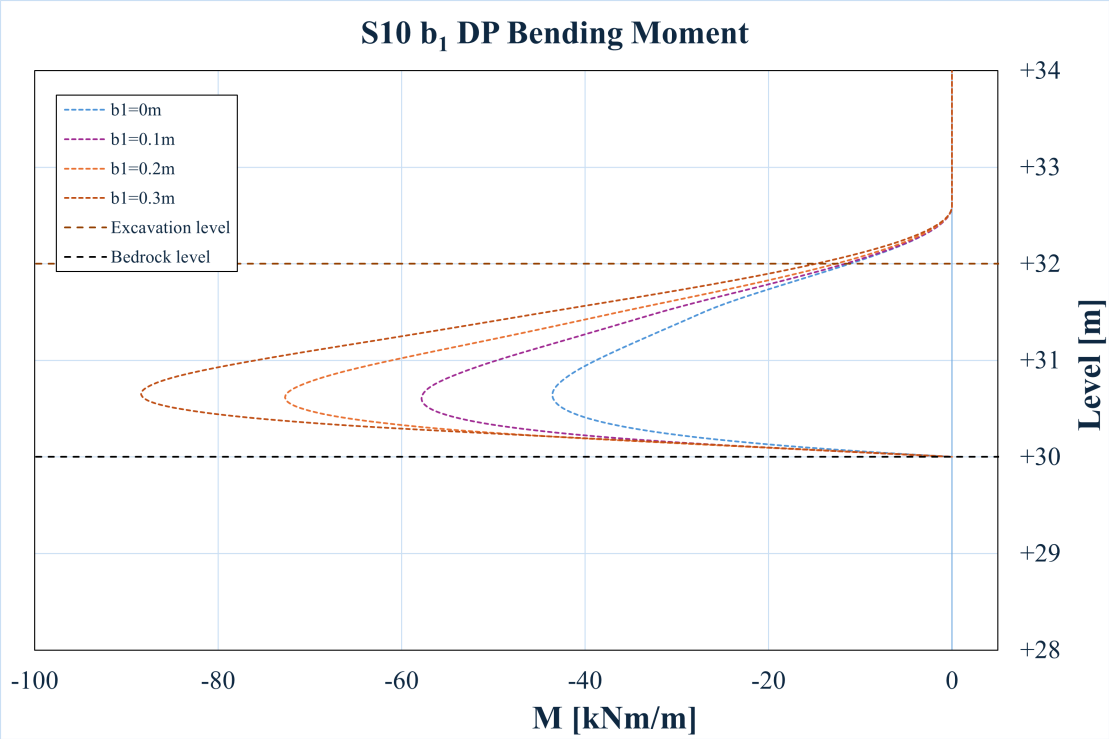

Figure 4.10: Section 10 Bending moment in the drilled pile for variations in b_1

4.1.4 Variations in b_2: S7

Similar to the variations in b_1 the most relevant parameters to investigate and visualize regarding variations i b_2 were phase and total displacement, shear forces and moments for both the sheet pile wall and the drilled pile.

4.1.4.1 Total Displacements

The results from PLAXIS displayed in Appendix B.2 visualized little to no variation when using different values for b_2. The spacing parameter b_3 was equal to the results from the variations in b_1, at approximately +32 meters for all iterations. In terms of total displacement for the drilled pile, the curves are very similar across the different iterations, indicating a stiff system. A small correlation with increasing b_2 is observed. The sheet pile wall shows somewhat greater variation, and for b_2 values greater than 0.35 meters, it is evident that the wall becomes more flexible at the top as the drilled pile is positioned further away.

4.1.4.2 Shear force

The shear force close to the toe of the sheet pile increases along with a larger distance b_2, the results are found in Appendix B.2. A peak shear force of ca 240 kN/m in the sheet pile and 50 kN/m in the drilled pile vary very little with the increases of b_2 in comparison with the variations of the vertical distance b_1. The results for the variations of shear force in the drilled pile are seen in Figure 4.11

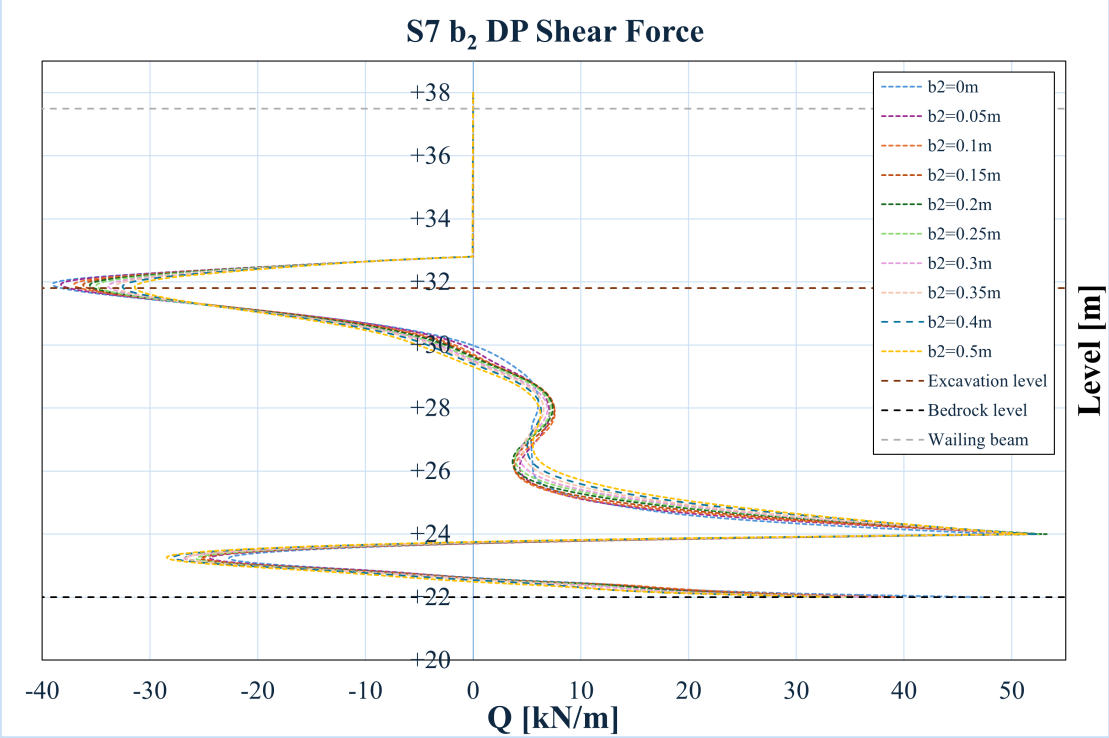

Figure 4.11: Section 7 Shear force in the drilled pile for variations in b_2

4.1.4.3 Bending moment

The result for the sheet pile bending moment showed minimal change in the curve for different values of b_2, see Appendix B.2. Figure 4.12 shows that the bending moment in the drilled pile is very low. However, it can be observed that a maximum negative moment occurs around 30 meters, while a maximum positive moment is found at approximately 23 meters. The curve indicates that the design moment for the drilled pile decreases only slightly. However, there is an increase in the positive moment near the base of the sheet pile wall. Still, the magnitude of this increase is small in relation to the design moment.

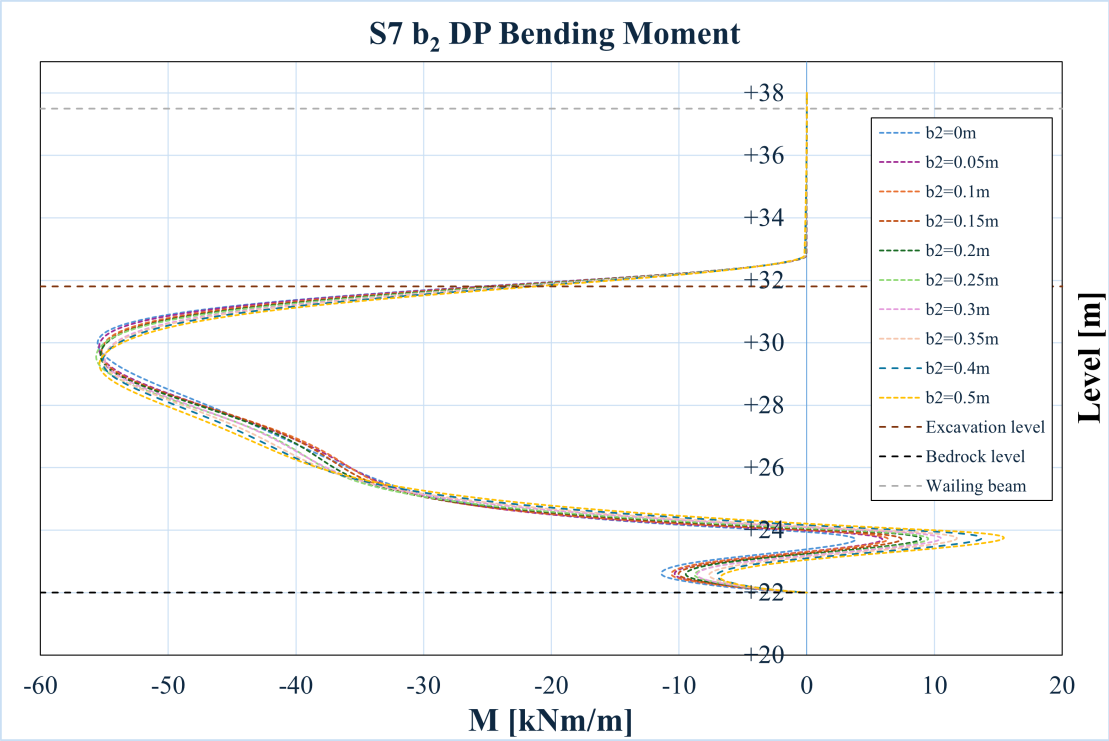

Figure 4.12: Section 7 Bending moment in the drilled pile for variations in b_2

4.1.5 Variations in b_2: S8

4.1.5.1 Total Displacements

As mentioned in Section 7 regarding the variations in b_2, the interaction distances vary only slightly between iterations, results are seen in Appendix B.3. The sheet pile wall and the drilled pile follow the same displacement curve down to approximately +32 meters.

4.1.5.2 Shear force

The shear force in the sheet pile has a decreasing effect as the lateral distance b_2 increases, seen in Appendix B.3. A similar observation can be made for the shear force in the drilled pile, which shows the peak at the joint with the bedrock. Figure 4.13 also illustrates the distribution of forces along the pile, which shows a trend that neutralizes the force in the middle of the interacting distance b_3, although not to a large extent.

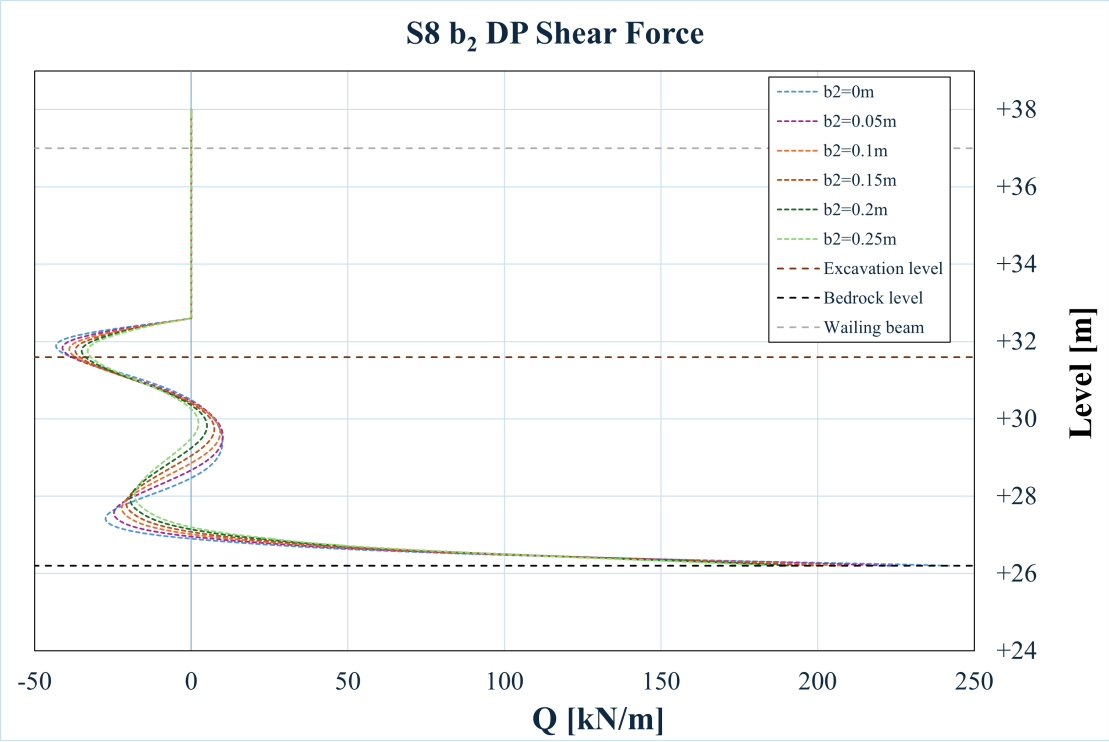

Figure 4.13: Section 8 Shear force in the drilled pile for variations in b_2

4.1.5.3 Bending moment

The visual interpretation of the Figure in Appendix B.3 shows that the bending moment in the sheet pile does not vary with an increase in b_2. This, in contrast to the drilled pile that shows a clear increase in peak bending moment, and a decrease in the first curve occurring at ca +31 m, seen in Figure 4.14. An interpretation of the intercept bending moment can be found in B.3, the trend illustrates a relatively even increase of the distance which the sheet pile appears to correlate with the drilled pile the most.

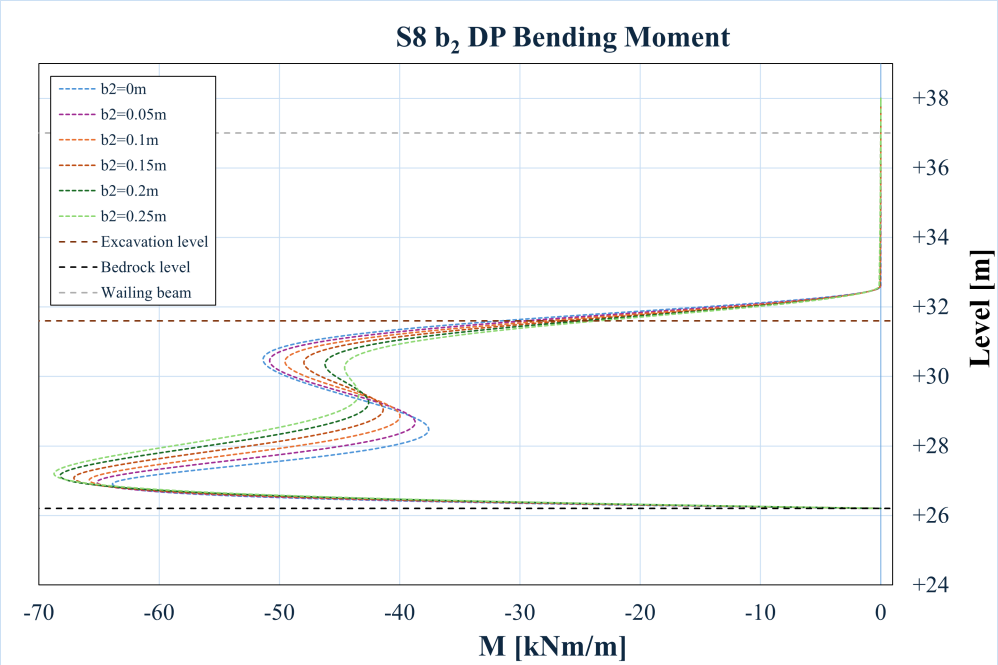

Figure 4.14: Section 8 Bending moment in the drilled pile for variations in b_2

4.2 Analysis of correlation for numerical results

In this chapter, a study of the correlation between the geometrical parameters b_1 and b_2 and their effect of the structural performance for both the drilled pile and the sheet pile in section 7, 8 ad 10 are presented.

The studied parameters are:

- $M_{\max}$: Maximum bending moment [kNm/m]
- $Q_{\max}$: Maximum shear force [kN/m]
- $u_{\max}$: Maximum total displacement [m]

The result is visualized in a set of comparative graphs, showing the impact of b_1 and b_2 individually to identify trends and sensitivities.

4.2.1 Section 7

As seen in Figure 4.15, $M_{\max}$ increases clearly with b_1, especially beyond 0.2 m. The moment peaks around $b_1 = 0.3$ m, indicating a sensitive relationship between vertical gap and bending demand. In contrast, b_2 shows minimal effect, with bending moment variations remaining small across the interval. This suggests that vertical spacing b_1 plays a more critical role than lateral spacing b_2 for moment development in the drilled pile. A similar pattern is observed for $Q_{\max}$. Shear force remains nearly constant up to $b_1 = 0.3$ m but increases with an inclination of ca 7 % per meter. Again, b_2 has limited impact, with only minor changes in shear force, further confirming the dominance of b_1 regarding the impact on the drilled pile.

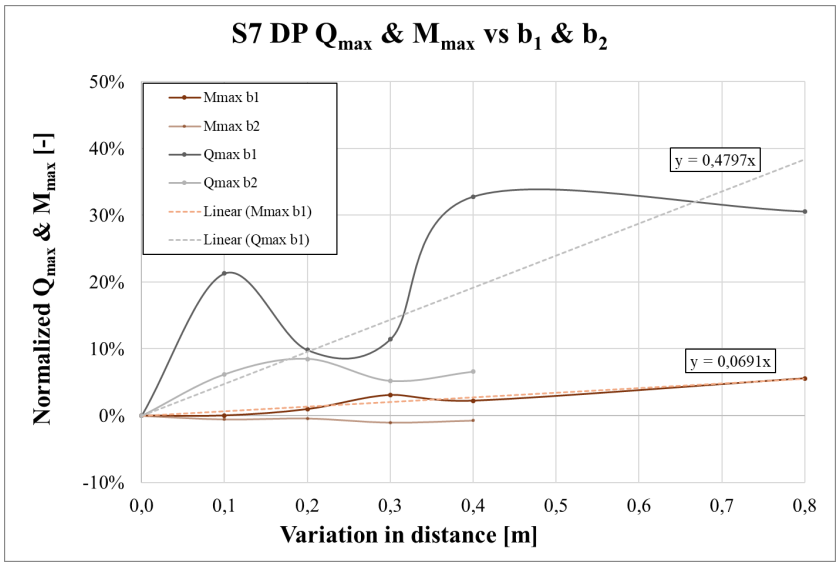

Figure 4.15: Correlations of $M_{\max}$ and $Q_{\max}$ and variations of b_1 and b_2 for the drilled pile in section 7.

In Figure 4.16, the sheet pile shows an increase in $M_{\max}$ with increasing b_1. This confirms a high sensitivity of the sheet pile to vertical spacing. b_2 causes only a slight increase in moment, reaffirming that it has minimal structural influence in

this case. Comparing the gradients of the curve between the drilled pile and the sheet pile shows that the sheet pile is less sensitive to changes in b_1 and b_2. b_2 affects $Q_{\max}$ slightly and non-linearly. There's a small initial drop followed by a slight increase again at $0.4m$, the variations in b_1 is the main influencing factor. Once again, b_1 clearly dominates the magnitude of the shear force in comparison to b_2.

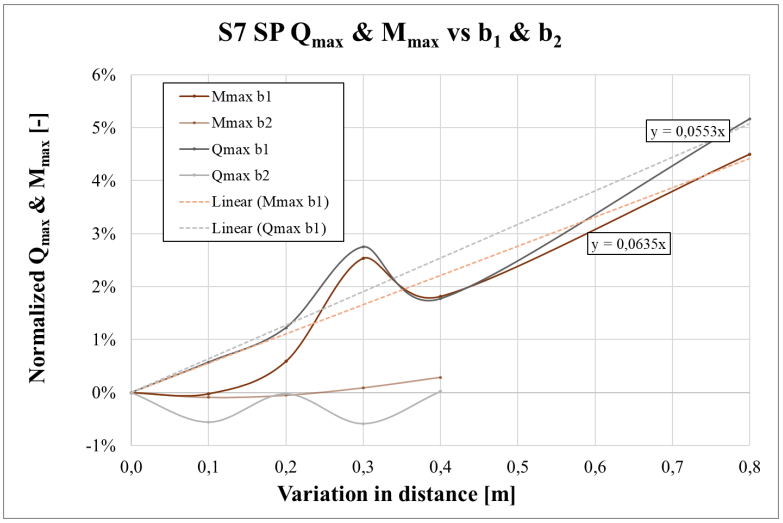

Figure 4.16: Correlations of $M_{\max}$ and $Q_{\max}$ and variations of b_1 and b_2 for the sheet pile in section 7.

In Figure 4.17 the maximum total displacement $u_{\max}$ increases linearly with b_1. Total displacement grows steadily up to an increase of 20% as b_1 increases, directly influencing wall deviation. b_2 has minimal effect on $u_{\max}$ and variations in b_2 lead to a displacement difference of less than 0.002 m, showing low sensitivity. b_1 is the dominant parameter for displacement.

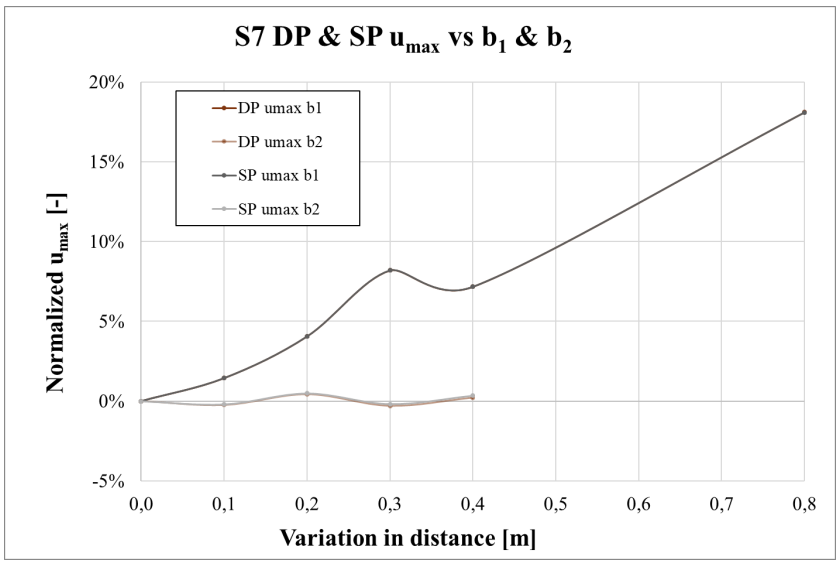

Figure 4.17: Correlations of $M_{\max}$ and $Q_{\max}$ and variations of b_1 and b_2 for the drilled pile in section 7.

4.2.2 Section 8

When conducting the results for section 8, the PLAXIS 2D model failed for $b_2 > 0.20m$ resulting in fewer input data.

Figure 4.18 shows that $M_{\max}$ increases almost linear with b_1, meanwhile $M_{\max}$ increases slightly to $b_2 = 0.1$ and then decreases, indicating a nonlinear trend. For $Q_{\max}$, b_1 causes a sharp rise up to 0.2 m followed by a slight drop, while b_2 steadily reduces the shear force. The inclination indicates a 3.10 factor increase per meter of gap, much higher than the factor for section 7.

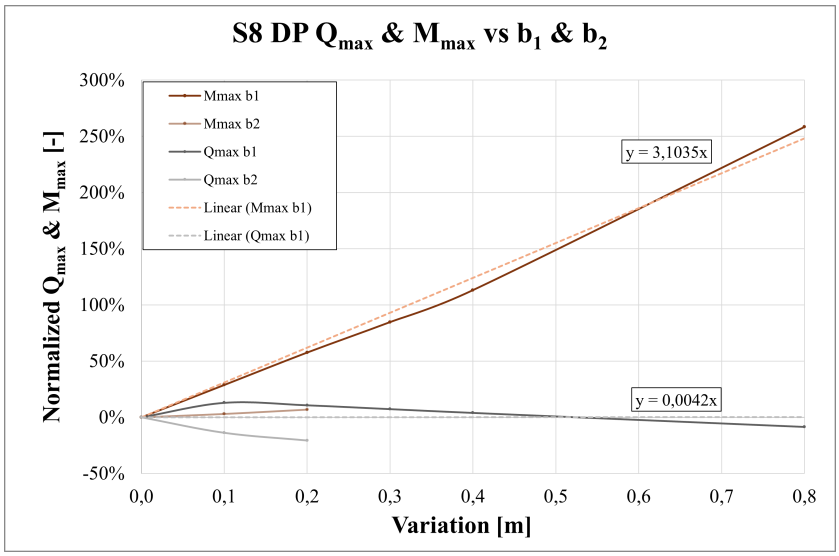

Figure 4.18: Correlations of $M_{\max}$ and $Q_{\max}$ and variations of b_1 and b_2 for the drilled pile in section 8.

Variations in b_1 show a clear decreasing trend in Figure 4.19, meaning higher b_1 results in lower bending moments in the sheet pile and the opposite effect is seen on the shear force, indicating that larger distance between the sheet pile toe and bedrock lead to greater shear force in the sheet pile. Variations of b_2 have almost no effect on $M_{\max}$ and $Q_{\max}$.

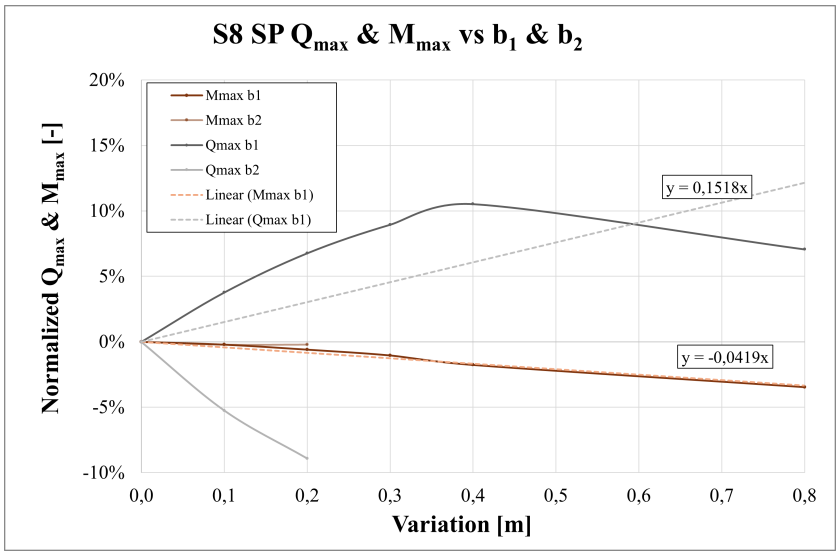

Figure 4.19: Correlations of $M_{\max}$ and $Q_{\max}$ and variation of b_1 and b_2 for the sheet pile in section 8.

Figure 4.20 shows that b_1 has limited effect on total displacement, with a slight dip around $0.2, \mathrm{m}$, while b_2 causes a clearer increase.

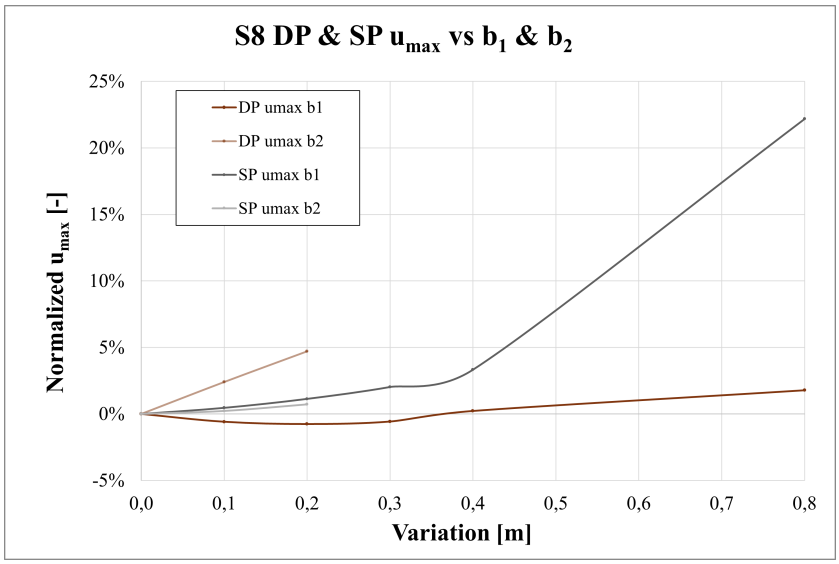

Figure 4.20: Correlations of maximum total displacement and variations of b_1 and b_2 for the drilled pile and sheet pile in section 8.

4.2.3 Section 10

Section 10 allowed iterations up to 0.8 m in b_1 and 0.15 m in b_2 from PLAXIS. As shown in Figure 4.21, the bending moment in the drilled pile increases linearly with b_1 and nearly doubles at 0.3 m, while b_2 has little effect. Shear force also rises with b_1, but less pronounced, and changes in b_2 remain minimal for both moment and shear.

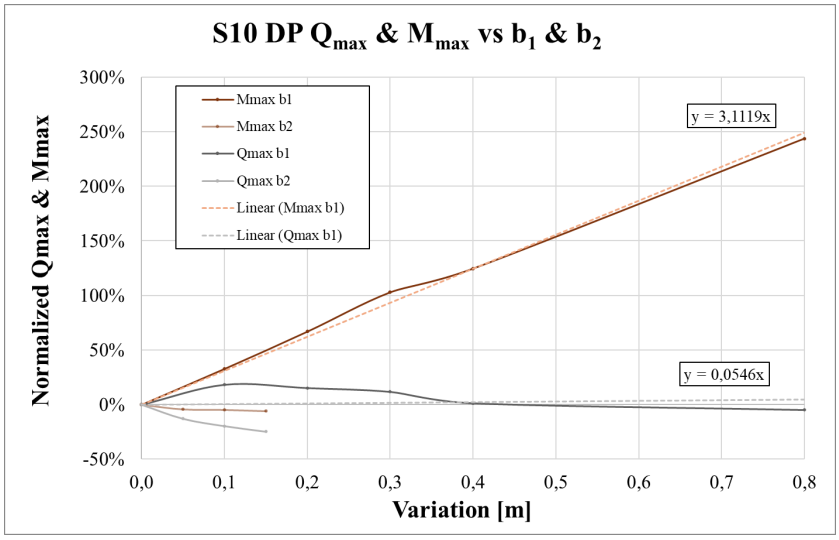

Figure 4.21: Correlations of $M_{\max}$ and $Q_{\max}$ and variations of b_1 and b_2 for the drilled pile in section 10.

On the other hand, Figure 4.22 shows that the bending moment in the sheet pile is relatively unaffected by variations in b_1 and b_2, with only small changes in size. The sheet pile shows almost no changes as the normalized value for b_1 increases by 1.5% and decreases by about 1% for increases in b_2. Figure 4.22 shows that the shear force in the sheet pile is almost unchanged for different values of b_1 and b_2.

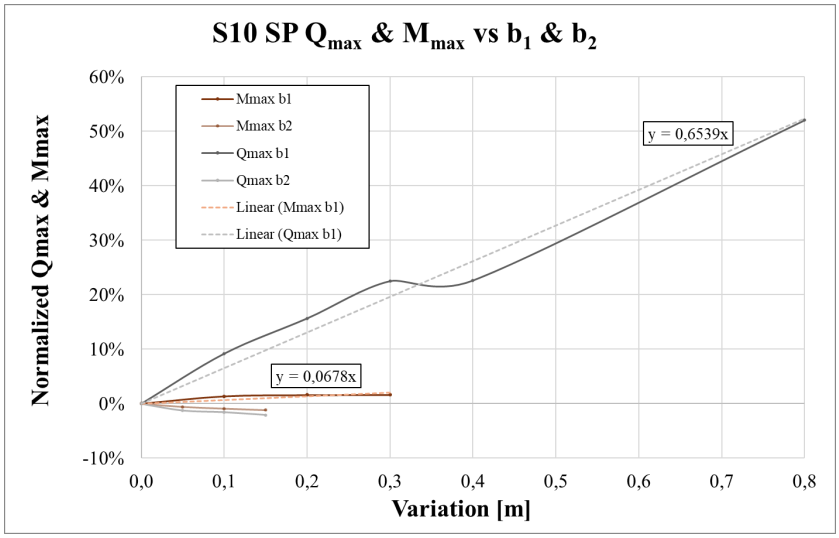

Figure 4.22: Correlations of $M_{\max}$ and $Q_{\max}$ and variations of b_1 and b_2 for the sheet pile in section 10.

4.3 Analytical results

Analytical earth pressure distributions have been calculated for Sections S7, S8, and S10 using the Equations presented in the methodology chapter, based on classical earth pressure theory. The following graphs illustrate the active and passive earth pressure envelopes, the net pressure acting on the sheet pile ($p_{\text{netto}} = p_a - p_p$), as well as the at-rest earth pressure p_0 and the redistributed net earth pressure σ_i. The soil layer profile for all three sections is seen in Figure 2.12.

Section 7 has a depth from excavation level to bedrock at ca 10 m, meaning that the passive earth pressure manages to build up, resulting in a net earth pressure which acts in favor of stabilizing the sheet pile, as seen in Figure 4.23. The redistributed earth pressure is therefore very low, at a σ_i of 10,31 kPa/m. This is in line with the low bending moments and shear forces observed from the numerical results.

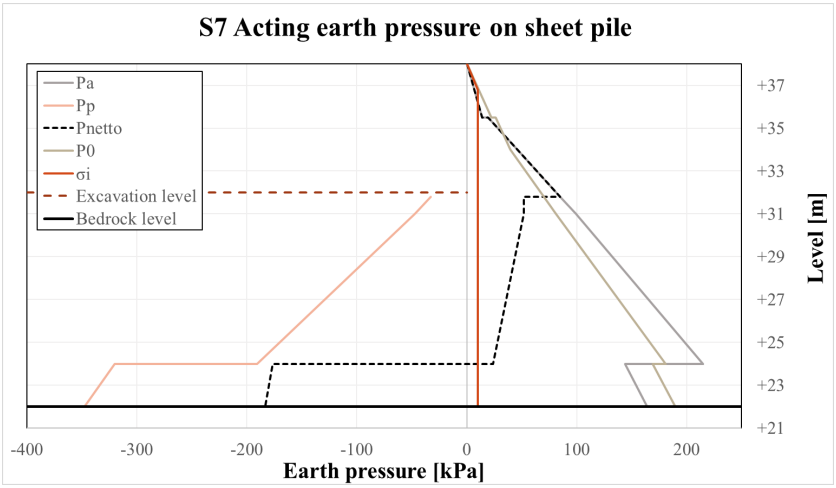

Figure 4.23: Analytical acting earth pressure on sheet pile for S7

The earth pressures acting on the sheet pile for section 8 are seen in Figure 4.24 and have an increase in redistributed earth pressure as the distance to bedrock is 5,4 m from the excavation level. This results in a σ_i of 36,7 kPa/m.

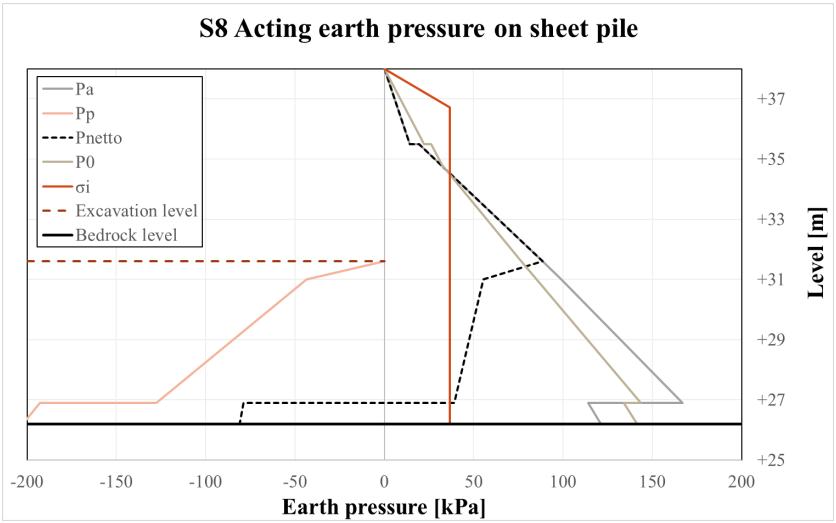

Figure 4.24: Analytical acting earth pressure on sheet pile for S8

Section 10 exhibits the highest redistributed earth pressure of 41,5 kPa/m, as a result of a distance to bedrock at only 1,6 m, seen in Figure 4.25. This section is therefore the most critical in terms of stability.

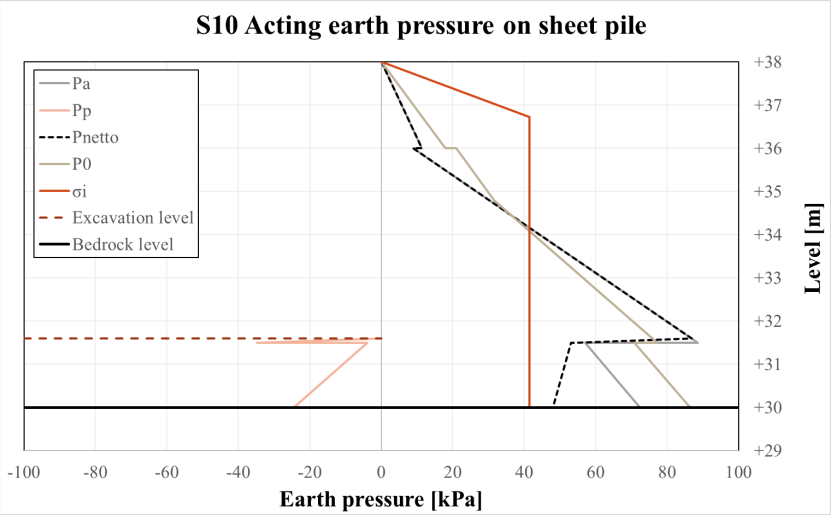

Figure 4.25: Analytical acting earth pressure on sheet pile for S10

The values of σ_i obtained from the different earth pressure calculations are showcased in Table 4.1 together with the gradient from the linear Equations of the numerical results. These show that there is a correlation between the magnitude of the resistributed earth pressure and the gradient of how $M_{\max}$ varies for the drilled pile as the gap b_1 increases.

Table 4.1: Comparison of σ_i from analytical results and $M_{\max}$ gradient from b_1 numerical results

Section	**σ_i from analytical result**	**$M_{\max}$ Gradient from b_1 numerical results**
7	10.37 kPa/m	0.0691
8	36.7 kPa/m	3.1035
10	41.5 kPa/m	3.3987

4.3.1 Comparison between analytical and numerical earth pressure

The results from the following graphs show a comparison of the earth pressure calculated for the earth pressure at-rest, and the initial phase lateral stress from the numerical moddel in PLAXIS. Figure 4.26 show a close alignment of the earth pressures until the ground water level at +34 m, where the analytical earth pressure deviate from the numerically calculated ones for the clay layer.

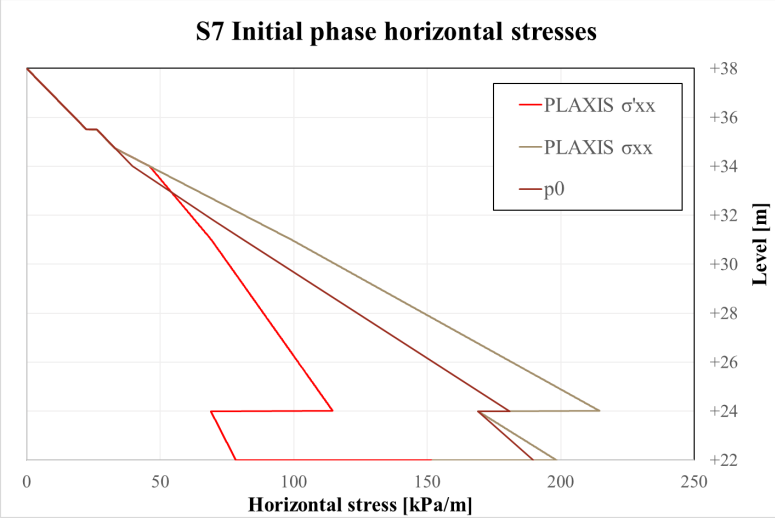

Figure 4.26: Comparison between numerical and analytical results for acting lateral stress in S7

Figure 4.27 shows that the correlation between σ_{xx} and p_0 follows the same pattern as observed for S7, however, the difference in magnitude is not significant. The same conclusion can be drawn for section 10, by interpreting the graph seen in Figure 4.28. Appendix C includes the results from the calculations made analyticallly.

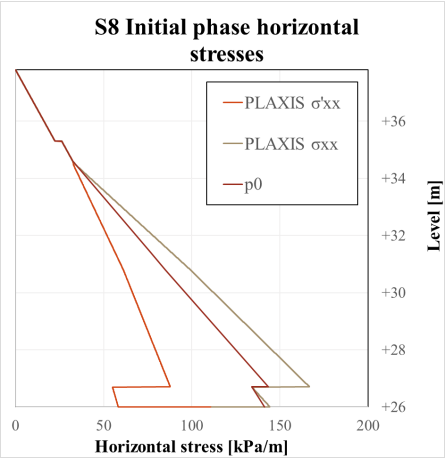

Figure 4.27: Comparison between numerical and analytical results for acting lateral stress in S8

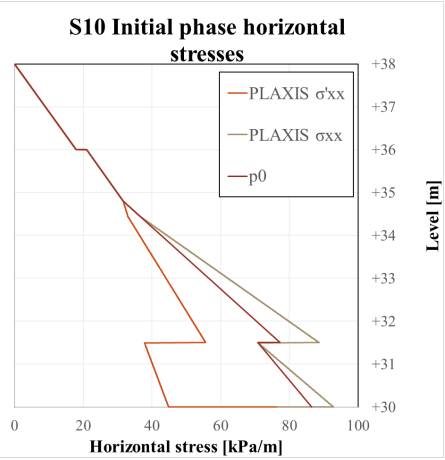

Figure 4.28: Comparison between numerical and analytical results for acting lateral stress in S10

4.4 Comparison of numerical results for different rock anchor designs

This section presents the results for the numerical analysis for the PLAXIS base models, comparing variations of fixed-end and free-end conditions for the drilled piles toe fixation on the horizontal plane. Values for total displacement, shear force and bending moment have been collected in PLAXIS and exported to Excel for graph generation. Because of the observed insignificant differences between the conditions, no graphs are deemed relevant to present and tables of the maximum values are therefore displayed instead, however these are included in Appendix D. Only section 7 and 8 are analyzed as the results from Chapter 4.1 showed a clear pattern in both cases, therefore the results for section 10 are excluded.

4.4.1 S7 variations in displacement conditions

The presented tables for this section includes shear force and bending moment for the drilled pile. Total displacement and all sheet pile centered graphs are deemed even less significant and are therefore excluded.

4.4.1.1 Variations in b_1

Table 4.2: Comparison of fixed and free ends for different b_1 values for section 7 for the drilled pile.

DP	$Q_{\max}$ [kN/m]				$M_{\max}$ [kNm/m]			
b_1 [m]	$x_{\text{Fixed}}, y_{\text{Free}}$	$x_{\text{Fixed}}, y_{\text{Fixed}}$	$x_{\text{Free}}, y_{\text{Free}}$	SP_{Fixed}	$x_{\text{Fixed}}, y_{\text{Free}}$	$x_{\text{Fixed}}, y_{\text{Fixed}}$	$x_{\text{Free}}, y_{\text{Free}}$	SP_{Fixed}
0	49,01	47,63	688,78	45,50	55,54	55,06	253,42	2,73
0,1	59,44	61,64	740,03	45,50	55,54	55,11	259,39	7,28
0,2	53,83	56,12	751,44	45,50	56,08	56,15	263,31	11,83
0,3	54,61	60,70	763,50	45,50	57,26	56,59	267,50	16,38
0,4	65,08	65,16	768,83	45,50	56,78	56,61	269,80	**20,93**
0,8	63,99	64,13	800,13	45,50	58,65	58,81	281,32	39,13

The results presented in Table 4.2 show minimal differences for the different horizontal conditions at the toe of the drilled pile for both the maximum bending moment and maximum shear force. The values for $Q_{\max}$ for x_{Free}, y_{Free} is significantly higher, reaching values more than 10 times the magnitude of the other displacement conditions. The values represented by SP_{fixed} are the values obtained for the method of assuming that the sheet pile is seen as a fixed end, and using the lateral load at the bedrock level. Although $M_{\max}$ for x_{Free}, y_{Free} is significantly higher, it is only approximately five times greater than the magnitude of the other displacement conditions. This indicates that the increase in bending moment is not proportional in the same way as assumed for the bending moment calculated for SP_{Fixed} using the design method for rock dowels.

4.4.1.2 Variations in b_2

Table 4.3 indicate that $M_{\max}$ for $x_{\text{Fixed}}, y_{\text{Free}}$ and $x_{\text{Fixed}}, y_{\text{Fixed}}$ is essentially the same for all b_2 values, while $Q_{\max}$, tends to be slightly higher for $x_{\text{Fixed}}, y_{\text{Fixed}}$ at higher b_2 values. The free end displacement conditions shows a decrease in both $Q_{\max}$ and $M_{\max}$ indicating that the loads are distributed differently compared to the other displacement conditions.

Table 4.3: Comparison of fixed and free ends for different b_2 values for section 7 for the drilled pile.

DP	$Q_{\max}$ [kN/m]			$M_{\max}$ [kNm/m]		
b_2 [m]	$x_{\text{Fixed}}, y_{\text{Free}}$	$x_{\text{Fixed}}, y_{\text{Fixed}}$	$x_{\text{Free}}, y_{\text{Free}}$	$x_{\text{Fixed}}, y_{\text{Free}}$	$x_{\text{Fixed}}, y_{\text{Fixed}}$	$x_{\text{Free}}, y_{\text{Free}}$
0	49	48	689	56	55	253
0,1	52	54	714	55	56	252
0,2	53	56	705	55	56	249
0,3	52	55	704	55	55	249
0,4	52	56	696	55	55	246

4.4.2 S8 variations in displacement conditions

The presented tables for this section includes shear force and bending moment for the drilled pile. Total displacement and all sheet pile centered graphs are deemed even less significant and are therefore excluded.

4.4.2.1 Variations in b_1

For section 8 with variations in b_1, $M_{\max}$ remains relatively comparable between the first two displacement conditions, as seen in Table 4.4. In contrast to section 7, the comparison between SP_{Fixed} and the horizontally fixed shoe that $M_{\max}$ is higher for the conventional design method, indicating an overdimensioning.

The differences in shear force are a little more pronounced, with $Q_{\max}$ somewhat higher for $x_{\text{Fixed}}, y_{\text{Free}}$ in comparison with $x_{\text{Fixed}}, y_{\text{Fixed}}$ for all b_1 variations except $b_1 = 0m$.

Table 4.4: Comparison of fixed and free ends for different b_1 values for section 8 for the drilled pile.

DP	$Q_{\max}$ [kN/m]				$M_{\max}$ [kNm/m]			
b_1 [m]	$x_{\text{Fixed}}, y_{\text{Free}}$	$x_{\text{Fixed}}, y_{\text{Fixed}}$	$x_{\text{Free}}, y_{\text{Free}}$	SP_{Fixed}	$x_{\text{Fixed}}, y_{\text{Free}}$	$x_{\text{Fixed}}, y_{\text{Fixed}}$	$x_{\text{Free}}, y_{\text{Free}}$	SP_{Fixed}
0	242	243	699	371	64	65	266	22
0,1	273	264	731	371	82	82	265	59
0,2	268	258	734	371	101	100	266	97
0,3	260	252	738	371	118	118	269	134
0,4	251	247	748	371	136	136	273	171
0,8	221	222	839	371	229	224	312	319

4.4.2.2 Variations in b_2

Table 4.5 show that the maximum moment, $M_{\max}$, is generally higher for the fixed end, while the maximum shear force, $Q_{\max}$, tends to be slightly higher for the free end. The results follow the same trend as the results for variations in b_2 for section 7.

Table 4.5: Comparison of fixed and free ends for different b_2 values for section 8 for the drilled pile.

DP	$Q_{\max}$ [kN/m]			$M_{\max}$ [kNm/m]		
b_2 [m]	$x_{\text{Fixed}}, y_{\text{Free}}$	$x_{\text{Fixed}}, y_{\text{Fixed}}$	$x_{\text{Free}}, y_{\text{Free}}$	$x_{\text{Fixed}}, y_{\text{Free}}$	$x_{\text{Fixed}}, y_{\text{Fixed}}$	$x_{\text{Free}}, y_{\text{Free}}$
0	242	243	699	64	65	266
0,1	209	207	720	66	66	262
0,2	192	189	713	68	68	259
0,3	-	176	710	-	69	257
0,4	-	166	704	-	70	254

5

Discussion

5.1 Influence of b_1 vs b_2

The parameters b_1, representing the vertical distance between the toe of the sheet pile and the bedrock and b_2, representing the lateral distance between the sheet pile and the drilled pile were varied to evaluate their effect on the structural behavior. The results of this study indicate a significantly greater impact on the structure for variations in the parameter b_1 compared to the variations of b_2, across all sections and output types as presented in Chapter 4.

The observed results for section 7 when increasing b_1 shows a clear reduction in maximum shear force within the drilled pile. Although some deviations were observed in the PLAXIS output, particularly at lower b_1 values, these appeared as local fluctuations or zigzag patterns in the shear force Figure 4.3, where the curve shows unrealistic trends. This behavior is likely caused by numerical effects rather than actual mechanical response. The corresponding bending moment in the sheet pile shows a peak near the excavation level and declines afterwards, indicating that the drilled pile no longer contributes to structural support above that point. The shear force in the sheet pile is zero at the excavation level, which agrees with expected structural behavior, where a change in shear sign corresponds to an turning point in the bending moment Figure 4.4.

The effect of variations in b_1 for section 8 presented in the sheet pile shear force Figure B.1 is even more distinct. As b_1 increases, the maximum shear force in the sheet pile increase significantly, following the same trend as discussed for section 7. This behavior indicates that a shorter load-transfer distance requires a more concentrated shear response, which is consistent with the increasing values of $Q_{\max}$. In contrast, the shear force in the drilled pile shows a decreasing trend with increasing b_1, where the force appears more widely distributed within the drilled pile.

The bending moment distribution in the drilled pile in section 8 shows a clear pattern. The magnitude of $M_{\max}$ increases significantly with b_1, but remains much lower than the bending moment in the sheet pile. The distance in which the bending moment appears to increase its amplitude between is roughly one third of the distance in which the drilled pile correlates with the sheet pile. This observation suggests that the interaction distance, b_3, is smaller than what can be seen in the bending moment diagram. It also supports the hypothesis that b_3 is affected more by excavation depth than by the total depth to bedrock, as the interaction zone ends around the same elevation in all three sections, regardless of the depth the bedrock.

In contrast, the results from lateral distance variations, b_2, results in minor changes in structural response across all sections and output types. Minimal increases are observed in $M_{\max}$, $Q_{\max}$, and $u_{\max}$ as b_2 increases, but these variations are very

small compared to those associated with parameter b_1. This behavior suggests that the modeled system behaves as a stiff structure, in which the interaction between the sheet pile and the drilled pile is not significantly affected by a lateral gap. While this may be a result of the stiffness of the modeled elements, it also indicates a limitation of the two-dimensional modeling approach, which does not capture three-dimensional soil deformation. In reality, the vertical separation could likely cause a redistribution of stress that is not visible in this analysis. A more accurate representation of this effect would require a three-dimensional modeling with more advanced soil-structure interaction definitions.

As for section 8, some local effects are seen for b_2 where both the intercept and peak values of moment in the drilled pile increase slightly. The corresponding shear force profile shows small variations, but with limited impact on the overall structural performance.

5.1.1 Numerical correlation between $M_{\max}$ and $Q_{\max}$

The results presented in Chapter 4.2 emphasizes the relationship between maximum bending moment and maximum shear force for both the sheet pile and the drilled pile, especially under variations in the vertical distance b_1. For the sheet pile, $M_{\max}$ and $Q_{\max}$ show a nearly proportional increase, which is consistent with the linear relationship assumed in conventional design guidelines presented in the theory section.

In contrast, the response of the drilled pile shows a significantly larger increase in $Q_{\max}$ compared to $M_{\max}$ for variations in b_1 when looking at section 7. This suggests that a larger portion of the load is being redistributed along the pile length, resulting in concentrated shear forces but lower bending moment. As such, the linearity assumed in traditional design for rock dowels may not be representative for drilled piles.

This observation changes however when comparing sections 8 and 10, where trends show that the bending moment increases with a gradient of ca $3.1 * b_1$. This in contrast to the increase of maximum shear force, which has a factor within a range $0.004 - 0.05$ for these two sections, meaning that the magnitude of Q_{max} varies much less in comparison to M_{max}. This still confirms the conclusion that the design method for rock dowels does not capture the variation in behavior of the drilled pile for vertical distances between the bedrock and the toe of the sheet pile.

The increase in gradient shows a positive trend as the redistributed earth pressure increases, as shown in Table 4.1. This correlation however, is not linear meaning that there is a more complex relationship between the bending moment, shear force, increase in b_1 and earth pressure.

5.1.2 Comparison of analytical and numerical earth pressure results

In Chapter 4.3, analytically calculated earth pressure distributions were compared with numerical results from PLAXIS 2D for sections 7, 8, and 10. One of the most clear differences is seen in the magnitude of the active net earth pressure in section 7, which was significantly lower than in sections 8 and 10. This observation corresponds well with expectations, as the shorter distance to bedrock in S7 allows

passive resistance to mobilize, thereby reducing the net pressure on the wall.

When comparing the analytical earth pressure profiles with those extracted from PLAXIS, a strong agreement is observed above the groundwater level, however, beyond that point, a small deviation appears. The analytical pressure values fall between the numerical effective stress (σ'_{xx}) and total stress (σ_{xx}) in the lateral direction, but remain significantly closer to σ_{xx}. This is consistent with the equations used for the analytical at-rest earth pressure p_0, where pore pressure is accounted for directly in the total stress calculation. Overall, the analytical approach provides a reasonable approximation of the horizontal stress distribution.

5.1.3 Influence of displacement conditions

The comparison of fixed- and free-end displacement conditions for the drilled pile in sections 7 and 8 shows that the modeled conditions at the pile toe have a limited influence on the overall structural response. This is true except for the case where both lateral and vertical directions are modeled as free, with the drilled pile embedded in the bedrock. This condition, represented by $x_{\text{Free}}, y_{\text{Free}}$ in Chapter 4.4, results in significantly higher internal forces, and are interpreted to be caused as a result of unrealistic point-loading effects at the transition from soil to bedrock, where the sharp contrast in stiffness leads to numerical effects in the form of concentrated loads.

For more realistic results from the boundary conditions, such as those for $x_{\text{Fixed}}, y_{\text{Free}}$ and $x_{\text{Fixed}}, y_{\text{Fixed}}$, the resulting values for both $M_{\max}$ and $Q_{\max}$ remain relatively close across all values of b_1 and b_2. The small differences observed are unlikely to affect practical design decisions. In both sections, variations in b_2 show an even smaller impact compared to variations in b_1, suggesting once again that the vertical gap is more critical when assessing the load transfer to the drilled pile. This analysis supports the assumption that modeling the pile as fixed horizontally is reasonable and contributes to a more stable numerical response. The extreme results for the fully free case underline the importance of choosing a representative toe displacement.

The most prominent conclusion that can be drawn from the various modeled cases is the relationship between $M_{\max}$ and $Q_{\max}$ for the same displacement condition. For the conventional design method for rock dowels, the design shear force is multiplied by a lever arm corresponding to the assumed vertical gap b_1, resulting in a linearly increasing bending moment with increasing distance. This contrasts with the behavior presented in the case where the drilled pile is modeled, suggesting that the load from the sheet pile is distributed along the length of the pile rather than concentrated at a single level. This continuous load transfer supports the conclusions established in chapter 5.1.1 regarding the pile´s distributed support behavior.

5.2 Comparison of drilled piles and rock dowels

When analyzing the structural behavior in comparison to traditional rock dowels, clear differences emerge in how the drilled piles respond to variations in loads from the site conditions. In addition to the observed differences in structural behavior, particularly how M_{max} develops in relation to shear force, additional

aspects of cost, time and installation are also taken into account when determining the advantages and disadvantages of rock dowels in comparison to drilled piles.

As previously presented, drilled piles are generally considered more expensive than rock dowels in the literature however, they also offer significant advantages in terms of installation time. During construction projects, time is a critical cost factor and therefore, the actual cost difference between drilled piles and rock dowels may be less substantial than often assumed. Additionally, drilled piles are structurally robust, well-suited to adapt to uncertain bedrock levels, and involve a less complex execution method. Their design however have a limitation in dimension which is the distance between the sheet pile and the wailing beam. In comparison, rock dowels benefit from an established analytical design method. However, they are dimensionally limited by the diameter of the casing tube, which can restrict their use in more demanding conditions. Moreover, casing tubes for rock dowels often require on-site or pre-welded assembly, which is time-consuming and reduces reusability. In contrast, drilled piles are not cast in place and typically only require spot welding, enabling faster installation and potential reuse. The distance parameter b_3 also enables shorter piles, however this can have negative consequences on installation effects. These aspects may have increased relevance in the industry, as options which prioritize reuse and other environmental benefits are becoming more important in design and planning.

Overall, observations suggest that drilled piles can achieve comparable or even better performances in terms of structural stability, construction time, and cost-effectiveness, due to their robustness and adaptability. These findings suggest that drilled piles could be considered more broadly in practice, particularly when taking into account practical design needs, construction conditions, and the potential for more efficient dimensioning.

5.3 Limitations

The study was subjected to a few limitations that could have affected the precision of the modeling. These included the exclusion of 3D effects, as the analysis was made with data from PLAXIS 2D, resulting in a soil-structure interaction that might not have been representative, especially for the drilled pile. The material parameters for the bedrock contributed to a sharp stiffness contrast, which led to an unrealistic point-loading effect on the drilled pile when modeled as embedded in the bedrock. Another limitation that could have affected the results was that the displacement limitations of the waling beam were not included in the model, which might have affected how forces were transferred in reality. Lastly, the whole thesis was based on input data from site-specific conditions at the Sahlgrenska Life-project, which limited the potential for generalization.

6

Conclusion

The aim of this study was to investigate the structural behavior of drilled piles when used as bedrock anchors for sheet pile walls, with a focus on the effects of the vertical and horizontal distance parameters b_1 and b_2, as well as to evaluate the interaction distance b_3. This as a basis for the comparison between drilled piles and rock dowels in terms of both structural performance and other relevant aspects.

Results from the numerical simulations show that variations in the vertical distance b_1 have a significantly greater impact on bending moment, shear force, and displacement than all variations in b_2. This trend was consistent across all sections, indicating that vertical separation is much more critical to the overall response of the retaining structure. The system displayed a generally stiff behavior for b_2, suggesting a limited effect caused by the numerical simulations. The correlation distance b_3 appears to only be affected by the excavation depth and not the bedrock level as all three sections result in similar b_3.

The results suggest a strong case for re-evaluating the current design methodology for drilled piles used as rock anchors. Numerical analyses concluded that the increase in design moment M_{Ed} due to variations in vertical distance b_1 does not follow the linear relationship assumed in conventional design handbooks, such as *Sponthandboken* (Fredriksson et al., 2024). The behavior implies that the current design approach may lead to over-dimensioning, particularly in cases with higher earth pressures. Furthermore, the results show that drilled piles are more tolerant to installation deviations and can accommodate a wider range of gap conditions without affecting the structural performance. This makes them especially suitable for projects with uncertain or varying bedrock levels.

Another important implication is the potential for reducing pile length based on the observed correlation depth b_3. This could lead to more efficient use of materials and a lower environmental impact. However, implementing such optimizations in practice would require further research, as it could have negative effects in the installation process. From a practical perspective, drilled piles were found to offer several advantages. Their structural robustness, adaptability to variations in bedrock levels, and tolerance for installation deviations make them a great alternative for complex geotechnical projects. While associated with higher material costs, this could be balanced by more time-efficient execution and potential for reuse. In contrast, rock dowels benefit from an established design framework but are more sensitive to field conditions and require more precise installation.

In conclusion, the findings suggest that drilled piles can provide a more flexible and efficient anchoring method. The correlation between redistributed earth pressure and an increase in bending moment gradient indicates a complex relationship which requires further research.

6.1 Future Research

In terms of further development of this work, there is great potential to compare the results from the thesis with measurements from the investigated site after excavation works have been done. By using measurements from inclinometers placed at the project Sahlgrenska Life, the numerical model can be validated and altered to represent the real conditions as well as possible. This could be combined with exploring the behavior for the drilled pile in three-dimension numerical modeling, in order to better capture the interactions between the soil and structures.

Furthermore, an interesting take to analyses the relationship between bedrock level and the behavior of the drilled pile would be interesting. To minimize the effects of variations of soil profiles, this could be done with a homogeneous clay layer which could result in a clear trend in increase/decrease as the earth stresses varies linearly.

Lastly, a more accurate modeling of the toe would be of interest for understanding the load transfers between the bedrock and the soil layer, as it has significant impact on the design values of the shear force for the drilled pile. Regarding displacement conditions, an analysis of the displacements at the top could also be done in order to assess the effect on the structural behavior for the drilled piles when anchored (welded) at the waling beam level.

7

References

ArcelorMittal Sheet Piling. (2018, December). *Horizontal toe support for steel sheet piles on bedrock: Rock Bolts* [Edition 12.2018]. ArcelorMittal Commercial RPS S.à r.l. Esch-sur-Alzette, Luxembourg. https://sheetpiling.arcelormittal.com

Bredenberg, H., Berglars, B., Rankka, W., Holmberg, G., Eronen, S., & Jokiniemi, H. (2010). *Borrade stålrörspålar: Anvisningar för projektering, dimensionering, utförande och kontroll* (tech. rep. No. 104) (Rapport 104, Pålkommissionen). Pålkommissionen. Linköping. https://www.palkommissionen.org

Das, B. M., & Sobhan, K. (2018). *Principles of Geotechnical Engineering* (9th). Cengage Learning. https://sheetpiling.arcelormittal.com/download-center/piling-handbook

Eriksson, J. (2025). *Interview Hercules* [Performed 5th of Mars 2025].

Fredriksson, A., Kullingsjö, A., Ryner, A., & Stille, H. (2024). *Sponthandboken Rapport 107*. Pålkommissionen.

Jin, Y., Biscontin, G., & Gardoni, P. (2021). *Adaptive prediction of wall movement during excavation using Bayesian inference. Computers and Geotechnics, 137*. https://doi.org/10.1016/j.compgeo.2021.104249

Knappett, J., & Craig, R. (2012). *Craig's soil mechanics* (8th ed.). CRC Press.

Matsman, M. (2025). *Interview Aarsleff* [Performed 10th of Mars 2025].

Piling, A. S. (2022). *Piling Handbook* (9th). ArcelorMittal. https://sheetpiling.arcelormittal.com/download-center/piling-handbook

Pomery, J., & Flyckt, A. (2024, October). *SAHLGRENSKA LIFE, HUS 1 Projekteringsbeskrivning-Sponter*.

Sahlgrenska Universitetssjukhus VGR. (2023, December). *Om sjukhuset* [Accessed: 2025-02-06]. https://www.sahlgrenska.se/om-sjukhuset/

SSAB AB. (2025). *RR® and RD® large diameter piles* [Accessed 23 May 2025]. Retrieved May 23, 2025, from https://www.ssab.com/en/brands-and-products/steel-categories/steel-piles-and-pressure-pipes/product-offer/large-diameter-piles

SSAB Europe Oy. (2024). *RR® and RD® Piles – Design and Installation Manual* [Version 17 (English)]. SSAB Europe Oy. Hämeenlinna, Finland. Retrieved May 23, 2025, from https://www.ssab.com/infra

Västra Götalandsregionen. (2025, January). *Förberedande arbete*. https://fastighet.vgregion.se/sjukhus/sahlgrenska-sjukhuset/projekt/forberedande-arbeten/

A

Appendix

Table A.1: Frictional Soil Parameters

General			
Identification	Frictional soil	Fill	-
Soil model	Mohr-Coulomb	Mohr-Coulomb	-
Drainage	Drained	Drained	-
Colour	RGB 247, 156, 29	RGB 122, 42, 59	-
γ_{unsat}	21,00	21,00	kN/m^3
γ_{sat}	21,00	21,00	kN/m^3
e_{init}	0,5	0,5	-
n_{init}	0,333	0,333	-
Mechanical			
E_{rm}	2,00E+04	2,00E+04	kN/m^2
ν	0,3	0,3	-
G_{ref}	7,69E+03	7,69E+03	kN/m^2
E_{oed}	2,69E+04	2,69E+04	kN/m^2
E'_{inc}	0,00	0,00	kN/m^2/m
γ_{ref}	0,00	0,00	m
V_s	6,00E+01	6,00E+01	m/s
V_p	1,12E+02	1,12E+02	m/s
c'_{ref}	0,00	0,00	kN/m^2
ϕ'	3,50E+01	3,50E+01	°
ψ	5	4	°
c'_{inc}	0,00	0,00	kN/m^2/m
γ_{ref}	0,00	0,00	m
Tension cut-off	yes	yes	-
Tensile strength	0,00	0,00	kN/m^2
Determination	v-undrained definition	v-undrained definition	-
v_u definition method	Direct	Direct	-
$v_{u,equivalent}$ (ν)	4,95E-01	4,95E-01	-
Skempton B	9,78E-01	9,78E-01	-
$K_{w,ref}/n$	7,50E+05	7,50E+05	kN/m^2

Table A.2: Bedrock Parameters

General		
Identification	Bedrock	-
Soil model	Hoek-Brown	-
Drainage	Non-porous	-
Colour	RGB 63, 80, 66	-
γ_{unsat}	22,00	kN/m^3
γ_{sat}	22,00	kN/m^3
e_{init}	0,5	-
n_{init}	0,333	-
	Mechanical	
E_{rm}	2,40E+07	kN/m^2
ν	0,2	-
G_{ref}	1,00E+07	kN/m^2
σ_{ci}	1,75E+05	kN/m^2
Determination	Direct	-
m_b	4,092	-
s	6,30E-03	-
a	5,02E-01	-
σ_t	2,69E+02	kN/m^2
σ_{ci}	-1,38E+06	kN/m^2
Tension cut-off	no	-
ψ_{max}	0,00	$^\circ$
σ_ψ	0,00	kN/m^2

Table A.3: Clay Soil Parameters

General						
Identification	Clay layer 1	Clay layer 1 ins	Clay layer 2	Clay layer 2 ins	Dry crust-clay	-
Soild model	Mohr-Coulomb	Mohr-Coulomb	Mohr-Coulomb	Mohr-Coulomb	Mohr-Coulomb	-
Drainage	Undrained B	Undrained B	Undrained B	Undrained B	Undrained B	-
Colour	RGB 241, 241, 95	RGB 214, 229, 46	RGB 224, 220, 143	RGB 228, 219, 37	RGB 161, 226, 232	-
γ_{unsat}	17.70	18.00	18.50	18.50	19.50	kN/m^3
γ_{sat}	17.70	19.00	18.50	19.50	20.00	kN/m^3
e_{init}	0.5	0.5	0.5	0.5	0.5	-
n_{init}	0.333	0.333	0.333	0.333	0.333	-
Mechanical						
E_{rm}	4.15E+03	4.15E+03	4.15E+03	5.40E+03	1.20E+04	kN/m^2
ν	0.3	0.3	0.3	0.3	0.3	-
G_{ref}	1.60E+03	2.08E+03	1.60E+03	2.08E+03	4.62E+03	kN/m^2
E_{oed}	5.59E+03	7.26E+03	5.59E+03	7.26E+03	1.61E+54	kN/m^2
E'_{inc}	0.00	0.00	250	325	0.00	kN/m^2/m
γ_{ref}	0.00	0.00	31	31	0.00	m
V_s	2.97E+01	3.36E+01	2.91E+01	3.32E+01	4.82E+01	m/s
V_p	5.56E+01	6.29E+01	5.44E+01	6.21E+01	9.02E+01	m/s
$s_{u,ref}$	0.00	1.65E+01	1.65E+01	1.65E+01	2.50E+01	kN/m^2
Φ'	0.00	0.00	0.00	0.00	0.00	°
Ψ	0.00	0.00	0.00	0.00	0.00	°
$s_{u,inc}$	0.00	0.00	1.00E+00	1.00E+00	0.00	kN/m^2/m
γ_{ref}	0.00	0.00	3.10E+01	3.10E+01	0.00	m
Tension cut off	yes	yes	yes	yes	yes	-
Tensile strength	0.00	0.00	0.00	0.00	0.00	kN/m^2
Determination	v-undrained definition	v-undrained definition	v-undrained definition	v-undrained definition	v-undrained definition	-
v_u definition method	Direct	Direct	Direct	Direct	Direct	-
$v_{u,equivalent}$ (nu)	4.95E-01	4.95E-01	4.95E-01	4.95E-01	4.95E-01	-
Skempton B	9.78E-01	9.78E-01	9.78E-01	9.78E-01	9.78E-01	-
Kw_{ref}/n	7.50E+05	7.50E+05	7.50E+05	7.50E+05	7.50E+05	kN/m^2

B

Appendix

B.1 Variations in b_1: S8

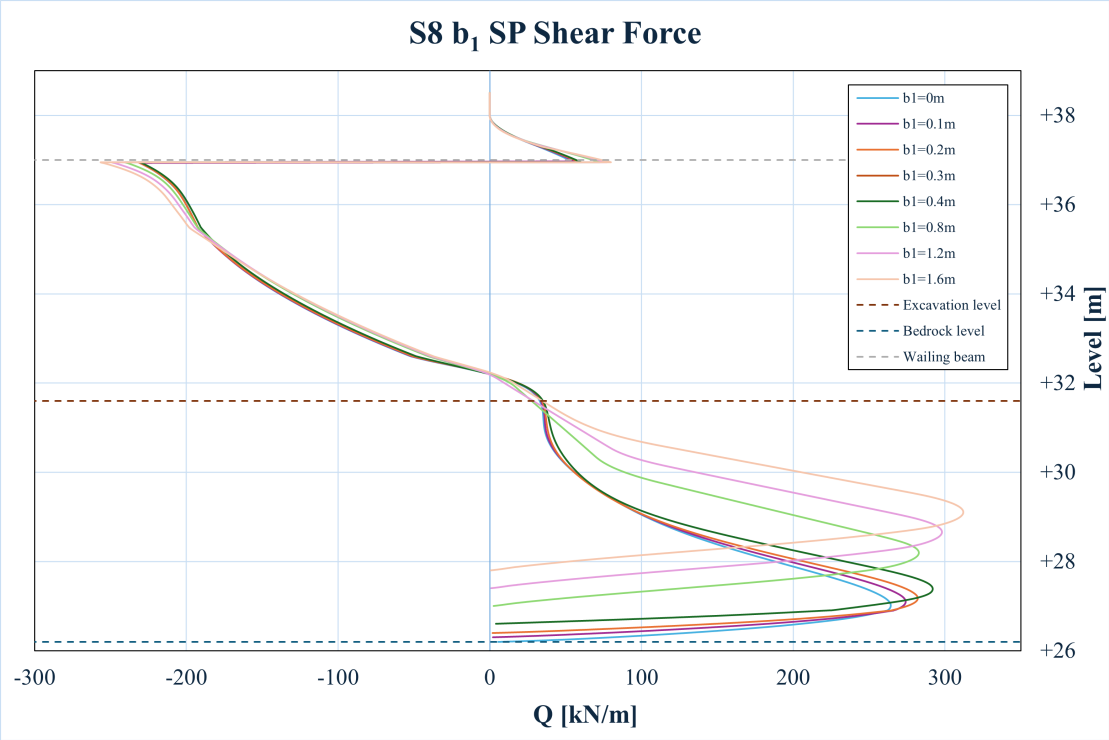

Figure B.1: Section 8 Shear force in the sheet pile for variations in b_1

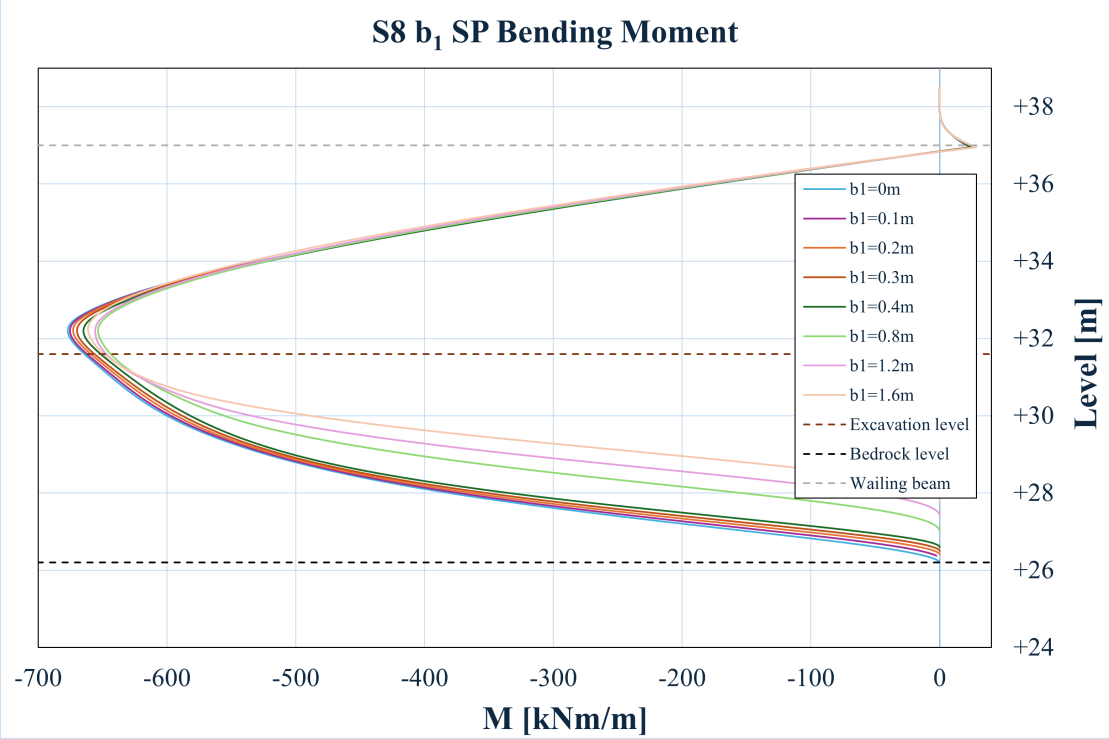

Figure B.2: Section 8 Bending moment in the sheet pile for variations in b_1

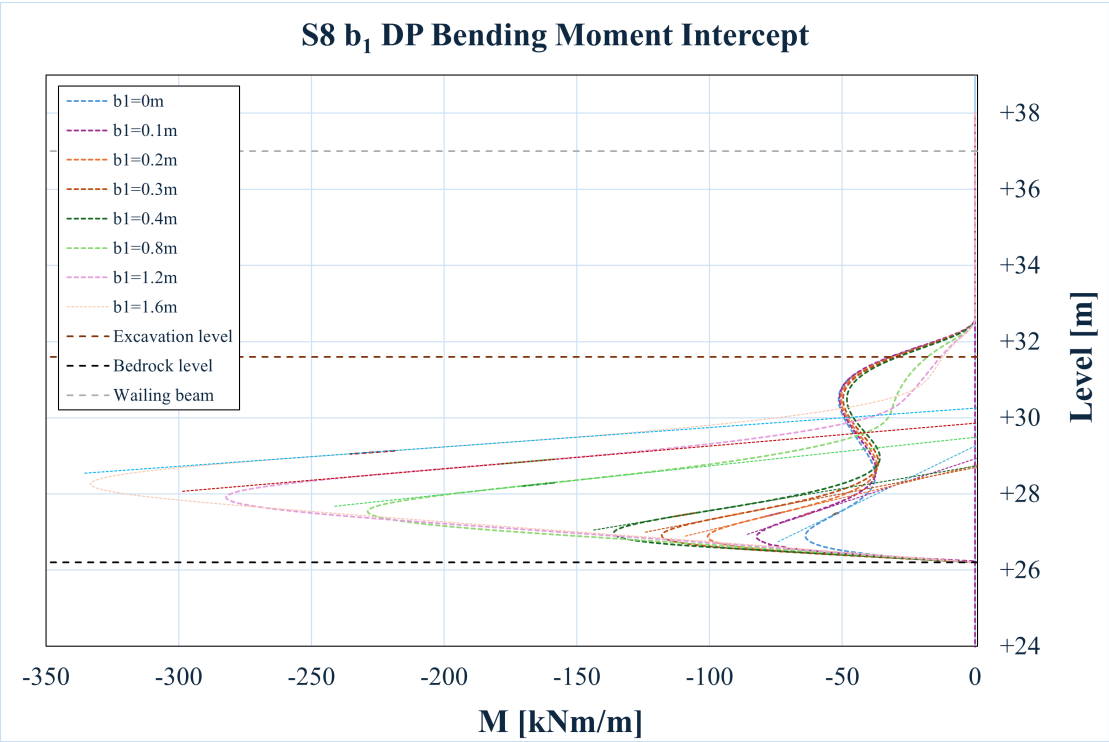

Figure B.3: Section 8 Bending moment including intercept in the drilled pile for variations in b_1

B.2 Variations in b_2: S7

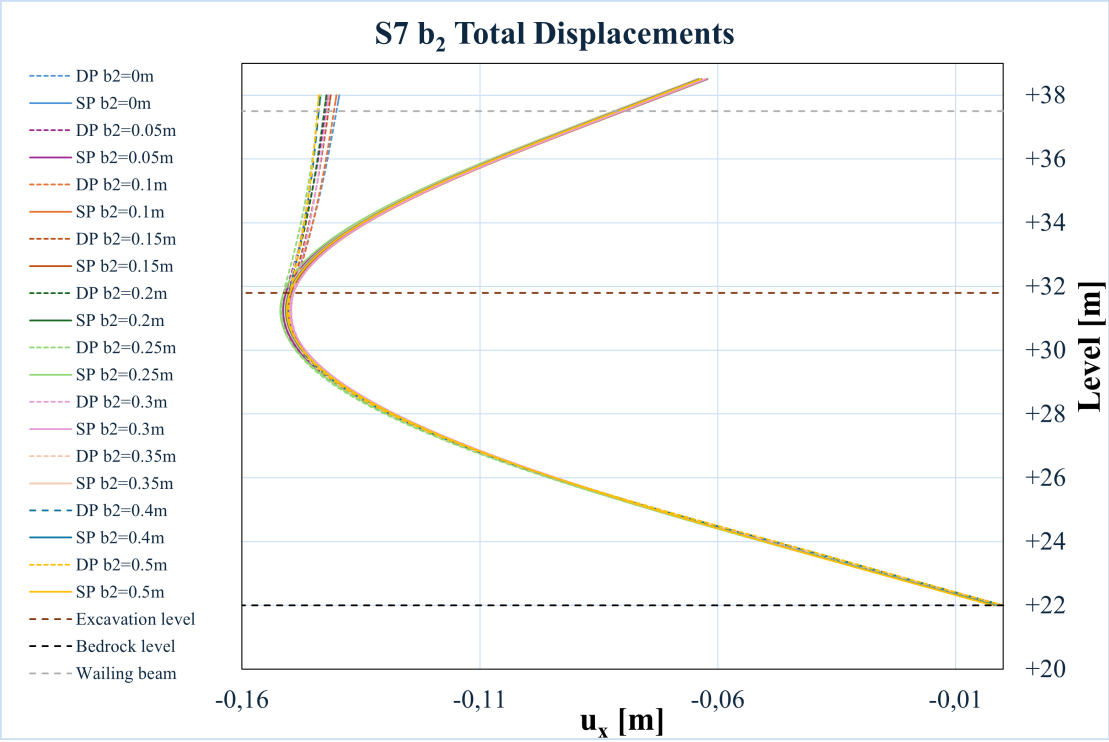

Figure B.4: Section 7 Total displacement for variations in b_2

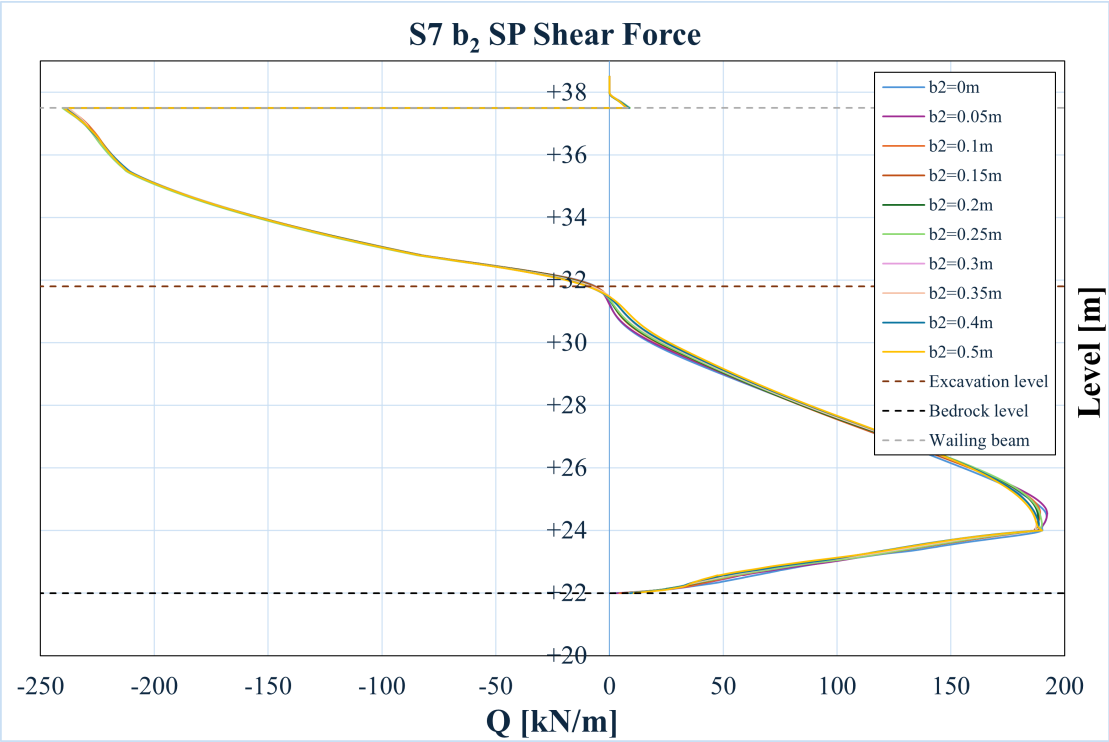

Figure B.5: Section 7 Shear force in the sheet pile for variations in b_2

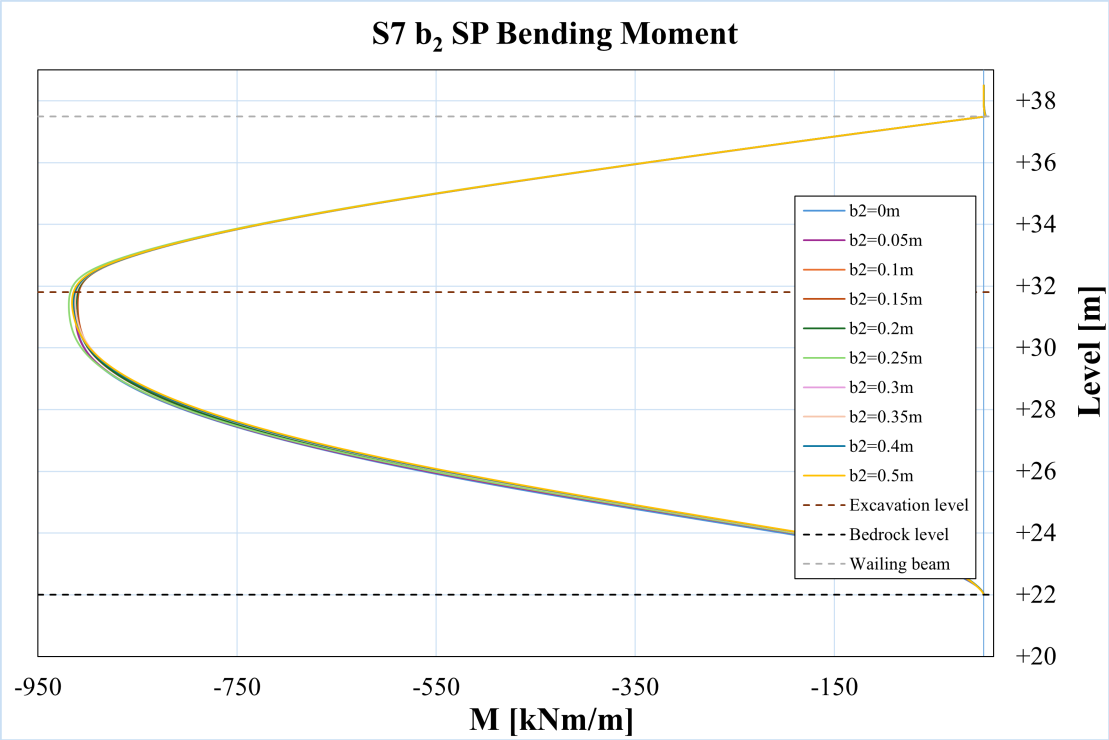

Figure B.6: Section 7 Bending moment in the sheet pile for variations in b_2

B.3 Variations in b_2: S8

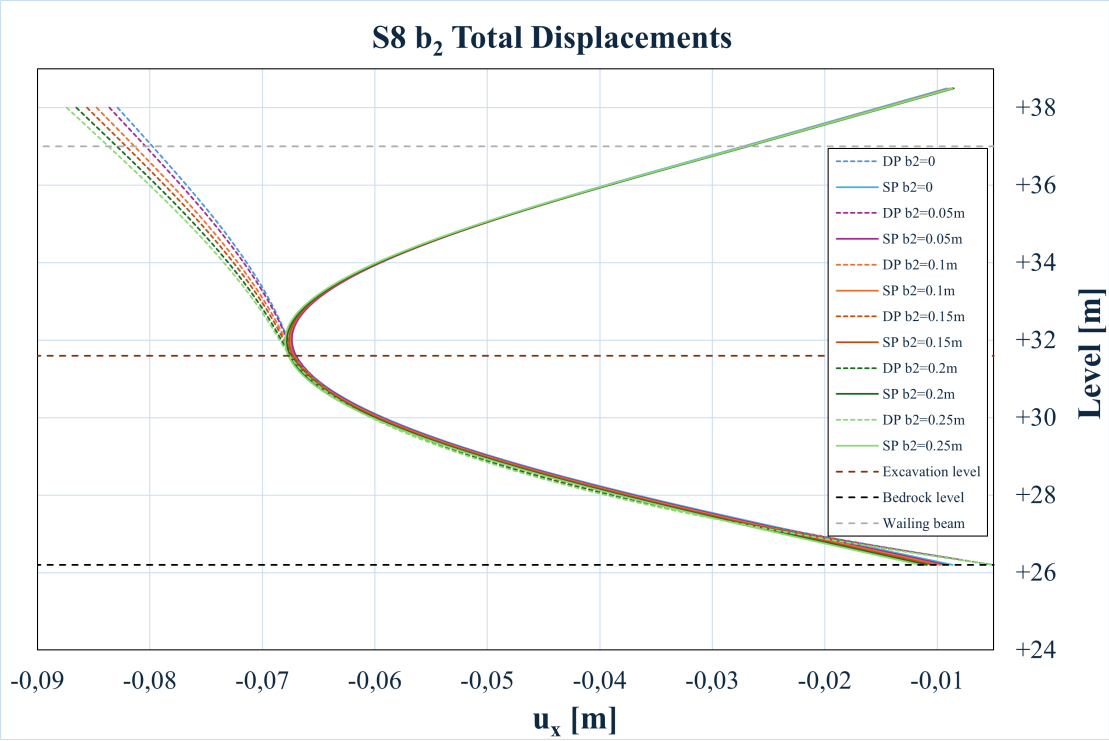

Figure B.7: Section 8 Total displacement for variations in b_2

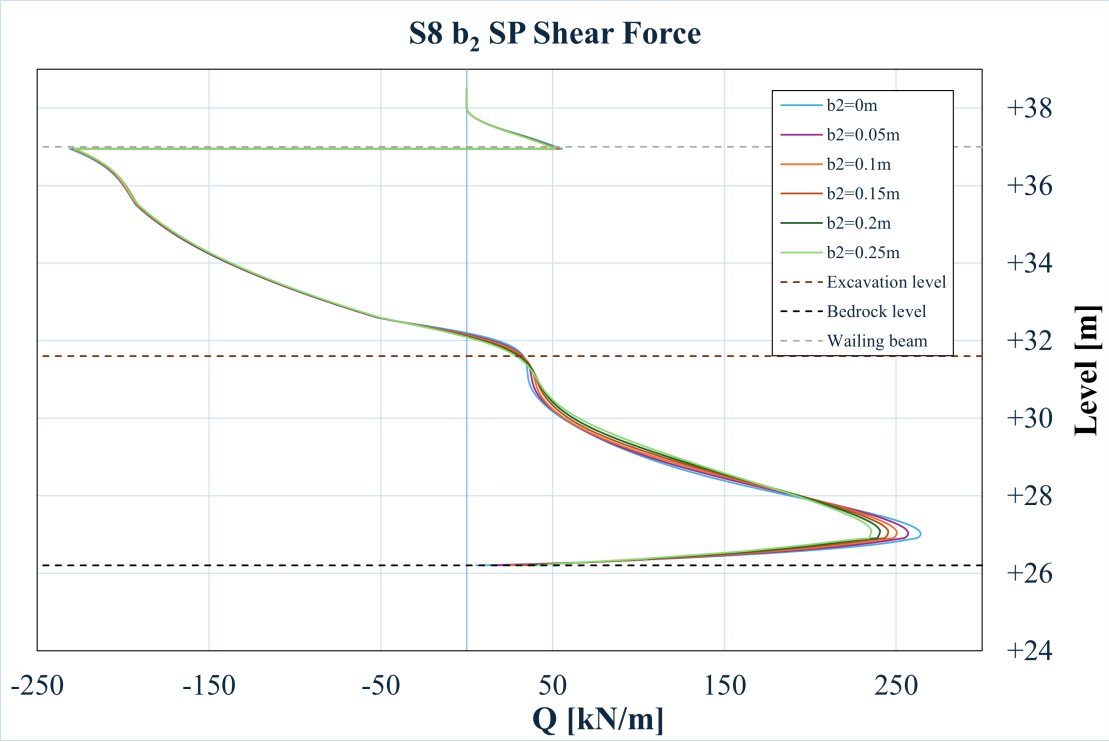

Figure B.8: Section 8 Shear force in the sheet pile for variations in b_2

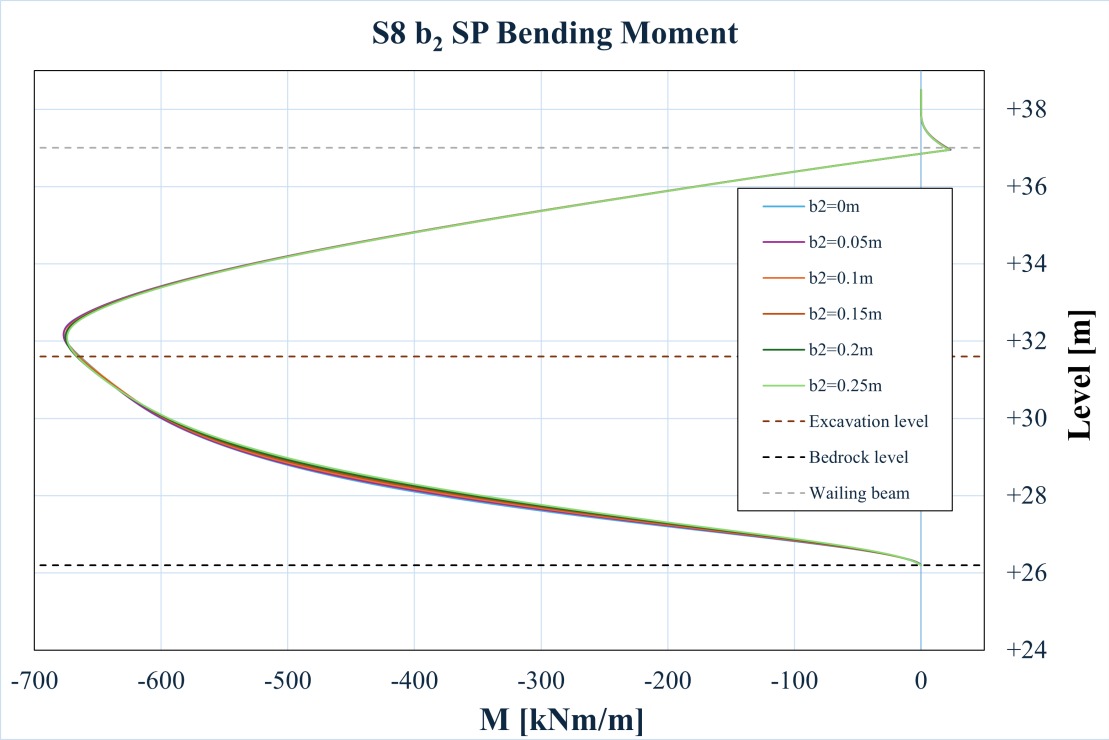

Figure B.9: Section 8 Bending moment in the sheet pile for variations in b_2

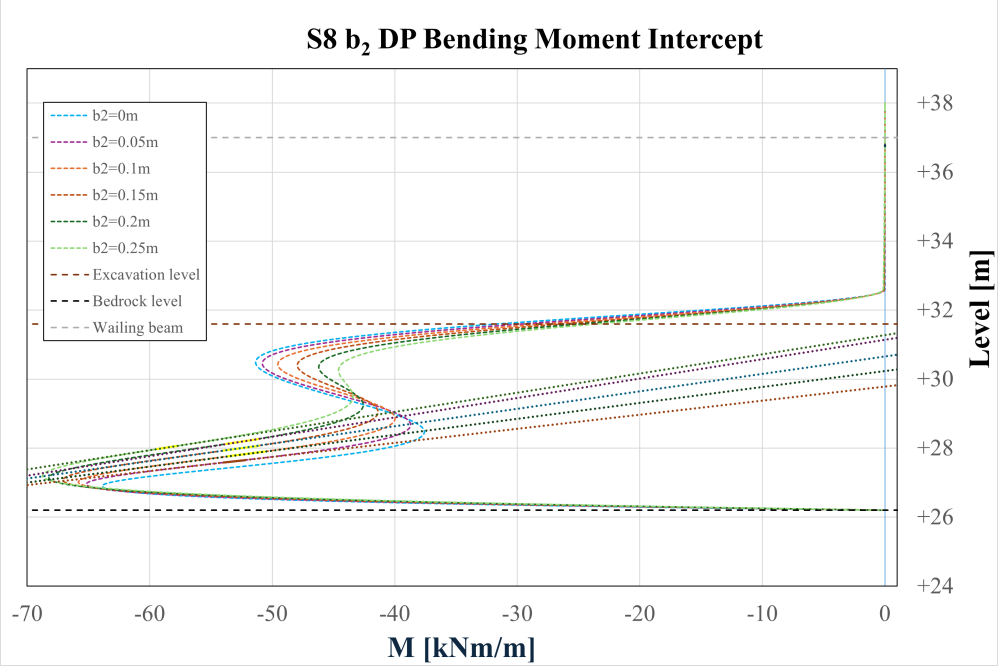

Figure B.10: Section 8 Bending moment in the drilled pile for variations in b_2 with intercept

C

Appendix

Table C.1: Analytically calculated earth pressure for section 7

	+m	z	σ_a	u_a	σ'_a	σ_p	u_p	p_a	p_p	$-p_p$	p_{net}	p_0
fill	38	0	0		0			0,00			0,00	0,00
	35,5	2,5	52,5		52,5			14,23			14,23	22,39
clay 1	35,5	2,5	52,5		52,5			19,50			19,50	26,25
	34	4	79,05		79,05			46,05			46,05	39,53
	34	4	79,05	0	79,05			46,05			46,05	39,53
	31,8	6,2	117,99	22	95,99			84,99			84,99	70,00
	31,8	6,2	117,99	22	95,99	0	0	84,99	33,00	-33,00	51,99	70,00
	31	7	132,15	30	102,15	14,16	8	99,15	47,16	-47,16	51,99	81,08
clay 2	31	7	132,15	30	102,15	14,16	8	99,15	47,16	-47,16	51,99	81,08
	24	14	261,65	100	161,65	143,66	78	214,65	190,66	-190,66	23,99	180,83
frictional soil	24	14	261,65	100	161,65	143,66	78	143,81	320,30	-320,30	-176,49	168,93
	22	16	283,65	120	163,65	165,66	98	164,35	347,68	-347,68	-183,33	189,78
bedrock												

Table C.2: Analytically calculated earth pressure for section 8

	+m	z	σ_a	u_a	σ'_a	σ_p	u_p	p_a	p_p	$-p_p$	p_{net}	p_0
fill	38	0	0			0		0,00			0,00	0,00
	35,5	2,5	52,5			52,5		14,23			14,23	22,39
	35,5	2,5	52,5			52,5		19,50			19,50	26,25
clay 1	34,8	3,2	64,89			64,89		31,89			31,89	32,45
	34,8	3,2	64,89		0	64,89		31,89			31,89	32,45
	31,6	6,4	121,53		32	89,53		88,53			88,53	76,77
	31,6	6,4	121,53	0	32	89,53	0	88,53	0,00	0,00	88,53	76,77
	31	7	132,15	10,62	38	94,15	6	99,15	43,62	-43,62	55,53	85,08
clay 2	31	7	132,15	10,62	38	94,15	6	99,15	43,62	-43,62	55,53	85,08
	26,9	11,1	208	86,47	79	129	47	166,80	127,67	-127,67	39,13	143,50
frictional soil	26,9	11,1	208	86,47	79	129	47	113,96	192,65	-192,65	-78,69	134,01
	26,2	11,8	215,7	94,17	86	129,7	54	121,15	202,23	-202,23	-81,09	141,31
bedrock	26,2											

Table C.3: Analytically calculated earth pressure for section 10

	+m	z	σ_a	u_a	σ'_a	σ_p	u_p	p_a	p_p	$-p_p$	p_{net}	p_0
fill	38	0	0			0		0,00			0,00	0,00
clay 1	36	2	42			42		11,38			11,38	17,91
	36	2	42			42		9,00			9,00	21,00
	34,8	3,2	63,24			63,24		30,24			30,24	31,62
	34,8	3,2	63,24		0	63,24		30,24			30,24	31,62
	31,6	6,4	119,88		32	87,88		86,88			86,88	75,94
	31,6	6,4	119,88	0	32	87,88	0	86,88	0,00	0,00	86,88	75,94
	31,5	6,5	121,65	1,77	33	88,65	1	88,65	34,77	-34,77	53,88	77,33
frictional soil	31,5	6,5	121,65	1,77	33	88,65	1	57,02	3,84	-3,84	53,18	70,80
	30	8	138,15	18,27	48	90,15	16	72,43	24,38	-24,38	48,05	86,44
bedrock												

D

Appendix

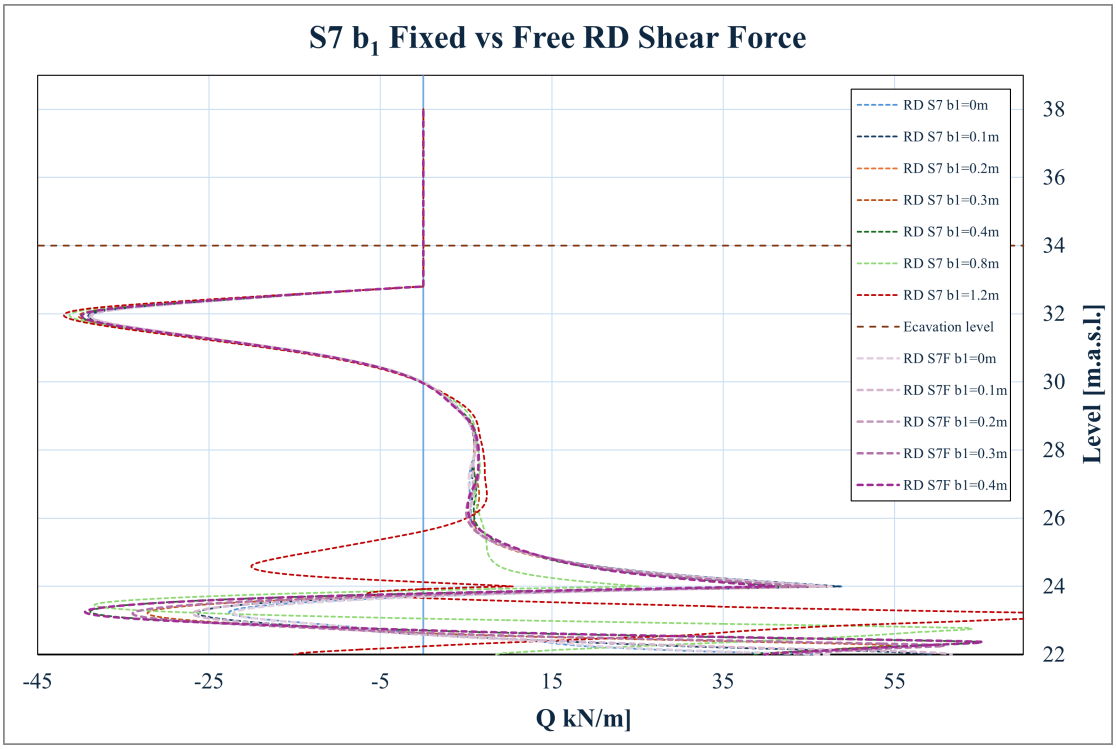

Figure D.1: Section 7 shear force in the drilled pile comparing fixed-end and free-end conditions for variations in b_1.

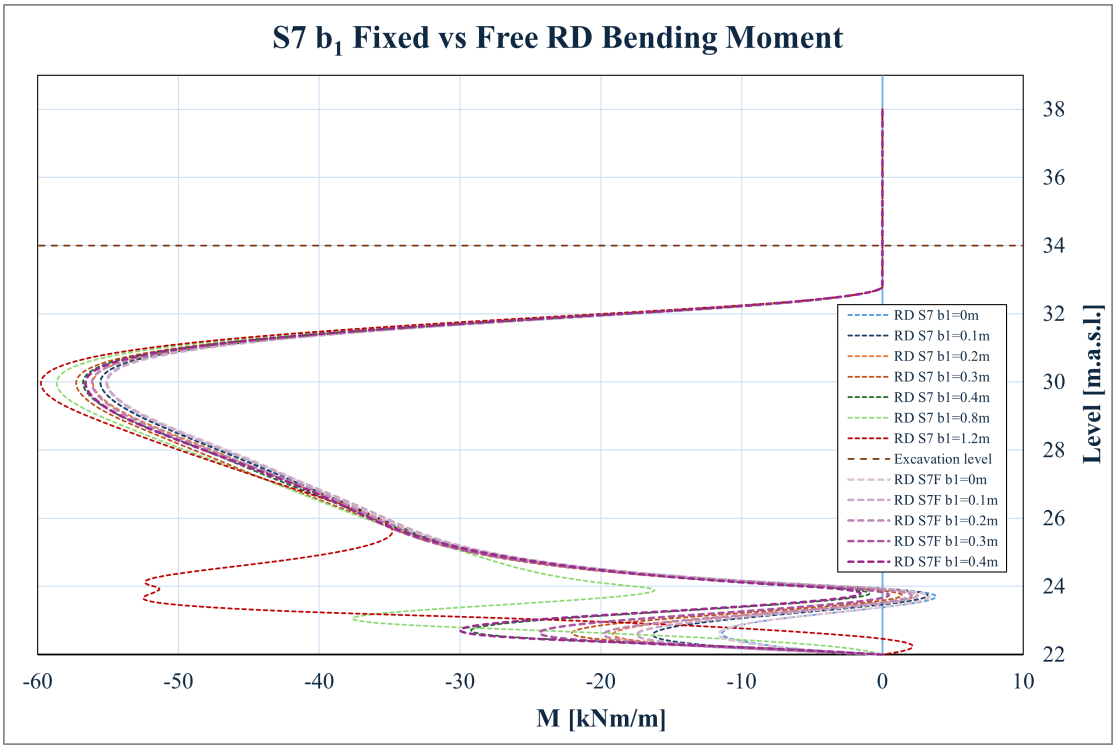

Figure D.2: Section 7 bending moment in the drilled pile comparing fixed-end and free-end conditions for variations in b_1.

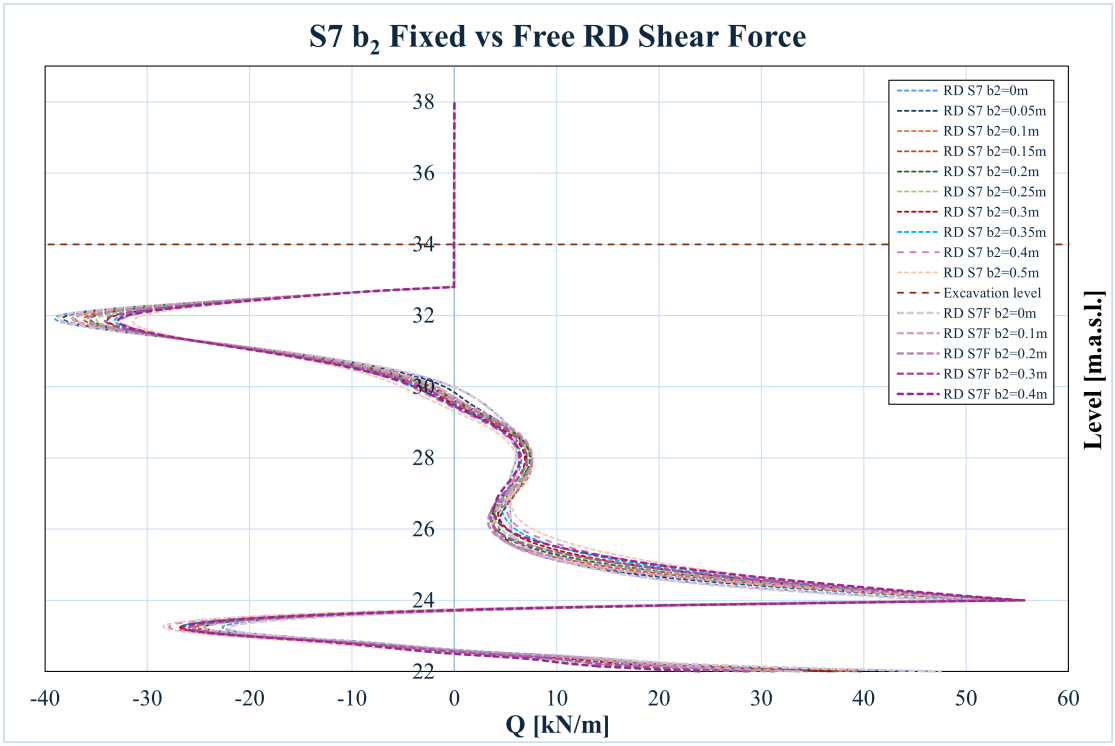

Figure D.3: Section 7 shear force in the drilled pile comparing fixed-end and free-end conditions for variations in b_2.

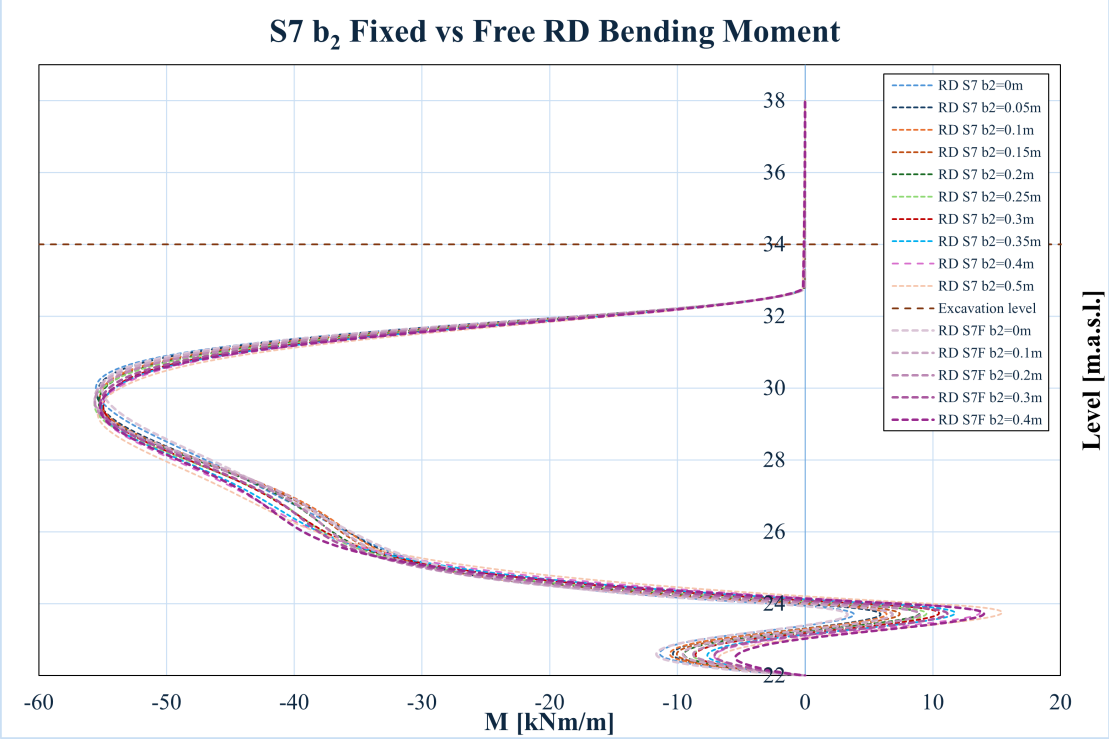

Figure D.4: Section 7 bending moment in the drilled pile comparing fixed-end and free-end conditions for variations in b_2.

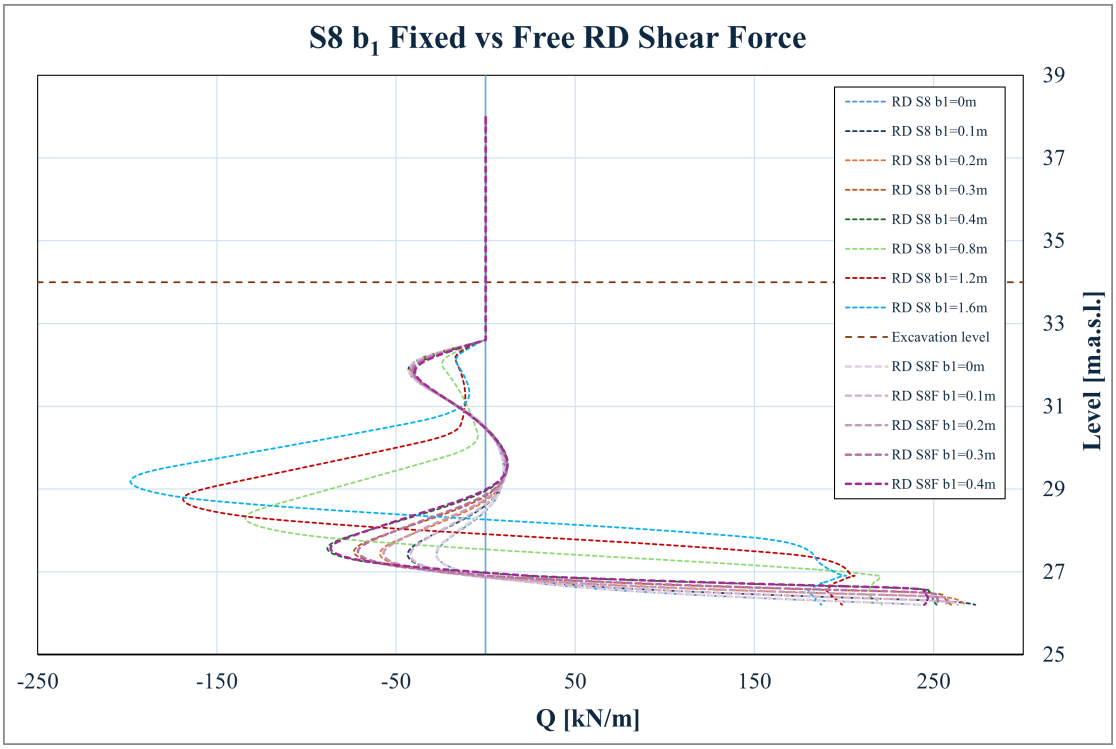

Figure D.5: Section 8 shear force in the drilled pile comparing fixed-end and free-end conditions for variations in b_1.

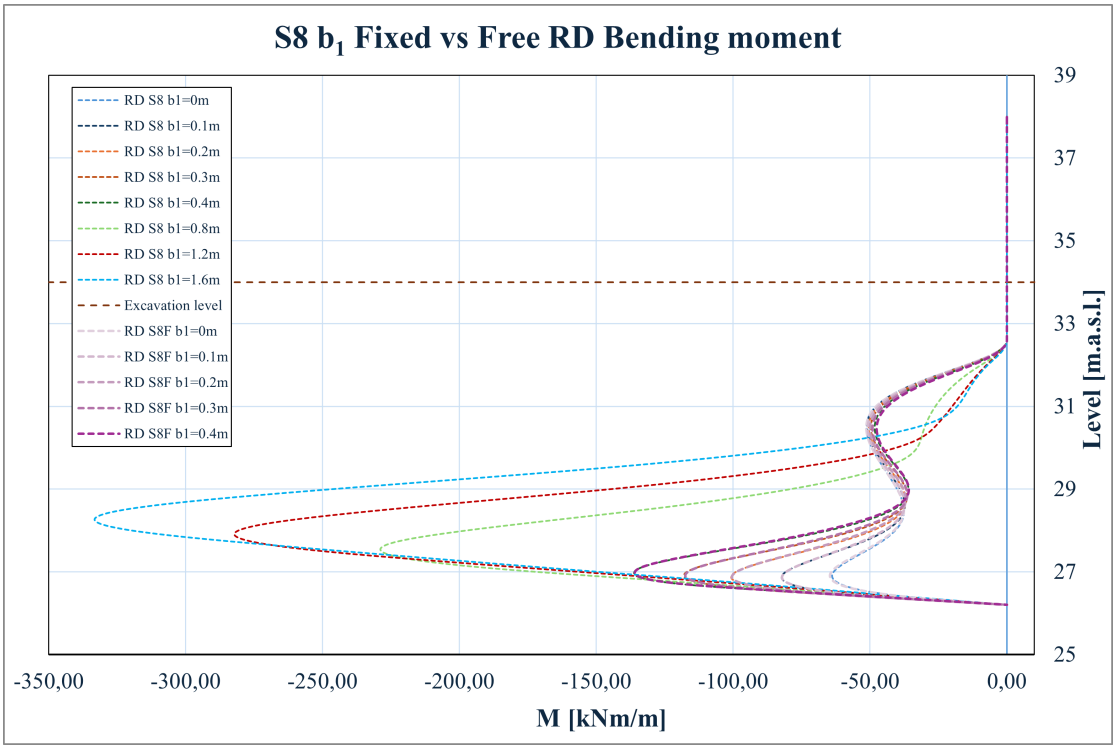

Figure D.6: Section 8 bending moment in the drilled pile comparing fixed-end and free-end conditions for variations in b_1.

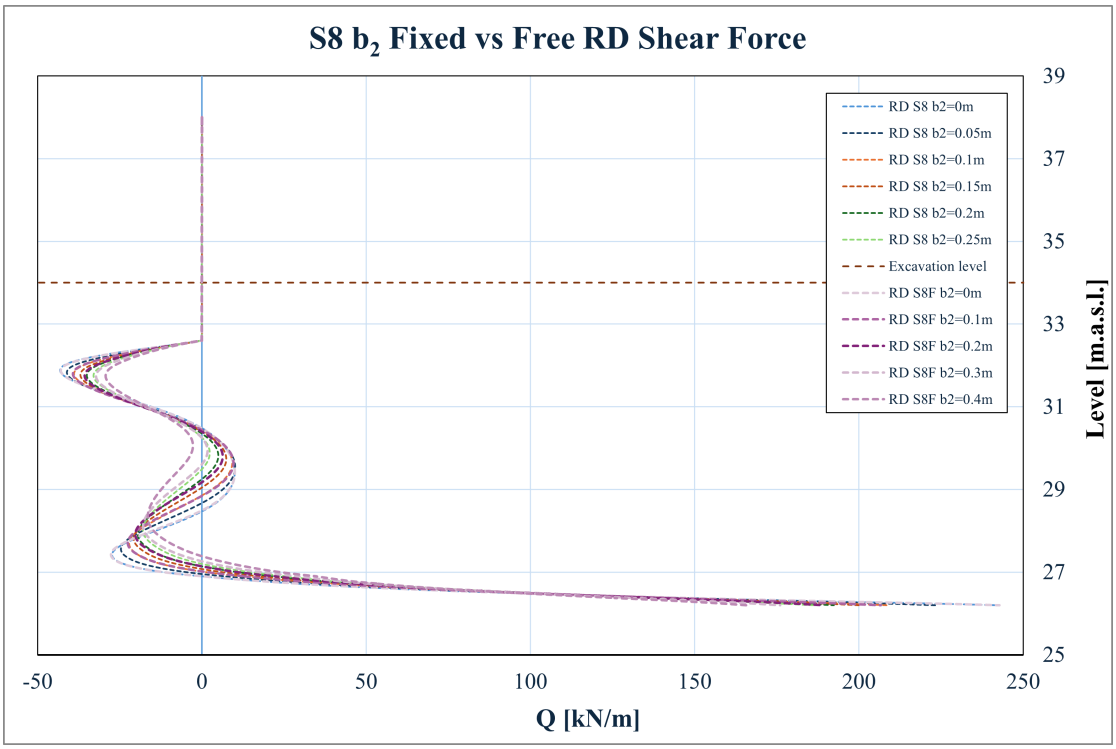

Figure D.7: Section 8 shear force in the drilled pile comparing fixed-end and free-end conditions for variations in b_2.

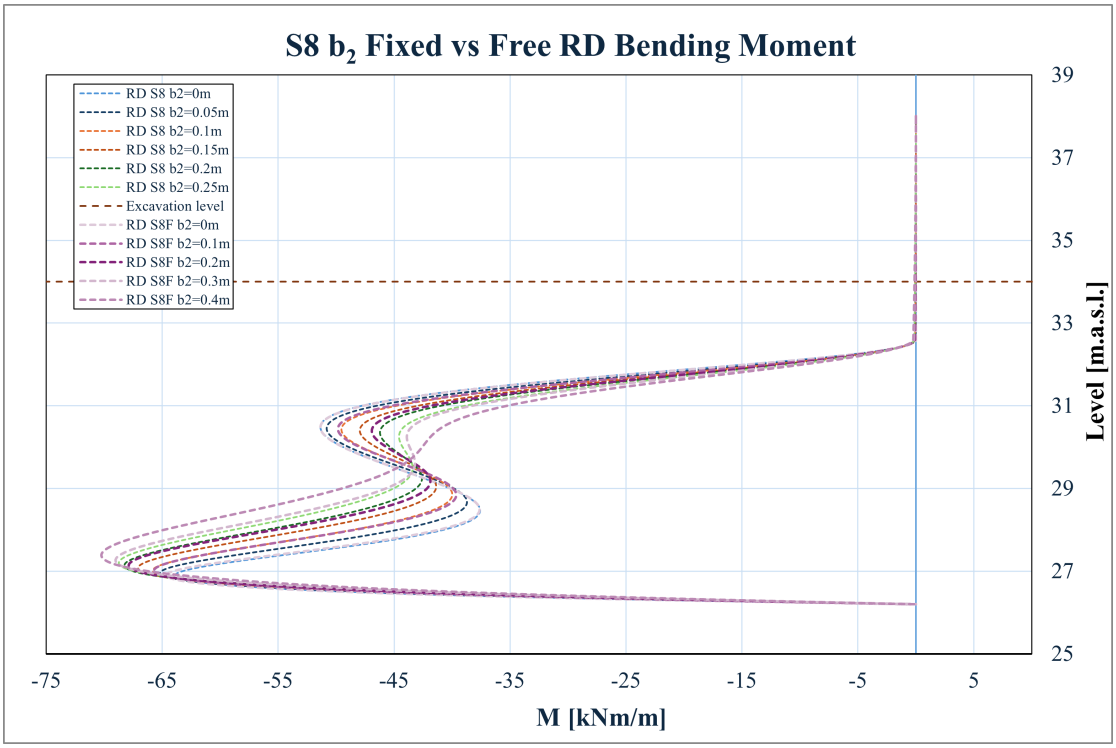

Figure D.8: Section 8 bending moment in the drilled pile comparing fixed-end and free-end conditions for variations in b_1.

E

Appendix

E.1 Transcription of interview Hercules

Date: 2025-03-5
Role of respondent: Supervisor for Hercules

[0:04 - 0:45]
Interviewer: Beskriv processen
Respondent: Vi sätter ett foderrör som vi svetsar på spontplankorna, liggande med en bottenplugg i som man ser på ritningen här. Här är foderröret och här har vi ett större foderrör, ett 219mm-rör som är gjutet från början. Som vi svetsar fast då. Då får vi en plugg här så när vi installerar spontplankan sen så kommer det inte gå upp massa skit och grejer, utan det här röret kommer vara tomt. I den bästa av vädrar så stannar ju spontplankan rakt mot berget så blir det ju ett litet glapp här nere, men inte så mycket.
[0:4 - 4:09]
Interviewer: Vet du ungefär vad ni brukar få? Mellan att ni borrar och. . . ?
Respondent: Ja, det vanliga skulle jag säga är mellan 10-20 cm. Och vi har ju en gräns på 50 cm, det är liksom max. Efter det så måste vi kontakta konstruktören. Vi har haft två där det var mer, den ena var 70 cm och den andra var 1,5 m. När det var 1,5 m då var det något annat antagligen som var lite galet där. Det var dessutom när de startade sponten eller slutade, jag kommer inte ihåg riktigt. Då går ju berget upp och lite sådär, sen så kommer vi och installerar eller vi borrar i den här cementpluggen med en vanlig bergkrona. Så går vi ner, borrar i berget, sen fyller vi med bruk och stoppar ner den. Så lätt är det ju tänkt då. Men så har vi haft problem i det här projektet, i det här glappet som blir. Nästan oavsett hur stort eller litet det är, så kryper det in material. Fint siltmaterial som går ner och lägger sig i här mellan att vi borrar och är färdigborrade, och stänger av hammaren, så rinner det in massa skit. När vi tar upp då, får vi inte ner dubben och vi kan inte se vart gjutningen tar vägen. Det märkte vi ganska fort, därför blev vi tvungna att göra en lösning i lösningen så att säga.
Respondent: Det vi kom fram till att vi skulle göra, det var att vi installerar ett nytt foderrör. I det här foderröret så att säga. Så här ser det ut då. Vi tänker oss att det här gula är ett foderrör och vi installerar ju helt enkelt det. Vi borrar igenom den här cementpluggen. Det här är vårt nya foderrör, ner så här, ner dit är grundtanken. Då hoppas vi då på att kunna täta glappet helt och hållet, sen installerar vi dubben i där då istället. Problemet med det då är ju att vi har ju redan 193mm rör så vi har liksom inte hur mycket plats som helst att jobba med. Och så ska vi in med ett nytt rör och så ska vi ha plats med dubben då. För den är 150mm. Problemet blev ju då som det står där att vi fick bara 4 mm

kringgjutning. Det var vi osäkra på om konstruktörerna skulle gå med på för de ville ju ha den här inspänd i botten. Men de räknade lite på det och såg att det är nog good enough. Och det är den bästa lösningen vi har just nu då. Så där står vi nu då och grejar med ute. Så vi installerade ett 6 meter långt foderrör.
Respondent: För vi hade under mer bekymmer när vi körde bara en halv meter fortfarande att det gick in silt. Både den vägen men vi tror även att vi gick in den vägen uppifrån också. För så länge vi är under sjöbotten så har vi ett tryck som går in då. Så vi har borrat en och en halv meter på vissa för att täta det lite grann. När man borrar ner det här foderröret så tätar det på utsidan mellan berget och foderröret. Ju längre man borrar ju mer kax och så får man täta igen där, och det har funkat. När de står där ute och borrar så gör de en slags bedömning. Man borrar en halv meter först, stänger av hammaren, väntar lite, ser vad som händer. Är det tätt och fint då så är vi nöjda.
[**4:1 - 4:48**]
Interviewer: Men då har det varit huvudproblemet med dubben här ute?
Respondent: Ja precis. Jag skulle säga att den här lösningen som var från första början, när man installerar ett färdigt foderrör och allting på sponten. När det funkar då är det jättebra på ett sätt och vis. Då är det skitbra men det är väldigt störningsosäkert. Det behövs verkligen inte mycket för att det ska bli problem. För då har du helt plötsligt ett foderrör som sitter i vägen istället. Struntar man i att sätta foderrören från början så har man ju din lösning där med en RD påle. Då kan du sätta den där du vill ha den och allting. Nu har du ett rör i vägen så du kan ju liksom inte...
[**4:49 - 6:28**]
Interviewer: Nej, precis. Och det är lite därför vi vill veta. Om vi bara kollar på det från första början. Är det smidigare för alla för att slippa de här problemen som kan uppstå?
Respondent: Jag tror många gånger är det nog så. Och särskilt om man tänker som här i Göteborgsområdet. Där vi har ett ganska osäkert berg. Det går ganska mycket upp och ner. Även där det är nära till berg så skiljer det rätt mycket. Det behöver inte skilja särskilt mycket egentligen för att det ska ställa till det. För så fort det är mer än en halv meter så blir det problem. Och då drabbas man ju inte av detta då, att man är väldigt strypt från början.
Interviewer: Ja, för vi hoppas ju på... Vi sitter ju lite i några olika program för att försöka se hur det samverkar. Men vi hoppas ju på att i och med att RD pålen verkar av en längre sträcka och tar upp kraft över en längre sträcka så kanske du har en större tolerans längre ner på det här glappet. Men det är väl lite det vi också jobbar med att komma fram till. Så vi vet ju inte riktigt än.
Respondent:Sen är problemet med en RD påle är att det är väldigt svårt att få den på rätt ställe där nere. Jag har ju varit med i många projekt och borrat RD pålar som dubb. Och när man sedan tar schakten så ser man det att man är ofta rätt så långt ifrån. Så ofta när du tar schakten så får du vara med och svetsa och plåta längre ner. För att få den att bli inspänd. Det är ju ett svårt alternativ här när man är i vatten. Det går ju givetvis där också men allting förvärras ju så att säga.

Interviewer: Skulle du gissa på att det är 10-20cm?
Respondent: Ja men det skulle nog vara någon slags medelvärde. Men de kan gå iväg ännu mer om det är så.

[**6:29–7:45**]
Jag har jobbat där på Skanska tidigare. Vi var på hamnbanan där borta. Där hade vi mycket bekymmer med just det. För där var väldigt mycket stora block liksom, träffar du det när du borrar så sticker den ju iväg. Men där uppe där du står och borrar, där ser ju allting jättefint ut. För du ser ju liksom inte riktigt vad som händer långt där nere.
Interviewer: Hur har ni toleranser och sånt? För jag vet att det pratas om vinklar och det får diffa med en grad och lite sådana. Är det oftast det som gäller? Vad gjorde ni för att åtgärda?
Respondent: Ja, här på sponten har vi 2 % som man får luta. Och det är ju lutningen det så att säga. Sen kan det fortfarande vara skev längre ner. Det är ju väldigt svårt att se och märka för oss när vi installerar det. När vi sen tog schakten så fick vi helt enkelt svetsa med s-plåt där nere. Men det är ganska vanligt i alla fall.
BULLER

[**9:23–9:33**]
Respondent: De har ju kalkberg och det är väldigt platt och fint. Så där jobbade vi med färdigsvetsade rör. Där hade vi en lösning så röret var bara att svetsa högst upp kan man säga.
[**9:40–9:47**]
Respondent: Sen när vi hade dubbat så skar vi bara loss det, och kunde svetsa dem på nya plankor.
[**9:48–9:59**]
Respondent: Vi hade liksom, jag kommer inte ihåg när det var 500 eller 600 plank. Men vi hade kanske bara 100 rör. Så vi sparade väldigt mycket pengar på att använda rören.
[**9:59–10:19**]
Interviewer: Hur gör man i vanliga fall?
Respondent: Alltså om det är det här projektet då, så lämnar du ju rören. Så då har du fortfarande en kostnad för rören, som man hade haft för en RD påle också. Visserligen så är RD påle dyrare, men du blir inte helt fri av materialet i köpet liksom.
[**10:19–11:05**]
Interviewer: Nej. Men i de fallen där man drar upp sponten igen, i temporära konstruktioner, brukar man... Vad sker med den, kan den återanvändas?
Respondent: Ja, sponten återanvänder man ju. Men röret är ju skrot oftast.
Interviewer: Ja, men ska man skära loss det då?
Ja, då blir det ju ett jobb. Ja. Och röret är liksom... De är ju inte så dyra de där rören. Så det är liksom inte värt att skära loss det och göra det snyggt för att kunna använda på ett annat projekt. Därför skrotar man. Sponten kan man däremot använda igen då, så att säga. Miljömässigt är det ju helt grymt. Den sponten har ju redan betalat sitt miljöpris. Den har ju kostat... Den är ju nästan helt miljömässigt gratis nästa gång man installerar den på ett projekt. Det är ju fantastiskt.
[**11:07 – 12:10**]
Här har du rörspont då. Vi borrar ju ner de här rören. Så borrar man dem bredvid varandra. Här är det lite konstigt. Vi driver varannan längre ner så därför ser den väldigt gles ut. Om du tänker, de två rören sitter i varandra. Så

ser det ut i vanliga fall, så att säga. Svindyrt, men bra. Du får ju en jävligt stabil spont. Den blir ganska bra när du går ner i berget. *Interviewer: Hur långt ner i berget brukar det vara?*
Respondent: Det brukar... Det beror lite grann på vad man ska göra. Här har vi då ner till 11 meter. Normalfallet är att antingen en meter ungefär eller den här klassiska tre gånger pålens diameter genomsyrar det man har även på vanliga borrade pålar, så att säga. Så de här är 400. Så då kan man ju snabbt räkna ut att det blir... 1200.
Respondent: Det här är någonting som kommer mer och mer. Det är en väldigt dyr lösning. Man inser ju oftare mer och mer är att det finns en vinst med att ta en dyr lösning. Som är rätt från början så att säga. Särskilt i grundläggning, det är så mycket problemlösning vi jobbar med. Vi startar på ett ställe och så ska vi göra det. Och så funkar inte det. Sen får vi ändra lite. Långsam framdrift och allt sånt liksom. Det är väl också för att vi väldigt sällan vet vad vi faktiskt har att jobba med. När vi väl har börjat jobba så ser vi inte det vi jobbar med heller. Vi kan bli osäkra från första början. Och det är inte alltid vi blir säkrare även när vi drar igång.
[**15:48 – 16:31**]
Respondent: Svetsningen ären annan grej som kan ställa till det. om man kan svetsa rören på plats så är det ju smidigt, då kan man ta ut sponten på lastbil så här och så kan man sätta den på plats. Kan man inte det så blir det väldigt mycket jobbigare att transportera. Det gäller ju även om man har dratt dem sen för då vill man kanske inte alltid rensa dem på plats., utan då måste man ju transportera dem från arbetsplatsen med en massa rör på. De ligger inte bra i stuvar, då blir det väldigt mycket dyrare. Oftast så lastar man ju spont efter vikt, du lastar så mycket som du får viktmässigt på bilen. I och med att det väger mer än vad det tar plats liksom. Men fyller du på en massa rör emellan så kan du inte lasta så mycket. Så då får du lägre vikt och det blir dyrare att transportera både dit och hem igen.

F

Appendix

F.1 Transcription of interview Aarsleff

Date: 2025-03-10
Role of respondent: Project manager for contractor Aarsleff

[**0:00–1:07**]
Interviewer: Hur ofta upplever du att ni använder er av den vanliga dubb-lösningen? Hur ofta har man problem med att stabiliteten inte är tillräcklig?
Respondent: Det beror lite grann på schaktnivåerna, det har ju med det att göra oftast. Det är nästan 50 procent av olika spontlösningar där man använder dubb. Det har också att göra med djupet på schaktet som styr om du behöver ha en dubb eller inte. Hur löst det är i backen också.
Interviewer: Vilka djup brukar det vara som man har denna lösning på ungefär?
Respondent: Om man drar en planka som är 10 meter och börjar komma ner på en schaktnivå under 5 meter så lär du ha något som håller emot. Ibland schaktar du ända ner till berg och då måste du ha någon typ av dubblösning som håller sponten.
[**1:07–2:07**]
Interviewer: Skulle du kort kunna gå igenom tillvägagångssättet för montaget av dubben?
Respondent: Det är olika, ibland har vi en påle som blir själva dubben som håller plankan, annars svetsas ett rör på spontplankan, och när den är fastsvetsad driver du ner den som du sen borrar ur och stoppar ner ett ämne i då som blir själva dubben, sen gjuts den fast. I detta fall har vi använt en påle som vi har borrat längs med spontplankan ner till berg, vid det angivna djupet.
[**2:08–2:39**]
Interviewer: Brukar ni svetsa dessa på plats?
Respondent: Nej, dubben svetsas inte utan den borras bara ner och behövs det kan du fästa med planka upptill. I detta fall behövs det inte. Kör man ett foderrör som det heter annars så svetsas det. Är det större jobb kan man försvetsa det hemma vid gården eller vid fabriken men annars gör man det bara på arbetsplatsen.
[**2:40–3:24**]
Interviewer: Vart brukar det uppstå problem? Vid vilka fall brukar ni behöva hitta en annan lösning?
Respondent: Det är ju när det är släntberg. Vi vet ju aldrig riktigt hur sponten beter sig och hur stort glapp du kan få. Det har vi lite där vi har idag också på Sahlgrenska när du har berg ganska nära.
[**3:26–4:29**]

Interviewer: Hur gör ni vid de fallen där det finns ett foderrör fastsvetsat? Hur gör ni då om något inte skulle stämma?
Respondent: Då kan det bli att du får stoppa i ett längre ämne, ett tjockare ämne alternativt att borra en RD-påle som vi gjort i detta fall, om det inte stämmer alls, så man verkligen vet att man får ner det.
Interviewer: Vi pratade med Hercules och de nämnde att problemet med att borra en RD-påle i efterhand när man har dimensionerat för foderrör är att det kan bli platsbrist. Har ni varit med om det, och vad gör ni då?
Respondent: Det finns massa olika typer av maskiner, så allting går ju att lösa. Det är bara en kostnadsfråga och tider, att kunna få till alltihopa.
[**4:30–6:22**]
Interviewer: Ser du någon kostnadsskillnad i att byta ut dessa två, dvs den vanliga dubblösningen mot RD?
Respondent: Pengamässigt vet jag inte men det är ju dyrare att borra med pålar. Det är mer tidseffektivt att köra med en borrad påle istället. Då får du mer exakta längderna ner till berg och du kan komplettera den också i värsta fall om det skulle bli större glapp. Och kunna nyttja den både som en påle och även stoppa in en dubb i den om det skulle vara så, för att verkligen stärka upp den.
Interviewer: Om det var upp till dig, vad hade du valt för standardlösning?
Respondent: Pengamässigt så är det foderrör, borra ur den och ha i en dubb, men att borra en påle är ju mest tidseffektivt. Alla jobb är olika, framför allt i utrymme som ni nämnde också, vart man står. Men oavsett måste det ändå borras, och då spar man tid på att borra en påle istället för att svetsa ett foderrör, borra ur och i med ett ämne som ska gjutas.
Interviewer: Tar det mer plats med den ena lösningen mot den andra eller hur ser det ut med vilka maskiner man behöver använda?
Respondent: Det beror på dubben och dimensionerna på röret, men de flesta som är upp till 270 mm klarar de flesta maskinerna, och det finns ganska små också som klarar av det.
[**6:34–7:12**]
Interviewer: Anser du att det finns ett behov av att utveckla metoden?
Respondent: Tror det är svårt att utveckla metoden, vet inte vart man skulle utveckla den på så sätt. Eftersom du måste ner och förankra plankan i berg så är borrlösningen den enda. Sen finns det väl olika sätt som man kan räkna på, det vet ni bättre än mig – hållfasthet och grejer, hur stort glapp man kan ha och hur grova eller klena ämnen man kan använda.
[**7:12–7:56**]
Interviewer: Det är lite det vi försöker komma fram till nu.
Respondent: Att optimera liksom.
Interviewer: Exakt, att kolla lite på hur mycket material kommer gå åt, det kan vara att en RD-påle kan ersätta ganska mycket mer, säg att den kan ersätta två dubb till och med men vi får kika lite mer på det.
Interviewer: Har du upplevt några komplikationer med de borrade RD-pålarna?
Respondent: Nej, det har jag inte.

DEPARTMENT OF ARCHITECTURE AND
CIVIL ENGINEERING
CHALMERS UNIVERSITY OF TECHNOLOGY
Gothenburg, Sweden 2025
www.chalmers.se

CHALMERS
UNIVERSITY OF TECHNOLOGY